Organic Functional Group Transformations in Experimental Hydrothermal Systems

by

Jessie Shipp

A Dissertation Presented in Partial Fulfillment
of the Requirements for the Degree
Doctor of Philosophy

Approved March 2013 by the
Graduate Supervisory Committee:

Hilairy Hartnett, Chair
Ian Gould
Everett Shock

ARIZONA STATE UNIVERSITY

May 2013

ABSTRACT

Hydrothermal systems are not the typical environments in which organic chemistry is studied. However the organic reactions happening there are increasingly implicated in non-trivial geochemical processes. For example, the origins of life, the formation and degradation of petroleum, and feeding the deep biosphere. These are environments where water is heated and pressurized until it has a polarity more typical of an organic solvent and an increased dissociation constant that decreases its pH. In addition, these environments host many transition metal oxide and sulfide minerals that are not inert bystanders to the chemistry happening around them. This thesis takes from the environment the complicated matrix of hot pressurized water, organic material, and minerals, and breaks it down, systematically, in the laboratory to probe the effects hydrothermal conditions and minerals have on the reactivity of model organic compounds. I conducted experiments at 300°C and 100 MPa using water, organic reactants, and minerals. Methyl- and dimethyl-cyclohexane based reactants provided regio and sterio-chemical markers to indicate reaction mechanisms. Without minerals, I found that the cyclic alkanes undergo a series of reversible stepwise oxidation and hydration reactions forming alkenes-alcohols-ketones, and alkenes-dienes-aromatic rings. I also found the reactions to be reversible; the ketone was readily reduced to the alkane. When the reactions were carried out in the presence of minerals, there were sometimes dramatic effects including reaction rate enhancement and changes in product distributions. Minerals pushed the reaction in the direction of oxidation or reduction depending on the type of mineral used. The hydration reaction could be essentially "turned off" using pyrite (FeS_2) and troilite (FeS), which eliminated formation of ketone

products. In contrast, hematite (Fe_2O_3) and magnetite (Fe_3O_4) favored the hydration reaction and enhanced ketone production. Sphalerite (ZnS) was shown to act as a heterogeneous catalysis for alkane isomerization by activating the C-H bond and increasing reaction rates until thermodynamic equilibrium was reached. This suggests that the types of minerals present in hydrothermal environments will affect the functional group composition of organic material. Minerals and hot pressurized water may also have useful applications in organic chemistry as "green" reactants and catalysts.

DEDICATION

To all the women who came before me.

To my mother and grandmother who gave me strength. To my family who always gave me someplace to run to, a place to call home, a place where nothing bad could ever happen. To Freeman for teaching me I can overcome any obstacle. And to Sidney, for keeping me sane and always reminding me what's important.

Thank you.

ACKNOWLEDGMENTS

There is an endless web of people who helped with this research, supported its author, and contributed to the science. I'd especially like to recognize my committee chair and research advisor, Dr. Hilairy Hartnett. She put countless hours into advising me, editing my work, and guiding my progress. I also appreciate the guidance and support from Dr. Lynda Williams and my committee members, Drs. Everett Shock and Ian Gould. I am honored to have worked with you. I also thank the members of the HOG group and CaNDy Lab, past and present, who shared ideas, discussed results, and helped with experiments. This includes Dr. Katie Noonan, Alex Hamilton, Zach Smith, Dr. Chris Glein, and especially Jesse Coe, who has given invaluable assistance with experiments and data processing. I also appreciate the financial support from the Department of Chemistry and Biochemistry at Arizona State University, and the National Science Foundation.

On a more personal note, I am thankful for the support from dear friends like Denise and Charlie Brigham, Katie Noonan, George Rivosecchi, and my two and four legged friends at the barn. Denise you are the best friend a girl could have, I never would have survived college without you. Charlie, thanks for feeding me meat and letting me hold down the couch while "doing homework". You and Denise took this homesick girl into your family and made my world a better place. Katie, thanks for all your advice and inspiration. Because of you I knew grad school was survivable, and there was light at the end of the tunnel. George probably took the brunt of my stress and emotional purges towards the final months of writing this thesis and job hunting- thanks for not only surviving it but also relieving my stress and always encouraging me. I also couldn't have

done it without my horse Sidney, who was always there to listen to me vent, cry on his shoulder, and cheer me up with early morning rides. He gave me an outlet and a sanctuary: the whole world went away when on his back. I also appreciate the girls at the barn, Kim, Julie and Dana, who probably had no idea what I did at work, but always cheered me on all the same. Thanks girls for sharing your positive energy. It's been a joy to ride with you these past few years.

Above all, this work wouldn't have been possible without the love and support of my mom and family. Mom, thanks for the countless care packages (I would have starved to death without them), endless phone calls when my mind was troubled, and for always making me feel like I could do anything. It's impossible to describe how much it meant to me. I always knew Grandma had my back, and her unwavering support and pride gave me strength when I wanted to quit. I am grateful to Seth and Leanne- thanks for all your visits that kept me from going insane in the city. Seth thanks for being there for every obstacle with encouragement and chocolate pudding. Dave, Bruce, Tom, you were like fathers instead of uncles. Thanks for being stewards of the most beautiful land on Earth and sharing with me its magic. Every time I went home I was inspired, refreshed, and ready to take on the world. That gift was priceless.

TABLE OF CONTENTS

Page

CHAPTER Page

LIST OF TABLES

Table Page

LIST OF FIGURES

Figure Page

Figure Page

Figure Page

Chapter 1

INTRODUCTION

What is Hydrothermal Organic Geochemistry?

This thesis is a culmination of experiments using organic reactants in hot, pressurized water, with and without minerals present. This area of science, where chemistry and geology meet under these extreme temperature/pressure conditions, is referred to as HOG: hydrothermal organic geochemistry. The purpose of this emerging area of research is to turn what we typically study in the laboratory (classical bench-top chemistry) into something relevant to processes happening in the environment where conditions aren't standard laboratory temperatures and pressures, and minerals are always present during chemical reactions.

The geochemical significance of organic material in hydrothermal systems is nothing new (Germanov, 1965) however up until recently HOG studies have been from more of a petroleum perspective, and focused on bulk organic matter effects (Engel and Macko, 1993; Kvenvolden, 1980). Here I present a systematic study of the behavior of specific organic molecules at hydrothermal conditions, from an organic chemistry perspective. I focus on how organic reactions behave in hot pressurized water and how different minerals can change that behavior. As a result, this work contributes to a molecular-level, mechanistic understanding of HOG. The insights gained into the reactivity of organic functional groups and the surface effects of minerals pushes future opportunities for HOG investigations further into the realm of mechanisms and heterogeneous catalysis.

Properties of Hot Pressurized Water

Hot pressurized water (HPW) is interesting from an organic chemistry perspective because of the physical and chemical changes that happen to H_2O molecules under high pressure and high temperature conditions. Under elevated temperatures and pressures, the shape of the water molecule changes; the bond angle increases, making the molecule less "bent", leading to a decrease in the dielectric constant. This changes the molecule's polarity, making HPW a better organic solvent than room temperature water. The ion activity product (K_w) for H_2O dissociation also increases. This increases the concentration of free H^+ and OH^- ions. The increase in H^+ concentration lowers the pH and makes H_2O a reasonable catalyst for acid-catalyzed reactions, while simultaneously making it an effective base catalyst due to the increase in OH^- ions. Details of these changes can be found in reviews by Akiya and Savage (2002) and Siskin and Katritzky (2001). For the experimental conditions used throughout this study, 300°C and 100 MPa, I calculated the neutral pH of water to be 5.3 using SUPCRT92 (Johnson J., 1992) with data and parameters from Shock et al. (1997). The solvent properties of water at 300°C are reported to be similar to those of room temperature acetone (Siskin and Katritzky, 1991).

Environments with HPW

Heating and pressurizing water has made it a better organic solvent, catalyst, and reactant, but this is not solely a laboratory-engineered state for H_2O. HPW is found naturally on Earth and possibly in extraterrestrial environments. At the bottom of the ocean, hydrothermal vents spew hot water ranging from merely warm to 400°C, that

comes from deep in the earth where reservoirs can reach temperatures >400°C (Simoneit, 2003). On land, there are also hot springs and geyser basins where the source waters are estimated to reach temperatures ranging from 90° to 350°C at depths between 100 and 4,500 m below the surface (Leviette and Greitzer, 2003).

On a young Earth, environments with HPW were likely more abundant than on the Earth we know today. Hydrothermal vents likely dominated the mostly submerged planet due to widespread volcanism and tectonic activity (Lunine, 1999; Shock et al., 2000). As we begin to think about the origins of life, thought to have emerged between 4.5 and 3.9 Ga (Russell et al., 2003), we have to consider that HPW was likely present when the first organic molecules were forming and eventually evolving into life (Chyba, 1993; Shock, 1996; Shock et al., 2000). Also, using our planet as an analogue for what other young planets and extraterrestrial bodies may be like, we'd also expect HPW to have been present during their history and could be involved in the origin of extraterrestrial life (Lunine, 1999).

Why organic chemistry?

Organic molecules find their way into environments with HPW. Organic material accumulates on the sea floor, is buried and makes its way deeper into these ocean sedimentary systems. Microbes consume most of the bioavailable carbon until what remains is recalcitrant, not very bio-available, organic compounds. These compounds eventually are buried deeply enough to encounter HPW. Similarly, deep sedimentary systems host compounds from oil/petroleum reservoirs that can come into contact with HPW. As mentioned previously, water behaves more like an organic solvent when heated

and pressurized, so conveniently these organic hydrocarbons are likely undergoing reactions in HPW; whereas, on the laboratory bench top water and hydrocarbons wouldn't even be miscible. This type of molecular behavior and reactivity is not well understood, nor often explored by classical organic chemists.

Why Minerals?

As we start to think about these natural environments with water at elevated temperatures and pressures, we quickly realize that these are not "clean" laboratory-like conditions. They are mostly sedimentary systems with an abundance of minerals (Simoneit, 1993). Minerals commonly found near hydrothermal vents and in deep sedimentary systems include the oxides and sulfides of a range of transition metals, for example, hematite (Fe_2O_3), magnetite (Fe_3O_4), pyrite (FeS_2), pyrrhotite ($Fe_{1-x}S$), and sphalertie (ZnS; Breier et al., 2012; Tivey, 1995). Clays in particular are theorized to be important for the synthesis of organic compounds in hydrothermal systems (Ferris, 2005; Williams et al., 2005; Williams et al., 2011). Therefore as we consider the chemistry of natural HPW we must also consider the presence of reactive mineral species and how their presence and composition may affect the organic chemistry happening in these environments. Several studies have observed mineral effects on organic reactions and theorized their prebiotic importance (Cody, 2004; Lahav, 1994; Russell et al., 1993; Vaughan and Lennie, 1991; Williams et al., 2005; Williams et al., 2011) but rarely are these studies conducted at hydrothermal conditions with the intent of investigating specific mechanistic effects (Schoonen et al., 2004).

Implications

There are several geochemical motivations for studying the chemistry of this pressurized matrix of H_2O, minerals, and organic material. First, it is essential to sustain the deep biosphere. Microbes have been found deeper than once expected in marine sedimentary systems, far below where bioavailable organic material, light, or other energy sources might be available (Colwell et al., 1997; Parkes et al., 1994; Zlatkin et al., 1996). It is hypothesized that the deep biosphere is "feeding" on small organic molecules generated from abiotic hydrothermal reactions of larger, once thought to be recalcitrant hydrocarbons (Horsfield et al., 2006; Mason et al., 2010; McCollom and Seewald, 2007; Windman et al., 2007). Degradation of petroleum-sourced hydrocarbons may also lead to bioavailable organic molecules that act as an energy source for microbes. This degradation not only affects the deep biosphere, it also affects the petroleum reservoir composition (Head et al., 2003; Larter et al., 2003; Oldenburg et al., 2006). Which brings us to the second implication of HOG: reactions between hydrocarbons and HPW can affect the formation, degradation, and resulting composition of petroleum reservoirs (Kvenvolden et al., 1990; Kvenvolden et al., 1994; Jones et al., 2008; Seewald, 2003; Simoneit, 1993; Siskin and Katritzky, 2001).

Third, on a much larger, global scale, HOG processes so must be considered when exploring the details of the carbon cycle. Most of the Earth's organic carbon is buried in sedimentary systems (Hedges, 1992). Reactions involving carbon compounds that reach hydrothermal conditions therefore may represent another branch of what happens to carbon as it cycles through the Earth system.

Lastly, organic reactions in HPW have an astrobiological implication. The building blocks for life and life itself may have formed in a hydrothermal environment (Kompanichenko, 2012; Martin et al., 2008; Russell et al., 2003; Shock et al., 2000; Shock and Schulte, 1998; Williams et al., 2011). As mentioned previously, a young Earth likely had HPW systems similar to present day geysers/hot springs and hydrothermal vents. The thermodynamics of these environments would have been favorable for production of molecules thought to be the precursors to life (Shock and Canovas, 2010; Shock, 1993, 1996; Shock et al., 1998). There is also evidence that these life-precursor molecules may have used clay sheets and minerals as templates or catalysts for prebiotic chemistry (Cody, 2004; Lahav, 1994; Russell et al., 1993; Vaughan and Lennie, 1991; Williams et al., 2005; Williams et al., 2011). Therefore as we study the origins of life, not only on our planet, but also as we go looking for extraterrestrial environments where life may be forming or has formed, it is important to have an understanding of the chemistry in these environments.

The role of this work

In summary, the study of how organic chemicals react in HPW and in the presence of minerals impacts the study of the deep biosphere, petroleum reservoirs, the carbon cycle, and aids in the search for the origins of life. Even with these vast and diverse implications, HOG is a relatively new field of inquiry but it is quickly gaining momentum from the need to bring a better chemistry-related understanding to real world environmental systems. I present three chapters that each push the HOG field towards a more mechanistic understanding of the reactions that can occur in HPW. I then tie

together the implications of the findings from these three data chapters in a final conclusions chapter. Chapter 2 is a study of the reactivity of various functional groups in HPW without minerals present; it showcases the unique reversible nature of the reactions and provides a deeper mechanistic understanding of functional group conversions at these conditions. Chapter 3 introduces how the addition of iron sulfide and iron oxide minerals affects hydrothermal organic reactions, using the same system of molecules studied in Chapter 2. Chapter 3 demonstrates how the reactivity and relative rates of different reaction pathways vary greatly depending on the type of mineral present. I emphasize why the presence of minerals therefore cannot be ignored while studying the chemistry of environmental systems. Chapter 4 investigates how sphalerite (ZnS), a common mineral found in hydrothermal environments, can be a heterogeneous catalyst for carbon-hydrogen bond breaking reactions. Not only does the ZnS mineral surface catalyze C-H bond breaking, it also allows a simple isomerization reaction to attain thermodynamic equilibrium on laboratory time scales. Chapter 4 also details the kinetic and mechanistic insights gained for the equilibrium between *cis*- and *trans*-alkanes in the presence of sphalerite. The concluding chapter, Chapter 5, summarizes the overall advancement in geochemistry gained from this work. I evaluate the complex, expensive, and sometimes hazardous reagents that are necessary to do the types of organic functional group conversions I studied at hydrothermal conditions under ambient laboratory conditions. Therefore this body of work not only advances the field of organic chemistry but also has "green" chemistry implications.

Chapter 2

ORGANIC FUNCTIONAL GROUP TRANSFORMATIONS IN WATER AT ELEVATED TEMPERATURE AND PRESSURE: REVERSIBILITY, REACTIVITY, AND MECHANISMS

Abstract

Many transformation reactions involving hydrocarbons occur in the presence of H_2O in hydrothermal systems and deep sedimentary systems. We investigate these reactions using laboratory-based organic chemistry experiments at high temperature and pressure (300°C and 100 MPa). Organic functional group transformation reactions using model organic compounds based on cyclohexane with one or two methyl groups provided regio- and stereochemical markers that yield information about reversibility and reaction mechanisms. We found rapidly reversible interconversion between alkanes, alkenes, dienes, alcohols, ketones, and enones. The alkane-to-ketone reactions were not only completely reversible, but also exhibited such extensive reversibility that any of the functional groups along the reaction path (alcohol, ketone, and even the diene) could be used as the reactant and form all the other groups as products. There was also a propensity for these ring-based structures to dehydrogenate; presumably from the alkene, through a diene, to an aromatic ring. The product suites provide strong evidence that water behaved as a reactant and the various functional groups showed differing degrees of reactivity. Mechanistically-revealing products indicated reaction mechanisms that involve carbon-centered cation intermediates. This work therefore demonstrates that a wide range of organic compound types can be generated by abiotic reactions at hydrothermal conditions.

Introduction

The chemical reactions of organic molecules at elevated temperatures and pressures are increasingly implicated in a suite of geochemical processes. Examples include the diagenesis and alteration of minerals and organic matter in marine sediments and sedimentary basins (Seewald, 2003; D'Hondt et al., 2004; Hinrichs et al., 2006; McCollom and Seewald, 2007), and organic and inorganic reactions that result in the accumulation of oil and natural gas deposits (Siskin and Katritzky, 2001; Head et al., 2003; Larter et al., 2003; Jones et al., 2008). It has also been proposed that hydrothermal transformations of organic compounds provide nutrient sources for microbial communities within deeply buried sediments and at hydrothermal systems in the oceans (Head et al., 2003; Horsfield et al., 2006; McCollom and Seewald, 2007; Windman et al., 2007; Mason, et al., 2010). Hydrothermal systems similar to those found in mid-ocean ridge environments are also thought to mimic the conditions where life, or the organic precursors to life, may have developed on early Earth (Baross and Hoffman, 1985; Nisbet, 1985; Shock, 1990; 1992; 1996; Shock and Schulte, 1998; Shock et al., 1995; 1998; 2000; Seewald et al., 2006; Martin et al, 2008; Shock and Canovas, 2010; Williams et al., 2011). Seewald et al. (2006) states that "despite the significant role that aqueous carbon compounds play in a broad spectrum of geochemical and biological processes, reactions that regulate the abundance of aqueous carbon compounds at elevated temperatures and pressures are poorly constrained." To some extent this is understandable, given the wide range of organic structures and reactions found in natural systems that can include both mineral and aqueous reactions. As an initial approach to understanding such complex systems, this work focuses on first understanding the

functional group transformations that connect alkanes to ketones without the added complexity of a mineral phase.

Product studies of hydrothermal reactions for a large number of specific organic functional groups have now been reported (Savage, 1999; Katritzky et al., 2001; Siskin and Katritzky, 2001; Watanabe et al., 2004). Notably, kinetic measurements on model systems have uncovered features of these processes that distinguish them from analogous reactions at ambient conditions; specifically, that these reactions may be controlled by thermodynamic rather than kinetic factors (Shock, 1988, 1989, 1994; Helgeson et al., 1993; Seewald, 1994, 2001). The first experimental evidence of metastable equilibrium states was provided by Seewald (1994) who demonstrated interconversion in simple alkane/alkene systems and showed that hydrogenation/dehydrogenation reactions for ethane and ethene using a pyrite-pyrrhotite-magnetite (PPM) mineral redox buffer attained metastable equilibrium in water at 350°C and 35 MPa. Interconversion between alkene and alcohol functional groups has also been demonstrated (Kuhlmann et al., 1994; Akiya and Savage, 2001).

Interconversions between alkanes, alkenes and alcohols are included in a general reaction scheme proposed by Seewald (2001) that connects alkanes to carboxylic acids (Figure 1). Alkanes and carboxylic acids represent some of the most abundant organic structure types found in natural hydrothermal systems and sedimentary basin fluids, and decarboxylation of carboxylic acids is considered to be an important mechanism for breaking larger organic structures into smaller ones. Figure 1 summarizes a proposed pathway that combines irreversible decarboxylation and reversible functional group interconversions to convert longer alkane chains into shorter ones, and also provides a

starting point for a molecular-level understanding of organic matter transformations and other process involving organic structures that can influence mineral reactions and may feed the deep biosphere.

Theoretical models for water-mineral-organic-microbe processes that drive diagenetic transformations, petroleum formation and habitat generation in the deep biosphere can be built using detailed kinetic and thermodynamic data about interrelated hydrothermal organic reactions. The present work has three goals relevant to furthering a kinetic and thermodynamic understanding of the reaction scheme presented in Figure 1. First, although interconversion between individual pairs of functional groups in the proposed reaction pathway has been demonstrated previously, the extent of reversibility across the entire reaction scheme has not yet been established. Therefore, one goal of the current work is to explore the reversibility and interconnectedness of as many of the functional group interconversions in Figure 1 as possible *within a single chemical reaction system*. Second, although kinetic results are published for several of the reactions in Figure 1, a comparison of the relative reactions rates of the various functional groups is not. Thus, a second goal is to obtain relative rate information for as many of the functional group interconversions in Figure 1 as possible, so that meaningful comparisons can be made among them. Finally, the third goal is to obtain mechanistic information for the reactions presented in Figure1, so that understanding can move from phenomenological to fundamental.

In the approach taken here, stereochemical and regiochemical probes are used to study the reversible reactions of model substituted cyclohexanes. For some of the reactions studied, these techniques also provide information on reactive intermediates,

thus yielding mechanistic information. By initiating the reaction scheme at different specific functional groups, information on relative reactivity and the extent of overall reversibility along the entire reaction scheme is obtained. Low extents of conversion are used to minimize secondary reactions of the functional groups.

Under the experimental hydrothermal conditions, we find the reaction path connecting alkanes to ketones is completely reversible, although for the cyclohexane structures investigated, formation of dehydrogenated aromatic structures eventually dominates the product distributions. The various functional groups exhibit quite different rates of overall chemical reactivity. Water is also observed to be a reactant. Interestingly, under the conditions and timescales of these experiments, no carboxylic acids are detected as products, although other products that require carbon-carbon bond fragmentation are observed.

Methods

Reactions were performed in capsules made from sealed gold tubes (3.35 cm long, with a 5 mm outer diameter and 4 mm inner diameter). Before use, the gold was annealed at 600°C for 15 h. One end of the tube was welded closed and the tube was purged with ultra high purity argon (Ar) for 15 min. The capsule was then immediately filled with 250 µL of Ar-purged 18.2 MΩ·cm water (NANOpure® DIamond™ UV, Barnstead International) and a measured volume of the organic reactant to give a final concentration around 0.2 M (Table 1 and Table 2 list the exact number of µmoles used in each experiment). The open end of the capsule was then welded closed while the bottom ¾ of the tube was kept cold in an ice-ethanol slurry (the measured temperature was -

15°C) to minimize reactant loss due to volatilization. The sealed capsules were weighed and placed in a stainless steel, cold-seal reaction vessel and pressurized to 100 MPa with deionized (DI) water. The reaction vessel was placed in a pre-heated furnace and heated to a maximum temperature of 300°C. A thermocouple inside the pressure vessel monitored the reaction temperature of the capsules. Typically, ca. 3 h was required to reach 300°C owing to the large thermal mass of the reaction vessel. The time zero point for each experiment was taken as the time when the vessel was put into the preheated furnace. This means the reported experiment duration includes the time it took for the system to reach 300°C.

After each experimental run, the reaction vessel was quickly cooled to room temperature in water while maintaining high pressure to avoid capsule bursting. The pressure was then relieved and the gold capsules removed and weighed to assure no leakage. The outsides of the capsules were rinsed in dichloromethane (DCM, 99.9%, Fisher Scientific) to prevent contamination and then the capsules were frozen in liquid nitrogen. Frozen capsules were sliced open with a scalpel and placed in glass vials containing 3 mL DCM with 5.85 µL of *n*-decane (99%, Alfa Aesar) added as an internal gas chromatography standard. Vials were capped and capsules were allowed to thaw. Vials were shaken to fully extract the contents of the capsule. The DCM/organic layer (lower layer, below the water) was removed with a disposable glass pipette and placed in an autosampler vial for analysis by gas chromatography (GC). Extraction blanks were also used to identify contaminants and/or impurities in the DCM or decane; blanks consisting of 3 mL DCM with 5.9 µL of *n*-decane were mixed alongside capsule

extractions, and treated identically to the experimental samples throughout the extraction/analysis process.

The experiments used a series of monomethyl- and dimethylcyclohexane molecules (Tables 1 and 2). The concentrations of the products were determined from calibration curves using authentic standards (methylcyclohexane, 99%, Sigma-Aldrich; 1-methyl-1-cyclohexene, 97%, Aldrich; 1-methylcyclohexanol, 97%, Alfa Aesar; 2-methylcyclohexanol, *cis* + *trans*, 97%, Alfa Aesar; 2-methylcyclohexanone, 99+%, Sigma-Aldrich; 3-methylcyclohexanone, >97%, Sigma-Aldrich; 4-methylcyclohexanone, 99%, Aldrich; 1-methyl-1,4-cyclohexadiene, 96+%, Sigma-Aldrich; toluene, 99.8%, Aldrich; *cis*-1,2-dimethylcyclohexane, 99%, Aldrich; *trans*-1,2-dimethylcyclohexane, 99%, Aldrich; 1,2-dimethylcyclohexene, 96+%, ChemSampCo; *o*-xylene, >99.5%, Aldrich; *p*-xylene, 99%, Alfa Aesar; and *m*-xylene, >99.5%, Aldrich). All quantitative work was performed using GC with flame ionization detection (GC-FID) on a Varian CP-3800 equipped with a 5% diphenyl/95% dimethylsiloxane column (Supelco, Inc). The injection temperature was set at 200°C and the temperature program used depended on whether the experiment utilized dimethyl compounds or monomethyl compounds. For dimethyl compounds the oven temperature started at 50°C then increased to 100°C at a rate of 5°C/min then increased to 200°C at 20°C/min, and finally increased to 300°C at 25°C /min where it was held for 10 min. For the monomethyl system the oven started at 40°C and was increased to 90°C at a rate of 2°C/min, followed by an increase to 300°C at 30°C /min where it was held for 2 min. Concentrations of structures that did not have authentic standards were determined using a calibration curve made from an authentic standard of an isomer of the structure. If an isomer was not available, the average GC

response factor for standards with similar structures was used. To determine concentrations of dimeric products, the average of the GC response factors from all the monomethyl standards was multiplied by two. Products that could not be identified using authentic standards on the GC-FID were characterized via gas chromatography-mass spectrometry (GC-MS; Agilent 6890/5973) using the same analytical column and temperature protocol as the GC-FID system. Identification of peaks was based on the interpretation of the mass spectra as well as comparison against the NIST Mass Spectral Library.

The mass balance for each experiment was assessed by summing the number of μmoles of quantified products with those of the remaining reactant, then dividing by the number of μmoles of reactant initially added to the capsule. The more volatile reactants yielded less than ideal mass balance due to evaporation prior to and while welding the capsules. This was particularly true for experiments with 1-methylcyclohexane (**1**), 1-methylcyclohexene (**2A**), 1-methyl-1,4-cyclohexadiene (**2C**), and toluene (**3E**), which yielded mass balances greater than 70%, but less than 90% (there were no unidentified product peaks in these experiments). The alcohol and ketone reactants, and most of the dimethylcyclohexane-derived reactants gave mass balances that were greater than 90% (Tables 1 and 2). The amount of conversion (also reported as % reacted) for each reaction was calculated by summing the quantifiable products and dividing by the sum of the products plus the unreacted starting material. This method avoids problems associated with volatile reactants, but underestimates the extent of conversion for any reaction that produced unquantifiable products (this occurred in the dimethyl system only; all products in the monomethyl experiments were quantified). The number of hydrogen atoms

produced or consumed in each experiment (Table 1) was calculated based on the degree of unsaturation for each product. Hydrogen balance cannot be calculated for experiments that resulted in a large amount of uncharacterized dimer (**D1**, **D2**) because the extent of unsaturation is unknown.

Results and Discussion

Experiments were performed using structures based on two simple cyclic alkane structures, methylcyclohexane (**1**) and 1,2-dimethylcyclohexane (**6**; *cis*- and *trans*-; Figure 2). Compared with the parent cyclohexane, the single methyl group in **1** serves as a *regiochemical* indicator for the formation of isomers. The two methyl groups in **6** have *cis*- and *trans*-stereochemistry on the cyclohexane ring and thus serve as a *stereochemical* indicator of isomer formation. The fact that many isomers are possible products in the reactions is a critical mechanistic tool, rather than a complicating factor. We show below that complete identification of all of the minor products is mechanistically revealing.

Experiments Based on Methylcyclohexane

We focus on the functional-group transformations that connect alkanes to ketones indicated in Figure 1. Experiments were started with each of the functional groups along the reaction path: alkane, alkene, alcohol, and ketone, as well as diene, and aromatic structures (i.e., 1-methylcyclohexane (**1**), 1-methylcyclohexene (**2A**), *cis*- and *trans*-2-methylcyclohexanol (**3A** + **3B**), 2-methylcyclohexanone (**4A**), 1-methyl-1,4-cyclohexadiene (**2C**), and toluene (**2E**)). Depending upon the starting structure and the

reaction time, a large number of products can be formed. A full summary of the products formed in the various reactions is given in Figure 3 and Table 1.

By comparing the percent of starting material reacted and the product distributions for each experiment (Table 1, Figure 4), information on the relative kinetic reactivities of the different functional groups can be obtained. The diene (**2C**) functional group is interpreted to be the most reactive compound under the experimental conditions, with the highest percent conversion (100%) exhibited after only 5.4 h reaction time. The alcohol (**3A** + **3B**) functional group was the next most reactive, with 95.4% conversion over the same time frame. The alkene (**2A**), ketone (**4A**) and alkane (**1**) were less reactive, with percent conversions decreasing as 76.4%, 6.8%, and 0.8%, respectively. The fully aromatic toluene was almost completely unreactive under the experimental conditions with only 0.4% conversion, mostly to benzene, after 144 h (6 days). Figure 4 not only depicts the percent of conversion for each experiment (pie charts), but also showcases the relative product distributions for the primary products (bar charts).

The products of the various reactions are discussed in detail below, but the product distribution of an example reaction is immediately revealing. The gas chromatogram of the products formed after a 3.5 h hydrothermal reaction of the alkene 1-methylcyclohexene (**2A**) is shown in Figure 5. Most of the other reactions gave fewer products, but the reaction of **2A** illustrates two notable features of the reactions in general. First, almost all of the functional groups are formed from the alkene, and this turns out to be the case for most of the different functional group reactants, implying extensive interconversion among the functional groups. Second, multiple isomers of the various functional groups were formed after only 3.5 h (with 76% conversion). This

implies that interconversion among the isomeric products and their common intermediates is rapid on the timescales of the reactions. Multiple alkene and ketone isomers also formed from the alkane reactant despite it's much slower reaction with only 0.6% conversion. In other words, not only do functional group interconversions occur, *but they occur reversibly on timescales that are rapid compared to that for overall decomposition of the starting material*.

Reaction of methylcyclohexane (**1**) under the experimental conditions was very slow. Only 0.6% conversion was observed after ca. 24 h at 300°C and 100 MPa. After almost 4 days the conversion increased, but non-linearly, to 0.8%. The same products were observed for both time periods, but with different distributions (Table 1; Figure 4). The main products are 1-methylcyclohexene (**2A**) and other methylcyclohexene isomers (**2B'**; Figure 3), toluene (**2E**), and all three possible methylcyclohexanone isomers (**4A**, **4B**, and **4C**; Figure 3). Of the methylcyclohexene isomers, 1-methylcyclohexene (**2A**) is the most abundant at both reaction times. Of the possible isomeric methylcyclohexanones, 2-methylcyclohexanone (**4A**) is the most abundant at both reaction times. Very small yields of the enone structures (**5'**) are also observed.

Toluene is presumably formed by two consecutive dehydrogenation reactions of the alkenes (**2A** and **2B'**), however, no methylcyclohexadiene isomers (**2C** or **2D**) could be detected at either reaction time (Figure 3). It appears that the dienes are short lived under the experimental conditions (see below). The small yields of the enones (**5'**) are likely formed by dehydrogenation of the cyclohexanones (**4A**-**4C**), i.e., analogous to the dehydrogenation of the starting alkane (**1**) to form the alkenes **2A** and **2B'**. Of the various possible methylcyclohexanol isomers that could have formed (**3A**-**3D**), none are detected

for either reaction time. However, the only viable reaction path to the enone structure must proceed via the alcohols, suggesting that the alcohols are also extremely short lived under the experimental conditions, and do not persist at measurable concentrations. Note that all three ketone isomers are observed, which requires three different alcohol structural isomer precursors. Not only do the alcohols apparently react very quickly under the conditions, but the observation of multiple ketone isomers suggests that either they interconvert rapidly, or they are formed from different isomeric alkene precursors that were generated rapidly.

The suggestion that the alcohols are short-lived under the experimental conditions is confirmed in an experiment starting with 2-methylcyclohexanol (as a mixture of *cis*- and *trans*-stereoisomers, **3A** and **3B**). After only 5.4 h, 95.4% of the alcohols had reacted. The products included an isomer of the starting alcohol, 1-methylcyclohexanol (**3C**) and minor quantities of other alcohol isomers **3D'**, all three isomeric ketones (**4A**-**4C**; although only trace quantities of **4B** and **4C** were found), methylcyclohexane (**1)** and a trace amount of toluene **2E** (see Table 1 for relative abundances). Due to this short reaction time, trace amounts of highly reactive dehydrogenated diene isomers (**2C** and **2D**) and enones (**5'**) could also be detected. The major products, by far, on this timescale were the alkenes, in particular 1-methylcyclohexene (**2A**), which constituted almost 50% of the products. It should be noted that rearranged cyclopentene products were observed, and trace amounts of uncharacterized dimeric structures **D1** and **D2** were also present in the gas chromatogram (Figure 3, Table 1). These observations, particularly the presence of 1-methylcyclohexanol (**3C**) and the 3- and 4-methylcyclohexanones (**4C**, **4B**), support the suggestion that alcohols react and interconvert rapidly and reversibly, and that

ketones form via dehydrogenation of the alcohols. A partial reaction scheme consistent with the observation of alcohol isomers is shown in Eq. (1) (NB, stereoisomers of the alcohols are not included in Eq. (1), but are observed in the experiments).

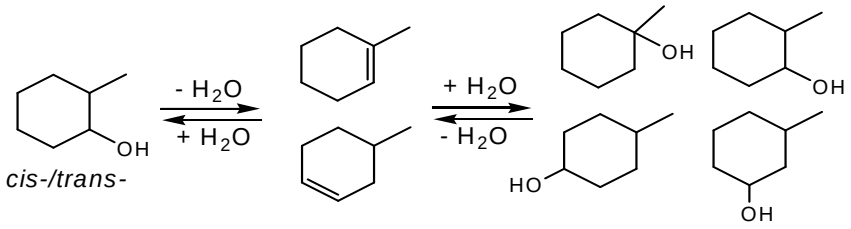

(1)

Dehydration of alcohols under hydrothermal conditions is known to be rapid (Xu and Antal, 1994; Kuhlmann et al., 1994; Xu et al., 1997; Antal et al., 1998; Akiya and Savage, 2001); so it is not surprising that alcohols were not found at measurable concentrations on the timescale of the alkane (**1**) experiments (1 and 4 days).

Ketones were observed as products in the reactions of alkane (**1**). This raises the question of whether the reaction can proceed completely in the other direction; i.e., can alkane (**1**) be formed during the reaction of a ketone? 2-Methylcyclohexanone (**4A**) was reacted under the same hydrothermal conditions (300°C and 100 MPa) and exhibited roughly 3% conversion after 5 h. Thus, while not as reactive as the alcohol, the ketone was considerably more reactive than the alkane (**1**; 0.6% conversion in 24 h). The most abundant products of the ketone were 1-methylcyclohexanol (**3C**), alkene isomers (**2A** and **2B'**), toluene (**2E**), and two methylcyclohexenone isomers (**5'**). Some rearranged alkene products were detected, in addition to a very small amount of a cyclohexadiene isomer (**2D**)**.** Notably absent were 2-methylcyclohexanols (**3A**, **3B**), and methylcyclohexane (**1**). Formation of 1-methylcyclohexanol (**3C**) again confirms rapid reversible reaction on the timescale of the experiment. The most likely mechanism for

formation of this alcohol is reduction of the ketone to 2-methylcyclohexanol (**3A**, **2B**), followed by dehydration to form an alkene and subsequent re-addition of water to the alkene, as illustrated by Eq. (2). Note this is similar to Eq. (1) with an additional hydration step.

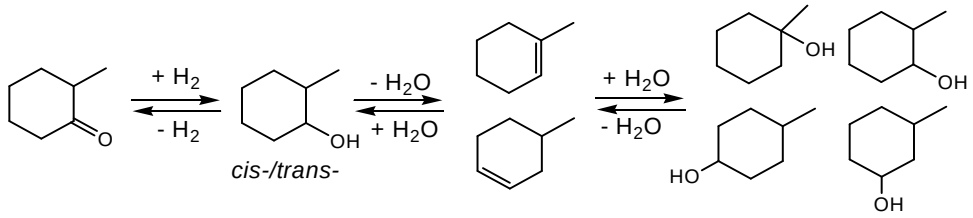

(2)

The re-addition of water could also occur at the carbocation intermediate precursor to the alkene after rearrangement. The absence of detectable alkane is presumably a consequence of the fact that the alkene undergoes dehydrogenation to form a cyclohexadiene and then toluene faster than it undergoes hydrogenation. Toluene is observed as a product in every experiment, which points to the propensity for dehydrogenation of the cyclic alkenes. Formation of aromatic products from cyclohexane has been observed previously in supercritical water, however the experiment differed in that a transition metal catalyst was used (Crittendon and Parsons, 1994). In order to form the alkane from the ketone, two formal additions of molecular hydrogen are required. At early reaction times the required hydrogen may not be available to form the alkane. Formation of toluene must liberate hydrogen, and this process may act as a hydrogen source for formation of alkane at later reaction times. Hydrothermal reaction of ketone **4A** for a longer time period (20 h) does in fact result in formation of alkane (**1**), in addition to many other low-yield products (Table 1). Interestingly, the alkene (**2A**) and toluene (**2E**) are the most abundant products after this longer reaction time. This result reinforces the time-dependence of the product distributions, discussed below.

As mentioned above, a common trend in all the experiments is the tendency to form aromatic products, specifically toluene (**2E**). A likely reaction path to toluene is via cyclohexadiene, itself formed by dehydrogenation of one of the alkene isomers (Figure 3). Diene isomers (**2D**, **2C**) are detected in very minor quantities in the short-term (5 h) experiments starting with the alcohols (**3A** + **3B**) and the ketone (**4A**; Table 1). However, dienes were not detected starting with the alkane (**1**), presumably due to the longer reaction times required for appreciable alkane conversion. Conversion of a diene to toluene would be expected to be rapid due to the relative stability of the aromatic system, and it is possible that the diene is too reactive to remain at detectable concentrations in experiments longer than a few hours.

The hypothesized reactivity of dienes is confirmed in an experiment starting with 1-methyl-1,4-cyclohexadiene (**2C**). After 5.4 h only trace amounts of the diene remained; the major product was toluene (**2E**), accompanied by significant amounts of alkene isomers (**2A**, **2B**□), the alkane (**1**), alcohol isomers (1- and 2-methylcyclohexanol; **3C**, **3A**, **3B**), and all three ketone isomers (**4A**, **4B**, **4C**). The diene also formed uncharacterized dimeric products (at low yields), similar to those observed starting with 1-methylcyclohexene.

A reaction starting with toluene (**2E**) resulted in almost no conversion even after 144 h (Table 1). Small quantities of benzene and some dimers were the only products. The absence of alkane, alkene, alcohol, or ketone products suggests that the formation of toluene may be irreversible. However, one must remember the reaction system consists of only toluene and H_2O, and a hydrogen source is necessary to form alkenes and alkanes, etc. The minor amount of benzene that formed could be coupled with H_2 and CO_2

formation, but evidently any reaction from this amount of H_2 generation was undetectable, and H_2O alone was an insufficient hydrogen source to reduce toluene under the experimental conditions. (Other experiments starting with dimethylcyclohexane suggest reversible formation of aromatic species maybe be possible when there are other sources of hydrogen, as discussed in the next section). Hydrogen balances were estimated for the alkane, alcohol, and ketone reactions only. An accurate hydrogen balance requires a complete description of the products, which precluded the reactions of toluene, alkene, and diene, since a large proportion of their products formed were dimers (**D1** and **D2**) with unknown structures. To determine the number of hydrogen atoms liberated, the number of hydrogen atoms in each product molecule was compared to the number in the corresponding reactant and the difference was multiplied by the final amount of that product. For all the reactions considered, there were fewer hydrogen atoms in the products than were present in the starting material. Normalization of these hydrogen amounts to 100% reaction, so comparisons could be made between experiments, gave about 140 µmoles of hydrogen atoms lost for both alkane reactions, between 95 and 102 µmoles lost for the alcohol reaction, and around 52 to 68 µmoles lost for the ketone reactions; the range is a result of how unsaturated we consider the dimers to be (Table 1). For the alkane reactions, each mole of alkane that reacted generated just over one mole of molecular hydrogen. For the alcohol reaction, one mole of molecular hydrogen was formed for each mole of alcohol reacted. The ketones are more oxidized than either the alkane or the alcohol, and in this case each mole of reacted ketone generated half a mole of molecular hydrogen (Table 1). This evidence indicates that hydrogen is produced in the course of these reactions. If all of the hydrogen atoms estimated in Table 1 were

actually present in the experiments as dissolved H_2 at the experimental conditions (near the critical point for water), the H_2 concentrations for most of the experiments would fall between 1.6 and 7.0 mmolar. The H_2 concentration evaluated in this manner for the alcohol experiment is ~188 mmolar. With the exception of the alcohol experiment, the estimated values are in the same range as H_2 concentrations measured in submarine hydrothermal fluids (0.4 to 16 mmolal; Shock and Canovas, 2010). Whether 188 mmolar H_2 is an attainable concentration in organic rich sediments where these reactions can occur remains to be determined.

The observation of multiple isomers of the various products that formed at essentially the same rate suggests both rapid interconversion and reversible reactions. Mechanisms that account for the reversible reactions involving the alkene and alcohol functional groups are shown in Figure 6. The conversion between the alkenes and alcohols is depicted as an E1 mechanism; however, previously published mechanisms for alcohol dehydration under hydrothermal conditions have suggested an E2 mechanism is possible (Kohlmann et al., 1994; Akiya and Savage, 2001). Either way, the central intermediates in the alkene-alcohol interconversions are the carbon-centered cations (Figure 6). The formation of rearranged 5-membered ring structures such as **R2B'** provides unequivocal evidence for these intermediates *via* 1,2-alkyl shift reactions of the cationic 6-membered ring. These rearranged products are also observed in the acid-catalyzed dehydration of **3A**/**B** under ambient conditions (Friesen and Schretzman, 2011) and in Akiya and Savage's (2001) dehydration experiments with cyclohexanol in high-temperature H_2O. Formation of the various alkene and alcohol isomers observed can be explained as a result of formation of these cations by alkene protonation followed by

deprotonation and/or hydration/dehydration. A different but related mechanism for isomer formation (not included in Figure 6) involves a 1,2-hydride shift reaction of the cation intermediates. The current experiments cannot distinguish between these two mechanisms, but the cation intermediates in Figure 6 are key for both pathways. The mechanisms of the hydrogenation/dehydrogenation reactions under hydrothermal conditions are not well understood at this time, and experiments using the monomethylcyclohexane system cannot provide insight because they lack stereospecificity. The mechanism outlined in Figure 6 implies that dehydrogenation of the alkane (**1**) mainly yields the most stable alkene isomer (**2A**). An alternate mechanism for formation of alkene isomers wherein irreversible dehydrogenation at all of the carbon-carbon bonds in the alkane ring occurs to give the different alkenes directly is unlikely given: 1) the demonstrated intermediacy of the cations, and 2) the observation that alkene isomers also formed when starting with both the alcohol and ketone functional groups. Experimental results from reactions of the dimethylcyclohexane ring systems (see the next section) provide additional information specific to the dehydrogenation/hydrogenation reactions.

In summary, essentially all of the cyclohexane variants with different functional groups can be formed starting from any of the other functional groups. These experiments demonstrate interconversion among the functional groups along the entire reaction path of Figure1 from alkane to ketone, and back again. Isomeric alkene, alcohol and ketone products are formed seemingly simultaneously, implying not only that the various functional groups are interconvertible, but also that reactions among them are rapidly reversible on our experimental timescales. Lastly, the interconversion between alkenes

and alcohols proceeds via a carbon-centered cation intermediate, as is evident by the formation of rearranged alkene and alkane products.

Experiments Based on Dimethylcyclohexane

The reactions of the monomethylcyclohexane system described above demonstrate almost universal interconversion *and* reversibility among a range of functional groups. Although the alkane can be converted into the alkene (and vice versa) the extent to which the dehydrogenation/hydrogenation reactions that couple the alkane and alkene are reversible cannot be demonstrated in the non-stereospecific monomethyl system. The stereochemical properties of 1,2-dimethylcyclohexane (**6**), which can exist as *cis*- and *trans*- diastereomers (*cis*-**6** and *trans*-**6**; Figure 2) can be exploited to explore the reversibility of the dehydration/hydration reactions. For one diastereomer to convert into the other, a common intermediate must be reached from both directions. In this section we show that the stereoisomers do indeed interconvert rapidly, and provide evidence that both a common transient intermediate *and* the alkene are involved in the interconversion reaction.

Hydrothermal reactions starting with either *cis*-**6** or *trans*-**6**, revealed a reaction that was considerably faster than starting with the monomethylalkane (**1**). At 300°C and 100 MPa in water, the alkane (**1**) exhibited only 0.6% conversion after 24 h, and only 0.8% conversion after 92 h (~4 days). The *cis*- and *trans*-dimethyl alkanes (*cis*-**6,** *trans*-**6**) exhibited 2.5% and 0.6% conversion, respectively, after 24 h, which increased to 3.1% and 1.1%, respectively, after 48 h (2 days). With two methyl substituents, the number of potential regioisomers of the alkene and alcohol functional groups that can form is much

larger, thus no attempt was made to identify every product peak observed in the gas chromatograms of the dimethyl structures. Instead, the products were divided into the groups summarized in Table 2. The major products of the reaction of both *cis*-**6** and *trans*-**6** are: the alternate alkane stereoisomer, small quantities of other alkane isomers, 1,2-dimethylcyclohexene (**7A**), dimethylcyclohexene isomers (**7B**□), several dimethylcyclohexanone isomers (**9**□, **R9**□), *o*-xylene (**11**) and small amounts of other xylene isomers (**11B**□; *m*-xylene and *p*-xylene are not separable under the GC conditions). After just one day the stereoisomer of the starting dimethylcycloalkane is among the major products, confirming facile interconversion between the *cis*- and *trans*-alkanes. However, the product distribution is time-dependent.

A partial mechanism for product formation from the dimethylcyclohexane system is shown in Figure 7. The mechanism is based on the one proposed for the monomethyl cyclohexane system. By analogy to the observed products in the monomethyl system, in particular the 5-membered rearranged products, we propose that the mechanism for formation of rearranged products in the dimethylcyclohexane system is via 1,2-alkyl shifts in carbon-centered cation intermediates (Figure 7). The alcohol (**8'**) and diene (**10**□) structures in Figure 7 are not actually detected by GC in the dimethylalkane experiments because longer reaction times were needed to increase conversions, therefore these highly reactive species are no longer present in detectable concentrations. This is analogous to the fact that diene and alcohol products were not detected in methylcyclohexane (**1**) experiments that were longer than 1 day.

Reactions starting with an alkene analogue, 1,2-dimethylcyclohexene (**7A**), were much faster, and exhibited 65.7% conversion after 3.5 h (0.15 days). The product

distribution was, not surprisingly, complex; major products identified include alkane, alkene, and ketone isomers, *o*-xylene and xylene isomers, in addition to other uncharacterized putatively dimeric structures. Importantly, *both* the *cis*- and *trans*-1,2-dimethylcyclohexane (*cis*-**6,** *trans*-**6**) were formed from the dimethylcyclohexene, along with other alkane isomers. This result confirms that the alkane and alkene are interconvertible, as observed in the monomethyl system. Significantly, both alkane stereoisomers appear to be formed simultaneously.

Compared to the hydration/dehydration reactions, the mechanisms of hydrogenation/dehydrogenation are not as well understood. The dimethylcyclohexane system offers some insight into possible mechanisms for the hydrogenation/dehydrogenation reactions. For the case of dehydrogenation of an alkane, we can consider three basic mechanism types: concerted removal of molecular hydrogen, stepwise removal of two hydrogen atoms, and stepwise removal of a proton and a hydride ion. Concerted removal of molecular hydrogen is unlikely because, in this case, microscopic reversibility would predict concerted addition of hydrogen to form the alkane from the alkene, and that process would favor one of the stereoisomers of dimethylcyclohexane (**6**). In fact, both stereoisomers are formed, with only a slightly higher abundance of the *trans*-isomer relative to the *cis*-isomer. The observed *cis*-to-*trans* ratio of 0.86 reflects the known thermodynamic stability of the *trans*- compared to the *cis*-isomer. Using thermodynamic data from Stull et al. (1969) the Gibbs energies of formation at 300°C for *trans*- and *cis*-dimethylcyclohexane were interpolated to be 245 kJ/mol and 250 kJ/mol, respectively. We conclude that removal of hydrogen from the

alkanes is therefore more likely to occur via a stepwise mechanism, as illustrated in Figure 8.

The common intermediate in the interconversion of the stereoisomers of the dimethylcyclohexane is indicated as **INT** in Figure 8. Carbon-hydrogen bond cleavage can occur homolytically to give a hydrogen atom and a carbon-centered radical, or heterolytically to give either a hydride and a carbon-centered cation, or a proton and a carbon-centered anion. The asterisks in Figure 8 denote the various possible atomic, radical or ionic intermediates. A stepwise heterolytic cleavage mechanism is unlikely since at one of the steps a hydride anion must be formed in the dehydrogenation reaction. Microscopic reversibility would then require that a hydride be added in one of the steps in the alkene hydrogenation reaction. Hydride would be extremely reactive in any aqueous environment and is thus unlikely to exist in a form or with a lifetime that could act as such a reagent. The more likely stepwise mechanism then is sequential liberation of a hydrogen atom with a carbon-centered radical as an intermediate. Generation of a free hydrogen atom at each step may not be necessary; for example, transfer of a hydrogen atom to another molecule capable of accepting it, perhaps an alkene, would allow carbon-hydrogen bond cleavage to occur together with formation of a new carbon-hydrogen bond. In the absence of hydrogen-atom transfer, the activation energy for the reaction is the carbon-hydrogen bond dissociation energy. Avoiding a free hydrogen atom by simultaneously forming another bond would also reduce the energetic demand on the reaction kinetics.

The *cis*-stereoisomer of the dimethylalkane (*cis*-**6**) reacts somewhat faster than the *trans*-isomer (*trans*-**6**). This difference can be understood within the context of Figure 8;

at the point of the intermediate (**INT**), addition of a hydrogen atom before the loss of a second hydrogen regenerates the starting alkane. Because the *trans*-isomer is favored thermodynamically over the *cis*-, a faster return to *trans*- from intermediate **INT** has the effect of apparently reducing the reactivity of the *trans*- and increasing the reactivity of the *cis*-isomer.

Time-series experiments were performed using both dimethylcyclohexane stereoisomers to gain an understanding of how product distributions changed through time (Figure 9). For both stereoisomers, the most abundant products at all times are the aromatic *o*-xylene (**11**), and the alkane stereoisomer (*cis*-**6** or *trans*-**6**). After short reaction times, the concentrations of the alkene and ketones are higher than they are after longer reaction times. Alcohols are involved in the interconversions of the ketones; however, they have comparatively short lifetimes (see previous section) and presumably quickly drop below detection. At the longer reaction times the ketones also drop below detection. After five days the primary products are *o*-xylene (**11**) and the alkane stereoisomer (*cis*-**6** or *trans*-**6**). Subsequent reaction appears to involve mainly interconversions between these functional groups. It should be noted that the system is sealed and the hydrogen concentration is not buffered, so liberated hydrogen atoms must increase in concentration presumably as hydrogen gas. In addition, in both experiments, the concentrations of the aromatic xylenes start to decrease slightly after steadily rising for the first 5-10 days. It is not clear what compounds are forming directly from the xylenes, but this result implies that formation of aromatic products may not be irreversible given a sufficient concentration of hydrogen in the mixture. In summary, as

in the monomethyl experiments, the concentrations of the various products respond quite rapidly to changes in the reaction environment.

Carbon-carbon bond cleavage

The appearance of products with rearranged carbon skeletons (Figs. 3 and 7) and minor products that have lost one carbon atom (Figure 3) provide evidence for carbon-carbon bond cleavage in these hydrothermal reactions. This is a necessary step for ketone-to-carboxylic acid reaction proposed by Seewald (2001; see Figure 1). However, carboxylic acids were never detected in any of our hydrothermal experiments. Instead, the only reactions observed for the ketones are formation/reformation of the alcohols, and dehydrogenation to form enones (Figure 3). The ability to extract and detect carboxylic acids by our analytical method was investigated using a cyclic carboxylic acid, benzoic acid, and a dicarboxylic acid, adipic acid, at concentrations of ~0.02 M (the average amount of mass missing based on mass balance calculations for the monomethyl system; Table 1). Benzoic acid was easily extracted and detected using the experimental analytical methods. Adipic acid is more water-soluble than benzoic acid and was not extracted/detected with our method. Heptanoic acid, a seven-carbon monocarboxylic acid, has aqueous solubility similar to that of benzoic acid and should be extracted and detected along with benzoic acid. Therefore long chain, or cyclic carboxylic acids would have been detected if formed at concentrations above our detection limits (<0.0004 M for benzoic acid). This suggests the sealed hydrothermal systems studied here do not achieve conditions that are sufficiently oxidizing to form detectable amounts of long chain or cyclic mono-carboxylic acids, at least for the reaction timescales studied here. Short

chain or dicarboxylic acids may have been formed and gone undetected, but given the high mass balances in the experiments and lack of evidence for broken ring structures missing multiple carbons, this seems unlikely. Seewald's experiments differed from these however, in that he used a mineral buffer to maintain hydrogen fugacity at a lower value than what is estimated to be present here. For example, Seewald's most reducing condition used a PPM mineral assemblage to maintain the H_2 concentration around 0.4 mmolal. As stated previously, if all of the estimated hydrogen atoms liberated (Table 1) were present as dissolved H_2 at the experimental conditions (near the critical point), then the concentrations fall between 1.6 and 7.0 mmolar for most experiments, (except for the alcohol experiment which is closer to 188 mmolar H_2). These concentrations are all higher than Seewald's H_2 concentration, and therefore his experimental conditions where carboxylic acid formation was observed were less reducing. Seewald stated that "these reactions may not be available in dry or mineral-free environments." This study shows that minerals are not necessary for the oxidation of alkanes to form ketones, although the conversions were small. The presence of minerals, and/or lower H_2 concentrations, may however, be necessary to promote the production of carboxylic acids.

The pH at experimental conditions was not measured in situ; however, using thermodynamic equilibrium calculations the pH can be estimated (Shock, 1995; Shock et al., 1989; 1997). The pH of neutral water at 300°C and 100 MPa was calculated to be 5.3. The organic compounds used should not affect pH, and the only potential products that would affect pH are undetectable amounts of carboxylic acids and CO_2. On average the experiments had about 10% missing mass; if all that mass was due to CO_2 the resulting pH is calculated to be 4.77. Similarly, if the missing mass was due entirely to carboxylic

acid products (benzoic acid was used for the calculations) the resulting pH would be 3.46. Therefore the lowest possible (i.e., worst case scenario) pH in the experiment would be 3.46, compared to a 5.3 neutrality. A lower pH could affect reaction rates for acid catalyzed reactions. However, we do not expect that CO_2 and carboxylic acids were formed to this extent.

Conclusions

The primary goal of this work was to obtain evidence for extended interconversion between the multiple functional groups presented in Figure 1 to provide support for this as a pathway for hydrothermal degradation of large organic structures. Evidence of this is clearly obtained from experiments in which detailed product analysis was performed starting at various points along the reaction pathway. Formation of all functional groups from alkanes to ketones is observed no matter what the starting point in the reaction scheme. Furthermore, the observation of multiple regio- and stereochemical isomers for all of the functional groups is consistent with multiple and rapid interconversions at each step, i.e., the reactions from one functional group to the next do not proceed in a purely linear fashion. These experiments provide the best experimental support to date for the extended reversible reaction scheme of Figure 1. The experimental results further suggest that we have explored large areas of the potential energy reaction surface, supporting the idea that the reaction product distribution may be controlled by thermodynamic rather than kinetic factors.

The observation of rearranged alkene and alkane products is entirely consistent with a cation intermediate in the alkene/alcohol interconversion, as is expected based on

evidence from prior literature. Water must be a solvent, a catalyst, and a reagent in at least some of the reactions. Water provides the acid catalyst and the reactant for hydration of the alkene, and it provides the catalyst and is the product of dehydration of the alcohol. The alkane/alkene and alcohol/ketone interconversions require addition and removal of hydrogen atoms, and the experiments do not provide direct evidence for or against water involvement in these reactions. The fact that conversion of the alkanes into alkenes proceeds faster than expected based on simple bond homolysis suggests a role for water in these reactions as well. The products that accumulate at longer reaction times are dehydrogenated aromatic systems, presumably with the formation of molecular hydrogen, suggesting that aromatization is thermodynamically favorable at the experimental temperatures and pressures.

Another goal of the present work was to obtain information on the relative rates of the reactions of the various functional groups. Under the experimental conditions the reactions proceeded with very different rates depending upon the starting functional group, yielding an overall reactivity order of: diene > alcohol > alkene > ketone > alkane > aromatic ring. This is the first time that such relative rate data has been obtained within a single reaction system. That dehydration is one of the fastest reactions points to the highly catalytic activity of hydronium ions under the experimental conditions.

Dehydration is an elimination reaction that is favored thermodynamically. Dehydrogenation to form the aromatic system represents an elimination that also appears to be favored thermodynamically. The high temperature apparently drives the reaction systems in the direction of elimination presumably because of the temperature dependence of the entropy contribution to the free energy. These observations may be

relevant to understanding the process responsible for maturation of organic material at high temperatures and pressures. For the cyclic structures studied here, the results indicate that aromatization processes compete with and connect to the other functional group interconversions, at least at the current experimental conditions. The fact that no carboxylic acids were detected under the present conditions and reaction timescales, suggests that carbon-carbon bond cleavage at the ketone functional group may be the rate determining step in the overall degradation process in natural systems. Alternatively, it might suggest other pathways for carboxylic acid formation (not included in Figure 1) may be the main routes that form carboxylic acids, which are known to accumulate in natural systems. One possibility is that carboxylic acids are formed in reactions that involve minerals as catalysts or reagents, and work is proceeding in our laboratory to explore this possibility. The fact that highly reactive species can be formed from simple alkanes, and that a wide range of functional groups can rapidly interconvert under laboratory hydrothermal conditions suggests these reactions may play an important role in generating the diversity of organic compounds known to exist in natural hydrothermal systems. This further implies that microbial ecosystems deep in Earth's crust or at seafloor hydrothermal vents may depend to some extent on organic molecules generated from thermodynamically controlled abiotic reactions.

Acknowledgements

We thank the members of the Hydrothermal Organic Geochemistry (HOG) group for lengthy discussions on this research. We also thank Zach Smith, Jesse Coe, Katie

Noonan, and Alex Hamilton for help in the laboratory and the rest of Carbon and Nitrogen Dynamics (CaNDy) Lab for edits and discussion on this manuscript. We also appreciate the help from Gordon Moore for lending his expertise in welding capsules, Loÿc Vanderkluysen for help formatting Figure 3, and Chris Glein for providing thermodynamic calculations. This work was funded by NSF grant 0826588.

References

Akiya N. and Savage P. E. (2001) Kinetics and mechanism of cyclohexanol dehydration in high-temperature water. *Ind. Eng. Chem. Res.* **40**, 1822-1831.

Antal, Jr., M. J., Carlsson M. and Xu X. (1998) Mechanism and kinetics of the acid-catalyzed dehydration of 1- and 2-propanol in hot compressed liquid water. *Ind. Eng. Chem. Res.* **37**, 3820-3829.

Crittendon R. C. and Parsons E. J. (1994) Transformations of cyclohexane derivatives in supercritical water. *Organometallics* **13**, 2587–2591.

D'Hondt S., Jørgensen B. B., Miller D. J., Batzke A., Blake R., Cragg B. A., Cypionka H., Dickens G. R., Ferdelman T., Hinrichs K.-U., Holm N. G., Mitterer R., Spivak A., Wang G., Bekins B., Engelen B., Ford K., Gettemy G., Rutherford W. D., Sass H., Skilbeck C. G., Aiello I. W., Guèrin G., House C. H., Inagaki F., Meister P., Naehr T., Niitsuma S., Parkes R. J., Schippers A., Smith D. C., Teske A., Wiegel J., Padilla C. N. and Acosta J. L. S. (2004) Distributions of microbial activities in deep subseafloor sediments. *Science* **306**, 2216-2221.

Friesen J. B. and Schretzman R. (2011) Dehydration of 2-methyl-1-cyclohexanol: new findings from a popular undergraduate laboratory experiment. *J. Chem. Educ.* **88**, 1141-1147.

Head I. M., Jones D. M. and Larter S. R. (2003) Biological activity in the deep subsurface and the origin of heavy oil. *Nature* **426**, 344-352.

Helgeson H. C., Knox A. M., Owens C. E. and Shock E. L. (1993) Petroleum, oil-field waters, and authigenic mineral assemblages: Are they in metastable equilibrium in hydrocarbon reservoirs. *Geochim. Cosmochim. Acta* **57**, 3295-3339.

Hinrichs K.-U., Hayes J. M., Bach W., Spivak A. I., Hmelo L. R., Holm N. G., Johnson C. G. and Sylva S. P. (2006) Biological formation of ethane and propane in the deep marine subsurface. *Proc. Natl. Acad. Sci. USA.* **103**, 14,684-14,689.

Baross J. A. and Hoffman S. E. (1985) Submarine hydrothermal vents and associated gradient environments as sites for the origin and evolution of life. *Origins Life Evol. B.* **15**, 327-345.

Horsfield B., Schenk H. J., Zink K., Ondrak R., Dieckmann V., Kallmeyer J., Mangelsdorf K., Primio R. D., Wilkes H., Parkes R. J., Fry J. and Cragg B. (2006) Living microbial ecosystems within the active zone of catagenesis: Implications for feeding the deep biosphere. *Earth Planet Sc. Lett.* **246 (**1–2), 55-69.

Jones D. M, Head I. M., Gray N. D., Adams J. J., Rwan A. K., Aitken C. M., Bennett B., Huang H., Brown A., Bowler B. F. J., Oldenburg T., Erdmann M. and Larter S. R. (2008) Crude-oil biodegradation via methanogenesis in subsurface petroleum reservoirs. *Nature* **451**, 176-180.

Katritzky A. R., Nichols D. A., Siskin M., Murugan R. and Balasubramanian M. (2001) Reactions in high-temperature aqueous media. *Chem. Rev.* **101**, 837-892.

Kuhlmann B., Arnett E. M. and Siskin M. (1994) Classical organic reactions in pure superheated water. *J. Org. Chem.* **59**, 3098-3102.

Larter S., Wilhelms A., Head I., Koopmans M., Aplin A., Primio R. D., Zwach C., Erdmann M. and Telnaes N. (2003) The controls on the composition of biodegraded oils in the deep subsurface- part 1: biodegradation rates in petroleum reservoirs. *Org. Geochem*. **34,** 601-613.

Martin W., Baross J., Kelley D. and Russell M. J. (2008) Hydrothermal vents and the origin of life. *Nat. Rev. Microbiol*. **6**, 805-814.

Mason O. U., Nakagawa T., Rosner M., Van Nostrand J. D., Zhou J., Maruyama A., Fisk M. R. and Giovannoni S. J. (2010) First investigation of the microbiology of the deepest layer of ocean crust. *PLoS ONE*. **5**, 1-11.

McCollom T. M. and Seewald J. S. (2007) Abiotic synthesis of organic compounds in deep-sea hydrothermal environments. *Chem. Rev.* **107**, 382-401.

Nisbet E. G. (1985) The geological setting of the earliest life forms. *J. Mol. Evol.* **21**, 289-298.

Savage P. E. (1999) Organic chemical reactions in supercritical water. *Chem. Rev*. **99**, 603-621.

Seewald J. S. (1994) Evidence for metastable equilibrium between hydrocarbons under hydrothermal conditions. *Nature* **370**, 285-287.

Seewald J. S. (2001) Aqueous geochemistry of low molecular weight hydrocarbons at elevated temperatures and pressures: Constraints from mineral buffered laboratory experiments. *Geochim. Cosmochim. Acta* **65**, 1641-1664.

Seewald J. S. (2003) Organic-inorganic interactions in petroleum-producing sedimentary basins. *Nature* **426**, 327-333.

Seewald J. S., Zolotov M. Y. and McCollom T. (2006) Experimental investigation of single carbon compounds under hydrothermal conditions. *Geochim. Cosmochim. Acta* **70**, 446-460.

Shock E. L. (1988) Organic acid metastability in sedimentary basins. *Geology* **16**, 886-890.

Shock E. L. (1989) Corrections to "Organic acid metastability in sedimentary basins." *Geology* **17**, 572-573.

Shock E. L. (1990) Geochemical constraints on the origin of organic compounds in hydrothermal systems. *Origins Life Evol. B.* **20**, 331-367.

Shock E. L. (1992) Chemical environments in submarine hydrothermal systems. In *Marine Hydrothermal Systems and the Origin of Life* (ed. N. Holm). *Origins Life Evol. B.* **22**, 67-107.

Shock E. L. (1994) Application of thermodynamic calculations to geochemical processes involving organic acids. In *The Role of Organic Acids in Geological Processes* (eds. M. Lewan and E. Pittman). Springer-Verlag. pp. 270-318.

Shock E. L. (1995) Organic-acids in hydrothermal solutions - standard molal thermodynamic properties of carboxylic-acids and estimates of dissociation-constants at high-temperatures and pressures. *Am. J. Sci*. **295**, 496-580.

Shock E. L. (1996) Hydrothermal systems as environments for the emergence of life. In *Evolution of Hydrothermal Ecosystems on Earth (and Mars?)*. Wiley, Chichester (Ciba Foundation Symposium 202). pp. 40-60.

Shock E. L. and Canovas P. C. (2010) The potential for abiotic organic synthesis and biosynthesis at seafloor hydrothermal systems. *Geofluids* **10**, 161-192.

Shock E. L. and Schulte M. D. (1998) Organic synthesis during fluid mixing in hydrothermal systems. *Jour. Geophys. Res.* **103**, 28513-28527.

Shock E. L., Helgeson H. C. and Sverjensky D. A. (1989) Calculation of the thermodynamic and transport-properties of aqueous species at high-pressures and temperatures: Standard partial molal properties of inorganic neutral species. *Geochim. Cosmochim. Acta* **53**, 2157-2183.

Shock E. L., McCollom T. and Schulte M. D. (1995) Geochemical constraints on chemolithoautotrophic reactions in hydrothermal systems. *Origins Life Evol. B.* **25**, 141-159.

Shock E. L., McCollom T. and Schulte M. D. (1998) The emergence of metabolism from within hydrothermal systems. In *Thermophiles: the keys to molecular evolution and the origin of life?* (eds. Wiegel and Adams). Taylor & Francis, London. pp. 59-76.

Shock E. L., Amend J. P. and Zolotov M. Y. (2000) The early Earth vs. the origin of life. In *The Origin of the Earth and Moon* (eds. R. Canup and K. Righter) University of Arizona Press. pp. 527-543.

Shock E. L., Sassani D. C., Willis M., and Sverjensky D. A. (1997) Inorganic species in geologic fluids: Correlations among standard molal thermodynamic properties of aqueous ions and hydroxide complexes. *Geochim. Cosmochim. Acta* **61**, 907-950.

Siskin M. and Katritzky A. R. (2001) Reactivity of organic comounds in superheated water: general background. *Chem Rev*. **101**, 825-835.

Stull D. R., Westrum E. F. and Sinke G. C. (1969) *The Chemical Thermodynamics of Organic Compounds*. John Wiley & Sons, Inc., New York. pp. 358-359.

Watanabe M., Sato T., Inomata H., Smith, Jr., R. L., Arai K., Kruse A. and Dinjus E. (2004) Chemical reactions of C_1 compounds in near-critical and supercritical water. *Chem Rev.***104**, 5803-5821.

Williams L. B., Holloway J. R., Canfield B., Glein C., Dick J., Hartnett H. and Shock E. (2011) Birth of biomolecules from the warm wet sheets of clays near spreading centers. In *Earliest Life on Earth: Habitats, Environments and Methods of Detection* (eds. Golding S. and Glikson M.). Springer Publishing. Chapter 4. pp. 79-112.

Windman T., Zolotova N., Schwandner F. and Shock E. (2007) Formate as an energy source for microbial metabolism in chemosynthetic zones of hydrothermal ecosystems. *Astrobiology* **7**, 873-890.

Xu X. and Antal, Jr., M. J. (1994) Kinetics and mechanism of isobutene formation from t-butanol in hot liquid water. *AIChE J.* **40**, 1524-1534.

Xu X., Antal, Jr., M. J. and Anderson D. G. M. (1997) Mechanism and temperature-dependant kinetics of the dehydration of tert-butyl alcohol in hot compressed liquid water. *Ind. Eng. Chem. Res.* **36**, 23-41.

Table 1. Product distributions for experiments with monomethylcyclohexane-based functional groups.

			Starting Structure							
			alkane (**1**)	alkane (**1**)	alkene (**2A**)	alcohol (**3A+3B**)	ketone (**4A**)	ketone (**4A**)	diene (**2C**)	toluene (**2E**)
experiment duration (h)			23.6	92.3	3.5	5.4	5.5	20	5.4	144
µmoles of starting material			60.3	60.3	49.7	49.7	50.3	50.3	49.8	49.6
% mass balance			89.7	70.5	85.2	103	92.9	94	83.8	85.4
% reacted			0.6	0.8	76.4	95.4	3.1	6.8	100	0.4
Products[a]			**% in final reaction mixture**							
alkanes	dimethylcyclopentane	**R1A'**[b]	0	0	0.23	0	0.02	0.04	0	0
	dimethylcyclopentane	**R1A'**	0	0	0.12	0	0	0	0	0
	dimethylcyclopentane	**R1A'**	0	0	0.14	0	0	0	0	0
	1-methylcyclohexane	**1**	**99.43**[c]	**99.21**	11.57	1.27	0	0.20	5.29	0
	ethylcyclopentane	**R1B**	0	0	1.15	0.06	0	0.01	0.02	0
alkenes	dimethylcyclopentene	**R2A'**	0	0	<0.01	0	0	0	0	0
	methylcyclopentene	**C2A**	0	0	0.11	0	0.28	0.43	0	0
	dimethylcyclopentene	**R2A'**	0	0	0.39	0.05	0	0	0.02	0
	dimethylcyclopentene	**R2A'**	0	0	2.19	0.29	0	<0.01	<0.01	0
	dimethylcyclopentene	**R2A'**	0	0	2.29	0.35	0	<0.01	<0.01	0
	dimethylcyclopentene	**R2A'**	0	0	2.23	0.45	0	<0.01	<0.01	0
	ethylcyclopentene	**R2B'**	0	0	0	1.04	0	0	0	0
	methylcyclohexene	**2B'**	<0.01	<0.01	11.74	21.64	0.12	0.65	9.14	0
	methylcyclohexene	**2B'**	0	0	0.72	1.86	0	<0.01	0.83	0
	dimethylcyclopentene	**R2A'**	<0.01	<0.01	8.67	1.32	<0.01	0.09	0.09	0
	ethylcyclopentene	**R2B'**	<0.01	<0.01	5.78	6.68	<0.01	0.21	0.60	0
	1-methylcyclohexene	**2A**	0.07	0.10	**25.39**	46.90	0.30	1.37	21.30	0
	ethylcyclopentene	**R2B'**	0	0	0.99	1.33	0	<0.01	0.07	0
	methylcyclohexene	**2B'**	0	0	0	<0.01	0	0	0	0
	dimethylcyclohexene	**R2A'**	0	0	0	<0.01	0	0	<0.01	0
alcohols	methylcyclopentanol	**C3A**	0	0	0	0	0.17	0.14	0	0
	1-methylcyclohexanol	**3C**	0	0	3.41	4.14	0.37	0.62	1.72	0

Table 1(cont.)

Products[a]			% in final reaction mixture (cont.) alkane (**1**)	alkane (**1**)	alkene (**2A**)	alcohol (**3A+3B**)	ketone (**4A**)	ketone (**4A**)	diene (**2C**)	toluene (**2E**)
	ethylcyclohexanol	**C3B**	0	0	0.19	0.27	0	0	0.03	0
	cis-2-methylcyclohexanol	**3A**	0	0	0.63	**1.24**	0	0	0.47	0
	methylcyclohexanol	**3D'**	0	0	0	0.19	0	0	0.05	0
	trans-2-methylcyclohexanol	**3B**	0	0	1.66	**3.35**	0	0	1.33	0
	methylcyclohexanol	**3D'**	0	0	0	0	0	0.01	0.18	0
ketones	dimethylcyclopentanone	**R4'**	0	0	0.11	<0.01	0.03	0.08	0	0
	2-methylcyclohexanone	**4A**	0.30	0.31	4.39	5.60	**96.93**	**93.25**	1.02	0
	3-methylcyclohexanone	**4C**	0.14	0.10	0.73	0.76	0	0	0.29	0
	dimethylcyclopentanone	**R4'**	0	0	<0.01	0.15	<0.01	0	0	0
	4-methylcyclohexanone	**4B**	<0.01	0	<0.01	<0.01	0	0	<0.01	0
enones	methylcyclohexenone	**5'**	<0.01	<0.01	<0.01	<0.01	0.16	0.18	0	0
	methylcyclohexenone	**5'**	<0.01	<0.01	0.92	<0.01	0.96	1.16	0	0
	methylcyclohexenone	**5'**	0	0	1.50	0	<0.01	<0.01	<0.01	0
dienes	methylcyclohexadiene	**2D**	0	0	0	<0.01	0.01	0	0.01	0
	1-methyl-1,4-cyclohexadiene	**2C**	0	0	0	<0.01	0.02	0	**0**	0
aromatics	benzene	**C2C**	0	0	0	0	0	0	0	0.17
	toluene	**2E**	0.06	0.28	5.09	0.13	0.41	1.40	49.20	**99.70**
	m/*p*-xylene	**C2D**	0	0	0	0	0.17	0.17	0	0
dimers	dimers	**D1**	0	0	6.89	0.93	0.07	0	7.11	0.12
	dimers2	**D2**	0	0	0.77	0	0	0	1.24	0
	hydrogen atoms liberated (μmol)		0.8	1.1	ND[d]	91 – 97	1.7 – 2.1	3.5	ND	ND
	H atoms normalized to 100% conversion (μmol)		140	140	ND	95 – 102	55 – 68	52	ND	ND

[a]Every product from each experiment is included in the table.
[b]**Bold symbols** refer to chemical structures illustrated in Figure 3.
[c]**Bold numbers** indicate % remaining starting material.
[d]ND- not determined due to large dimer production

Table 2. Quantified products from experiments with dimethylcyclohexane-based functional groups.

Reactant	Experimental Conditions: time (d)	initial μmoles	% MB[b]	% reacted	Products (μmoles)[a]: *trans* alkane	*cis* alkane	alkane isomers	1,2-alkene	alkene isomers	*o*-xylene	xylene isomers	ketone isomers	toluene
cis-1,2-dimethylcyclohexane (*cis*-**6**)	1	61.0	94 (2)[e]	2.5	0.76 (0.02)	**55.9**[c] **(0.9)**	0.055 (0.006)	0.009 (0.002)	0.17 (0.02)	0.264 (0.002)	0.199 (0.002)	trace	nd[d]
	2	61.0	83.8 (0.5)	3.1	0.827 (0.004)	**49.6 (0.3)**	0.056 (0.003)	0.021 (0.001)	0.11 (0.03)	0.46 (0.01)	0.103 (0.002)	trace	nd
	6	61.0	86.5 (0.3)	4.5	1.164 (0.007)	**50.4 (0.2)**	0.165 (0.002)	0.0168 (0.0009)	0.241 (0.006)	0.640 (0.001)	0.151 (0.003)	nd	trace
	16	61.0	84 (2)	4.6	1.35 (0.03)	**49.1 (0.9)**	0.194 (0.006)	0.013 (0.002)	0.282 (0.008)	0.441 (0.005)	0.110 (0.002)	nd	trace
trans-1,2-dimethycyclohexane (*trans*-**6**)	1	60.0	96.5 (0.2)	0.6	**57.6 (0.1)**	0.0883 (0.0005)	trace	0.040 (0.001)	0.091 (0.009)	0.08 0.01)	trace	0.04 (0.03)	nd
	2	60.0	97.0 (0.5)	1.1	**57.6 (0.3)**	0.093 (0.008)	0.02 (0.01)	0.053 (0.004)	0.16 (0.01)	0.272 (0.006)	0.046 (0.002)	trace	nd
	10	60.0	99.9 (0.2)	1.8	**58.84 (0.09)**	0.22 (0.02)	0.152 (0.005)	0.010 (0.002)	0.096 (0.008)	0.450 (0.004)	0.152 (0.002)	nd	trace
	19	60.0	96.4 (0.8)	1.9	**56.8) (0.5)**	0.237 (0.004)	0.180 (0.006)	0.007 (0.004)	0.13 (0.01)	0.395 (0.008)	0.134 (0.005)	nd	trace
	24	60.0	99.0 (0.5)	2.0	**58.2 (0.3)**	0.327 (0.004)	0.213 (0.009)	0.007 (0.002)	0.160 (0.002)	0.351 (0.002)	0.147 (0.002)	nd	trace
1,2-dimethylcyclohexene (**7A**)	0.15	49.9	86.8[f] (0.4)	65.7	2.66 (0.02)	2.30 (0.02)	*1.55*[g] (*0.06*)	**14.92 (0.09)**	*15.7* (*0.1*)	4.42 (0.03)	0.076 (0.002)	*1.81* (*0.01*)	trace
o-xylene (**11**)	10	63.5	91.6 (0.2)	0.4	nd	nd	nd	nd	nd	**57.9 (0.1)**	0.051 (0.001)	nd	0.203 (0.002)
	21	63.5	89.5 (0.2)	0.6	nd	nd	nd	nd	nd	**56.6 (0.1)**	0.045 (0.004)	nd	0.275 (0.006)
	37	63.5	93.3 (0.2)	0.7	nd	nd	nd	nd	nd	**58.8 (0.1)**	0.063 (0.002)	nd	0.363 (0.004)

[a]Dimers were not quantified. [b]MB- mass balance [c]**Bold**- remaining amount of starting material [d]nd- not detected [e]numbers in parentheses are the analytical error (μmols) in the number above them. [f]The alkene generated a significant number of unquantifiable isomer peaks [g]*italic*- semi-quantitative due to possible unidentified isomers

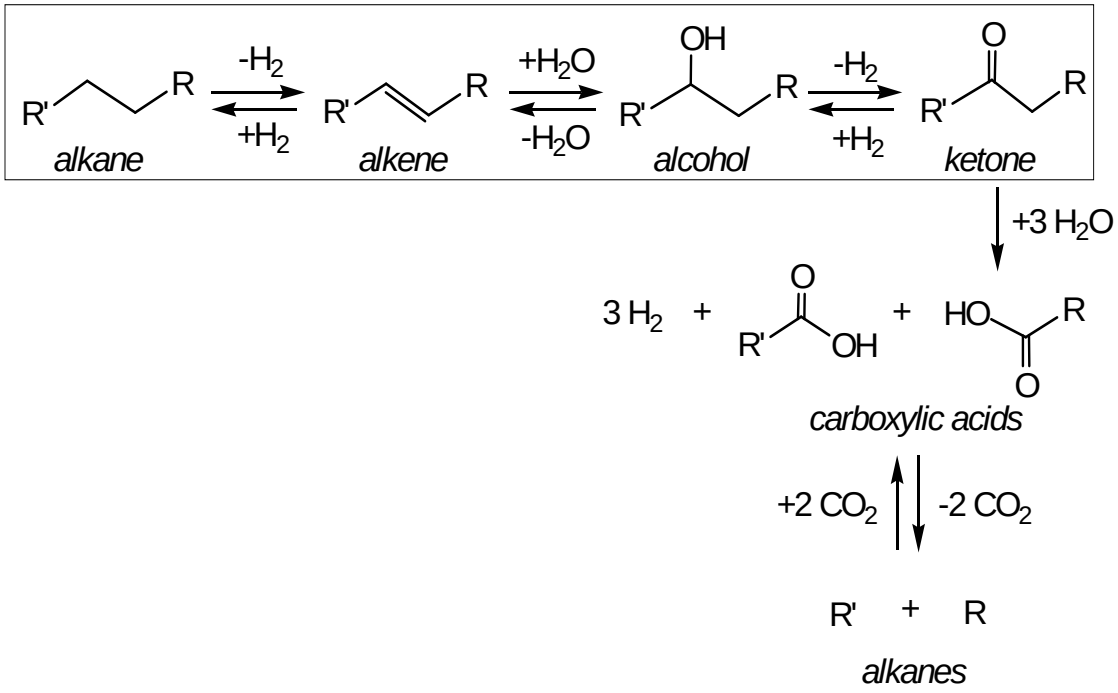

Figure 1. Schematic illustration of functional group interconversions (horizontal arrows), and carbon-carbon bond cleavage reactions (vertical arrows) that convert larger alkanes into smaller alkane fragments. The functional group interconversions consist of oxidation/reduction and hydration/dehydration reactions. The part of the reaction scheme that is contained in the box, from alkanes to ketones, is the focus of the present work.

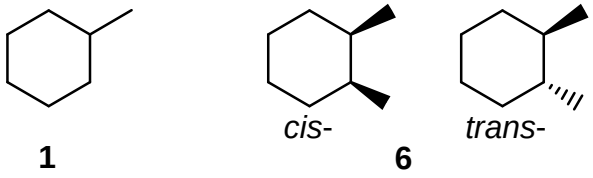

1 **6**

Figure 2**.** Model cyclic alkanes used throughout the study: methylcyclohexane (**1**) and *cis*- and *trans*-1,2-dimethylcyclohexane (**6**). Various functional groups were added to these basic structures to investigate interconversion reactions.

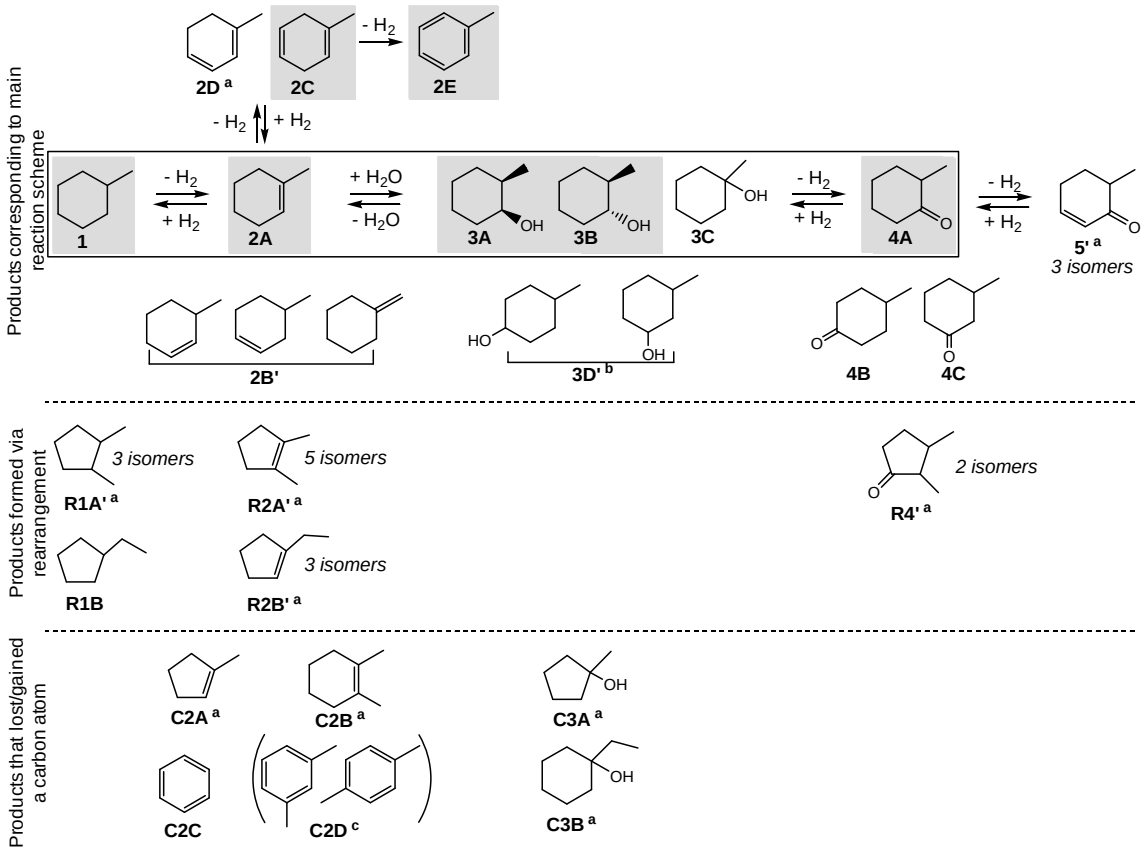

Figure 3. Summary of the products of the hydrothermal reactions starting from any of the structures highlighted in grey. The structures in the box correspond to the reaction scheme from alkane (structure 1) to alkenes (structures numbered 2) to alcohols (structures numbered 3) to ketones (structures numbered 4) shown in Figure 1. Structures designated with " ' " represent more than one structural isomer. Products formed via rearrangement carry the designation "R". Minor products that lost or gained a carbon atom are designated "C". Not shown are uncharacterized dimeric structures that are formed in some reactions in small yields. [a] The actual structure was not characterized and may be an isomer of the one shown. [b] *Cis* and *trans* stereoisomers of these alcohols may also have been formed that are not separable under the analytical conditions. [c] *m*-Xylene and *p*-xylene are not separable under the GC conditions, either or both may be formed. Note dimer structures (**D1**, **D2**) are not included.

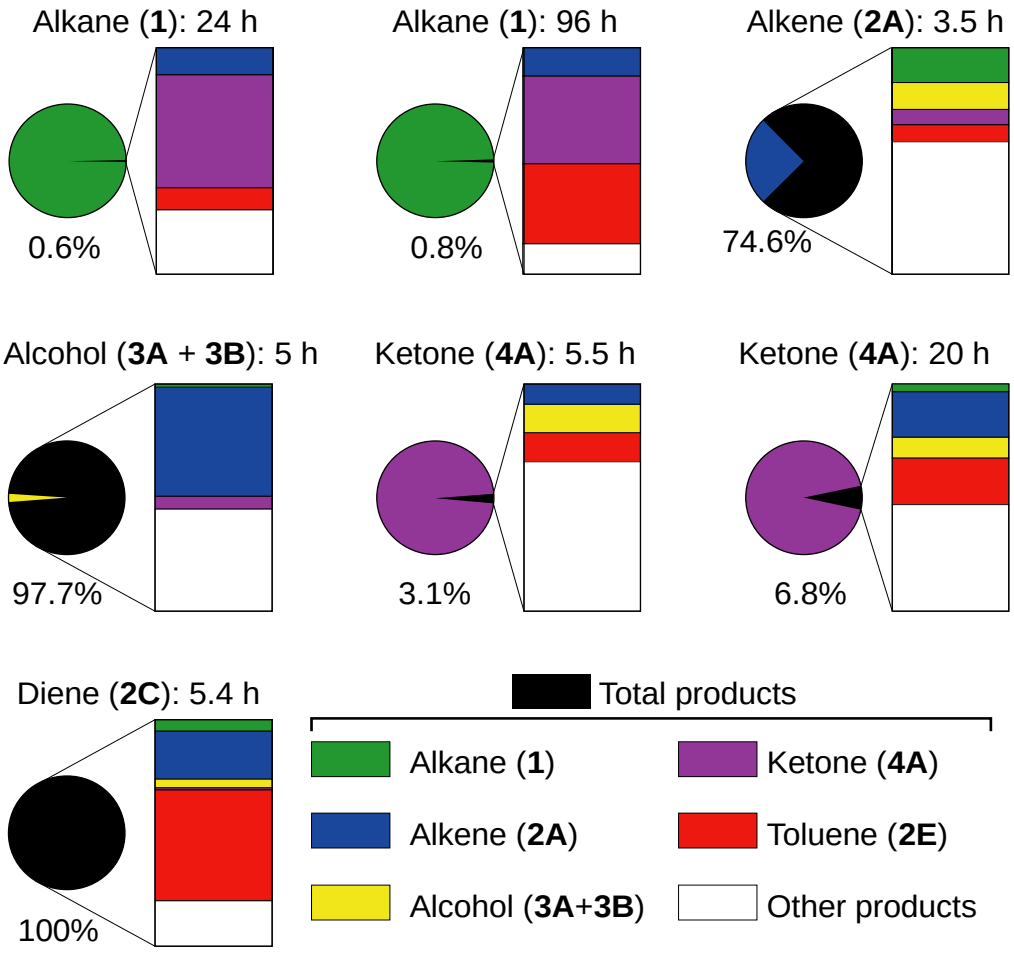

Figure 4. Pie charts show percent conversion for seven individual experiments with various starting materials; the black slice represents total products formed. Bars illustrate the relative distribution of primary reaction products that comprise the total products. The bar segment representing “other products” is the sum of products that are not part of the primary reaction scheme.

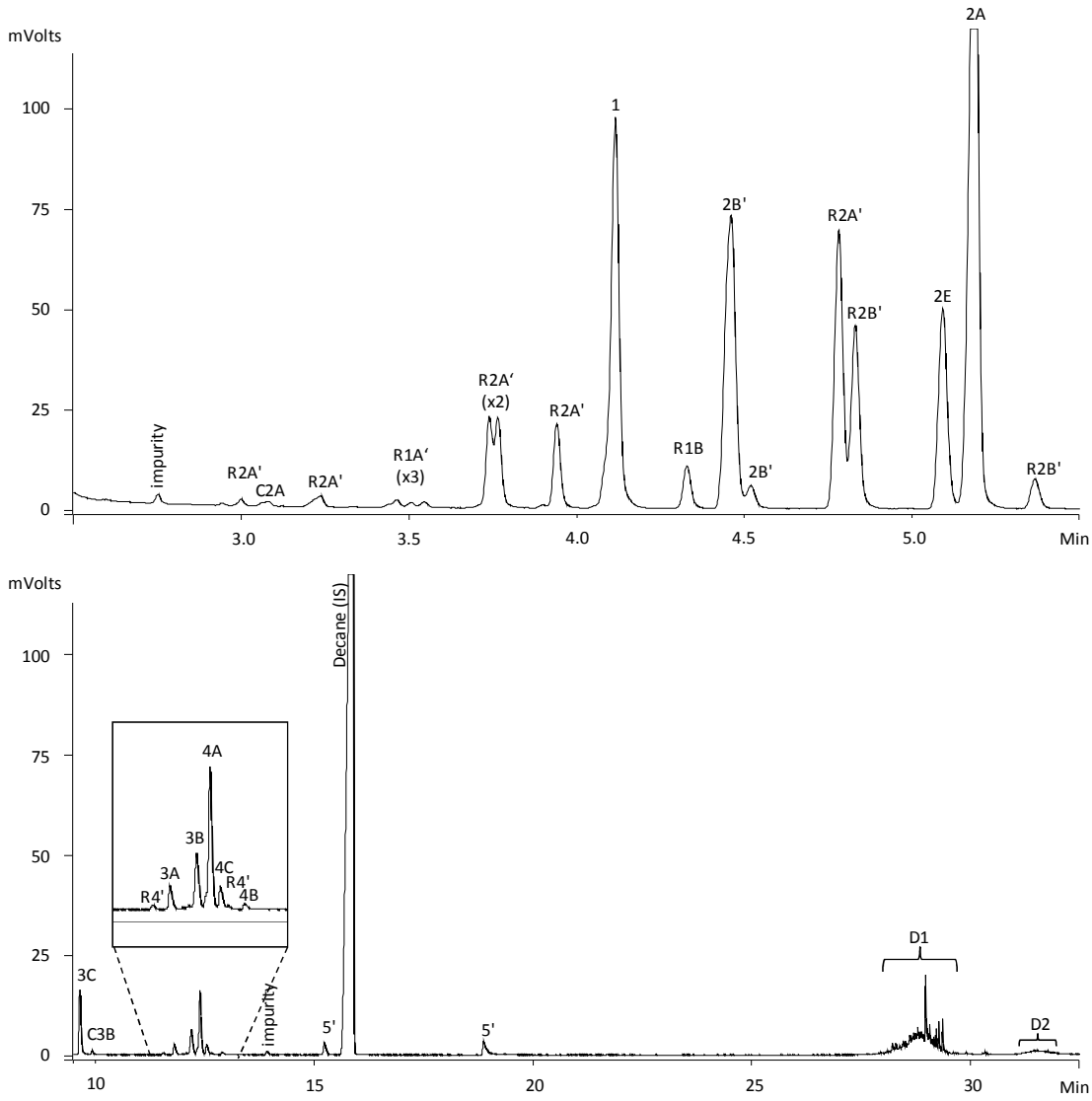

Figure 5. Chromatogram of products formed from 1-methylcyclohexene (**2A**) reacted at 300°C and 100 MPa for 3.5 hours. Top panel is retention times from 2.5 to 5.5 min, bottom panel is retention times from 9.5 to 32.5 min, both on the same vertical scale (-1 to 120 mV). No products were observed between 5.5 and 9.5 min. "Impurity" represents an impurity in the DCM or decane (used as an internal standard; IS). Peak labels are defined in Table 1 and structures are shown in Figure 3.

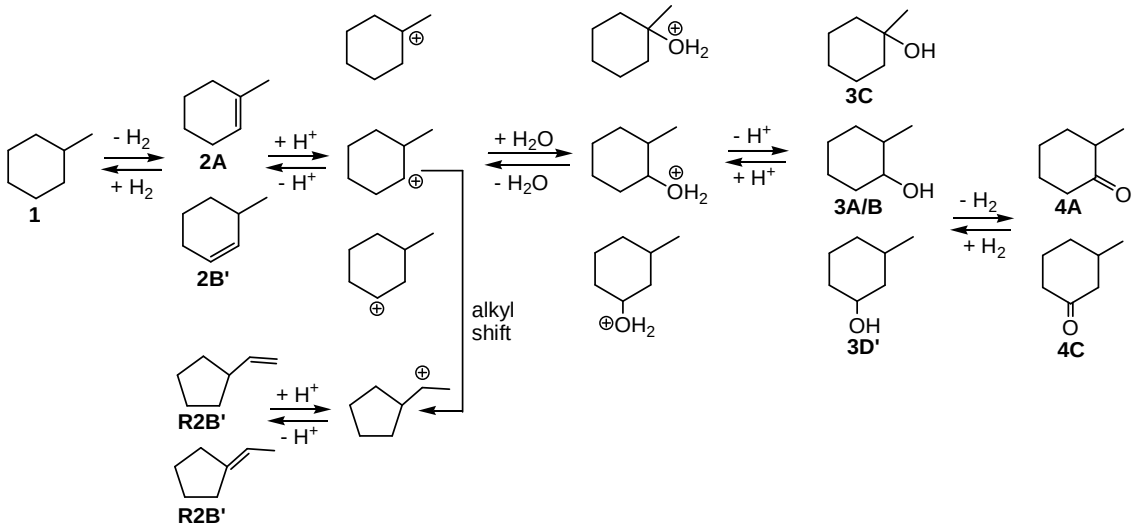

Figure 6. Partial mechanism for reversible interconversion of alkene, alcohol and ketone functional groups. Formation of all of the observed isomers for each functional group is not shown, and stereochemistry is ignored.

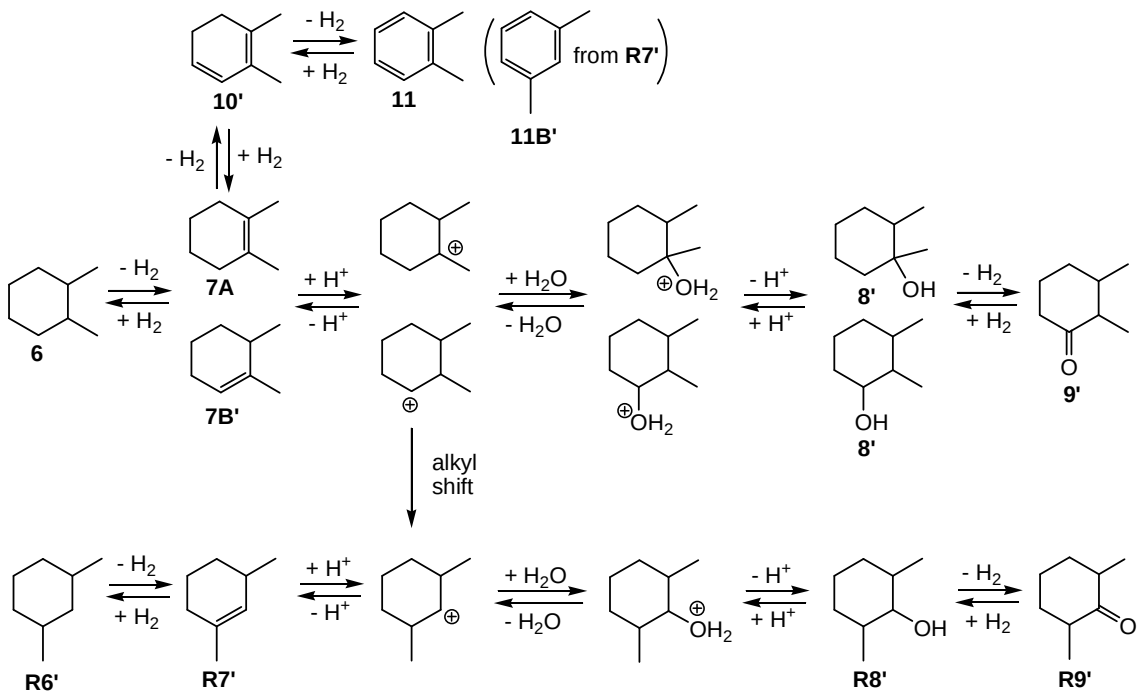

Figure 7. Partial summary of products and a partial proposed mechanism for hydrothermal reaction starting with *cis*- or *trans*-1,2-dimethylcyclohexane (**6**) or 1,2-dimethylcyclohexenes (**7**). The overall pathway links alkane and ketone functional groups according to the scheme in Figure 1. Structures designated with " ' " represent more than one structural and/or stereoisomer, the actual isomers were not characterized. Products formed via rearrangement carry the designation "R". Uncharacterized dimeric structures formed in small yields when starting with the alkene (**7A**) and xylene (**11**) are not shown. Rearranged xylene isomers (**11B'**) are presumably formed from rearranged alkenes (**R7'**).

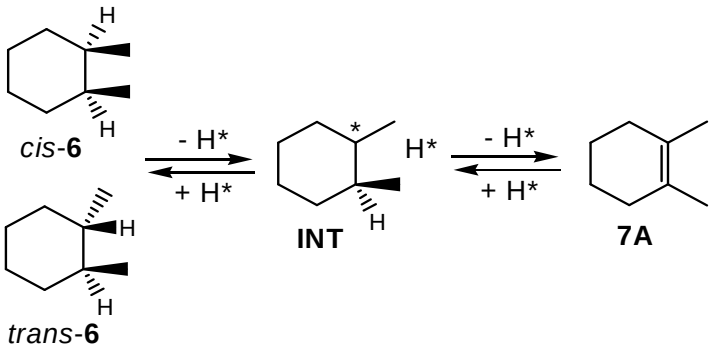

Figure 8. Proposed mechanism for the step-wise dehydrogenation of 1,2-dimethylcyclohexane (**6**) and hydrogenation of 1,2-dimethylcyclohexene (**7A**) under hydrothermal conditions. The star represents either the unpaired electron of a cation site or an anion site on the intermediate (**INT**).

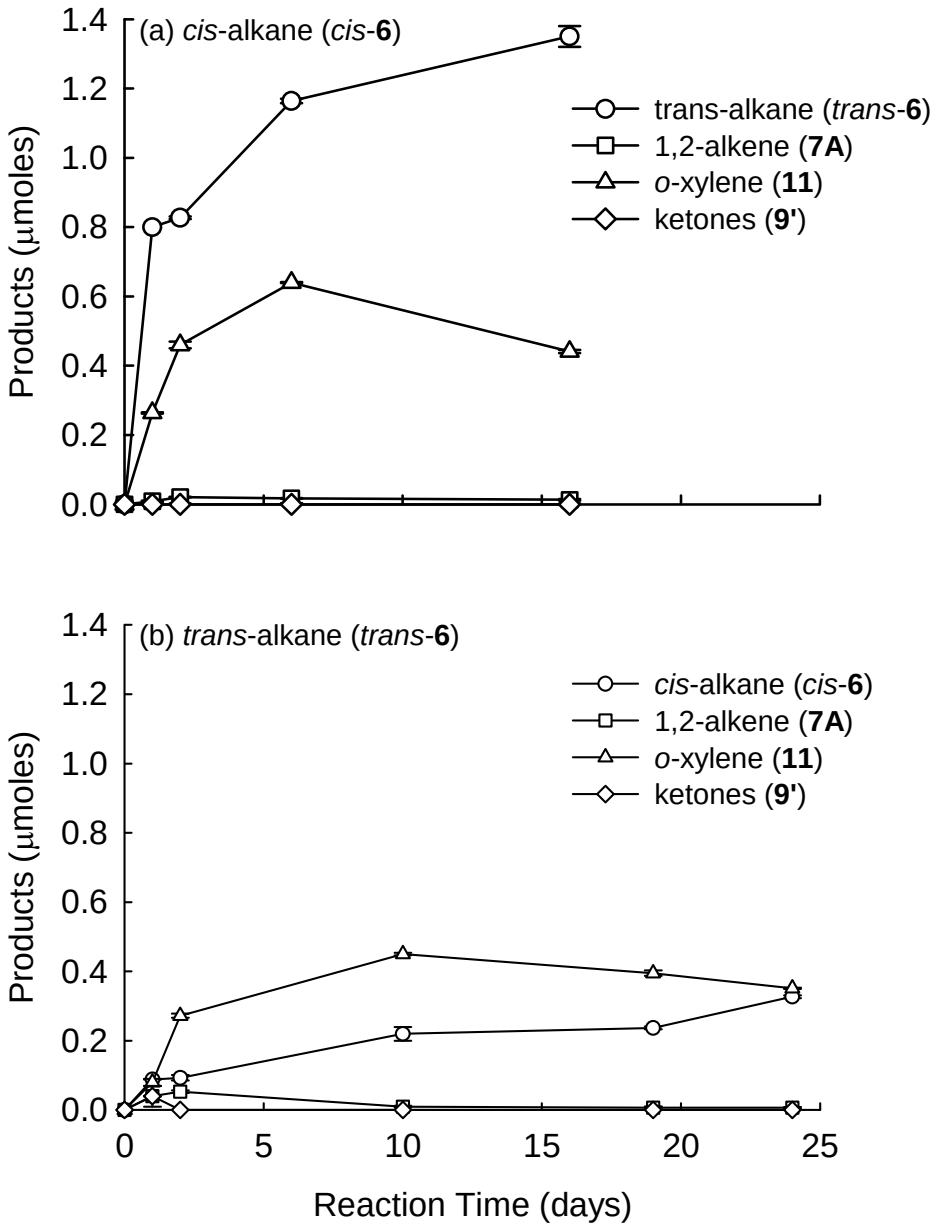

Figure 9. The amounts of products formed from hydrothermal reactions using two different alkane sterioisomers as the starting reactant: (a) *cis*-1,2-dimethylcyclohexane (*cis*-**6**) and (b) *trans*-1,2-dimethylcyclohexane (*trans*-**6**). Each point represents an individual capsule experiment (300°C and 100 MPa in H_2O) of a given duration.

Chapter 3

THE EFFECTS OF MINERALS ON ORGANIC FUNCTIONAL GROUP TRANSFORMATIONS IN HYDROTHERMAL SYSTEMS

Abstract

Hydrothermal environments in deep sedimentary systems are composed of three major constituents: hot pressurized water, organic material, and inorganic minerals or clays. There have been studies of the reactivity of organic compounds in high pressure, high temperature water, but few have investigated how the inorganic mineral phase affects organic reactions under these conditions. This study takes the complex environmental matrix of mineral assemblages and bulk organic material and simplifies it, to systematically study the effects of pyrite (FeS_2), pyrrhotite ($Fe_{1-x}S$), magnetite (Fe_3O_4) and hematite (Fe_2O_3) on an alkane, *trans*-1,2-dimethylcyclohexane, and a ketone, 2-methylcyclohexanone, in water at 300°C and 100 MPa.

Without minerals, alkane and ketone functional groups can reversibly interconvert at these conditions through alkene and alcohol structures via reduction/oxidation and hydration/dehydration reactions. The work presented here describes how the addition of minerals can shift these reactions to selectively enhance or inhibit the formation of specific products and, sometimes, dramatically affect the amount of reactant conversion. The oxide and sulfide minerals had different effects; for example, when pyrite and troilite (FeS; used as a pyrrhotite analogue) were added to the reaction the dehydration reaction rates were enhanced; in contrast, hydration reactions, were enhanced by hematite and magnetite.

I observed redox effects and correlations between the amount of available mineral surface and the amount of specific products formed. With pyrite, the alkane reactant formed the oxidized product xylene, whereas with FeS it did not. In reactions starting with the ketone reactant, FeS enhanced formation of the reduced alkane and alkene products, whereas pyrite again favored more oxidized products, i.e., toluene and eneones. For experiments with FeS, varying amounts of surface area had no effect on the extent of conversion, or the product distributions observed. This suggests the FeS mineral effects were a result of solution-phase reactions, likely caused by mineral-dissolution driven H_2 and H_2S concentrations. Conversely, hematite and, especially, pyrite reactions had marked correlations between surface area and reactions involving the breaking and reforming of C-H bonds. This observation suggests the reaction rate enhancement from these minerals may be due to surface interactions catalyzing C-H bond cleavage. I conclude that minerals in hydrothermal systems have significant and varied effects on organic functional group reactivity. The minerals used here are found in many natural environments and likely influence the distribution of organic molecules present in those environments through both surface interactions and mineral-driven solution phase chemistry.

Introduction

Hydrothermal reactions of organic compounds play an important role in many geochemically relevant systems. Examples include: the formation, degradation, and therefore composition, of oil and petroleum deposits (Head et al., 2003; Jones et al., 2008; Kvenvolden et al., 1990; Kvenvolden et al., 1994; Seewald, 2003), the chemical

transformations associated with submarine hydrothermal vents (Simoneit, 1993; Tivey, 1995), and the metabolic pathways of subsurface microbes (Horsfield et al., 2006; Mason et al., 2010; Oldenburg et al., 2006; Simoneit, 2003; Windman et al., 2007). Many studies of hydrothermal reactions of organic compounds have now been reported (Akiya and Savage, 2002; Katritzky et al., 2001; Savage, 1999; Shipp et al., 2013; Siskin and Katritzky, 2001; Watanabe et al., 2004; Yang et al., 2012) and some general principles are starting to emerge. For example, organic reactions under these conditions can be quite different from corresponding reactions under ambient conditions. One reason for this is the increased importance of thermodynamic rather than kinetic control, as evidenced by the fact that hydrothermal organic reactions are shown to be highly reversible (Reeves et al., 2012; Seewald, 1994; Shipp et al., 2013; Shock, 1993). Although there have now been many reported studies of the hydrothermal chemistry of a wide range of organic functional groups (Akiya and Savage, 2001; Katritzky et al., 2001; McCollom et al., 2001; McCollom et al., 1999; Reeves et al., 2012; Savage, 1999; Shipp et al., 2013; Watanabe et al., 2004; Yang et al., 2012), only a few of these have included the inorganic components relevant for geochemical systems, such as clays and other minerals (Bebie and Schoonen, 2000; Bell et al., 1994; Breier et al., 2012; Cody et al., 2004; McCollom et al., 1999; Seewald, 2001; Williams et al., 2005; Williams et al., 2011).

The role of inorganic solids such as minerals in hydrothermal organic reactions has gained attention within the last decade, with some dramatic effects observed when minerals were incorporated into experimental studies (Foustoukos and Seyfried, 2004; Fu et al., 2008; Schreiner et al., 2011; Shipp et al., submitted). Mineral assemblages are sometimes used as redox (H_2/O_2) buffers during studies of hydrothermal organic

reactions (Andersson and Holm, 2000; Seewald, 1994; Seewald, 2001). However, studies that focus on specific mineral effects and how minerals influence the reactivity of specific organic functional groups (beyond controlling solution redox conditions) are essentially absent from the geochemical literature. Understanding the ways in which minerals control organic reactivity is important since minerals have been proposed to act as early life catalysts (Cody, 2004; Cody et al., 2000; Ferris, 2005; Lahav, 1994; Martin et al., 2008; Mulkidjanian, 2009; Russell et al., 1993; Wang et al., 2012; Wang et al., 2011) and as templates for organic synthesis reactions (Fu et al., 2008; Holm and Andersson, 2005; Schoonen et al., 2004; Williams et al., 2005; Williams et al., 2011). Perhaps more importantly, determining how minerals control the mechanisms of organic reactions is critical if we are to establish guiding principles on which to build predictive models of organic reactivity in geochemical systems. The goal of the present work is to study the effects specific minerals have on the hydrothermal chemistry of organic functional groups, and whether these effects can be rationalized in terms of properties of the minerals that are independently understood.

An important class of inorganic materials commonly found in natural hydrothermal systems is the iron-bearing oxide and sulfide minerals. Examples include magnetite, Fe_3O_4, hematite, Fe_2O_3, pyrite, FeS_2, and pyrrhotite, $Fe_{1-x}S$. These are among the most abundant minerals in deep sedimentary systems (Simoneit, 1993; Vaughan and Lennie, 1991). But, more importantly for the present work, these minerals are related to each other via redox equilibria involving water, H_2, and H_2S. In the presence of water these four minerals occupy adjacent stability fields in a Fe-S-O-H stability diagram and are dependent only on the H_2 and H_2S fugacity, Figure 10. At equilibrium in an aqueous

system, the distribution of iron minerals (e.g., magnetite, hematite, pyrite, and pyrrhotite) will be determined by the solution phase activities of H_2 and/or H_2S (when these are in excess). Alternatively, when the minerals are in excess they can be used to alter the aqueous concentrations of H_2 and/or H_2S. As mentioned above, mineral assemblages have been used to buffer the concentrations of H_2 and H_2S in previous studies of hydrothermal reactions. In this way minerals can control how reducing or oxidizing the hydrothermal environment is, and thus, potentially control the organic reactions occurring under these conditions.

In water at elevated temperatures and pressure, simple alkanes undergo a series of interconnected reactions that give a range of products containing functional groups including alkenes, alcohols, ketones and aromatic structures. Shipp et al. (2013) recently reported on the reactivity of 1,2-dimethylcyclohexane under hydrothermal conditions (300°C and 100 MPa), and observed oxidation via hydrogen loss to form alkenes and aromatic xylenes, as well as oxidation to form cyclic ketones through a combination of dehydrogenation and hydration reactions. The reaction steps are illustrated in Figure 11. The reactions along horizontal arrows represent oxidation (hydrogen removal, to the left) and reduction (hydrogen addition, to the right) reactions. The reactions along vertical arrows represent hydration (addition of water, going up) and dehydration (loss of water, going down). An important feature to note is that these reactions are all reversible under hydrothermal conditions. For example, starting with a ketone, the products formed include alkenes, xylenes, and some alkane. Further evidence of reversibility is obtained from stereochemical studies. Specifically, when starting with the *trans*-isomer of 1,2-dimethylcyclohexane, the *cis*-stereoisomer of the starting structure is formed in addition

to the alkene, xylene, and ketone products. The alkane stereoisomer acts as a stereochemical probe for reaction reversibility, and also as a probe for the most elementary reaction step, cleavage of a single covalent bond.

The reaction scheme shown in Figure 11 for dimethylcyclohexane based compounds allows the hydrothermal chemistry of individual functional groups to be directly compared within the same chemical system. For example, Shipp et al.'s 2013 study with water alone compared the relative rates of reaction of the various functional groups. In that study the alcohol and the diene were the most reactive; by far, alkanes were the least reactive, and the alkene and ketone exhibited intermediate reaction rates. For all of the starting structures, the product distributions tended to be complex in reactions without minerals.

Here, I extend my previous work on the dimethylcyclohexane system to study the influence of minerals on these same hydrothermal reactions. In principle, the mineral influences on specific functional groups could be obtained by starting at different points along the reaction scheme in Figure 11, as in the water alone experiments. However, the goal of the present work is to investigate whether there are systematic differences in this sequence of reversible reactions that can be attributed to changes in mineral composition, changes in the surface area of the added mineral, or changes in the redox conditions that result from adding specific minerals. Therefore, we have chosen to start at opposite ends of the reaction scheme, utilizing a fully reduced and dehydrated reactant, the alkane, *trans*-1,2-dimthylcyclohexane, and an oxidized, hydrated reactant, the ketone, 2-methylcyclohexanone.

As mentioned above, mineral assemblages have previously been used to control equilibrium redox conditions by buffering solution phase H_2 and H_2S (Holm and Andersson, 2005), in order to study organic chemistry under these conditions (Seewald, 2001). Here we take a different approach asking whether, and how, the chemistry responds to changes in redox *potential* upon addition of a mineral. Figure 10 shows the equilibrium stability fields for the common iron oxides and sulfides in the presence of water at 300°C and 100 MPa. Addition of one of these minerals to a hydrothermal organic reaction effectively initiates reactions that must trend toward different pseudo-equilibrium concentrations of H_2, H_2S, and organic products. The question is, are the reactions far enough from equilibrium, and sufficiently influenced to change reaction pathways or efficiencies? I find that although the mineral effects are not simple and cannot be assigned to only one property (e.g., changes in bulk composition vs. changes in surface area or crystal structure), the answer to this question is yes. Experiments in the presence of troilite (used as a pyrrhotite analogue), pyrite, magnetite, and hematite affect the extents of conversion (relative to a no-mineral condition) and selectively enhance or inhibit specific reaction pathways. The mineral effects are different not only for different functional groups, but also for different minerals. For some minerals there is a dependence on surface area, implying reaction at the mineral surface, and for others there is no dependence on surface area, consistent with effects due to solution phase reactants.

Methods

Experiments were conducted in small gold capsules (4.3 cm long, 5.0 mm outer diameter and 4.0 mm inner diameter). Cut gold tubes were annealed at 600°C for 15

hours prior to use. One end of the tube was arc welded closed and the capsule was loaded with 250 µL argon purged de-ionized water (18.2 MΩ·cm, NANOpure® DIamond™ UV, Barnstead International), 60 µmoles organic reactant, and a weighed amount of mineral (amounts were determined based on the desired mineral surface area, see below for surface area measurements). The capsule head space was purged with ultra high purity argon before being welded closed. Capsules were placed in a cold-seal reaction vessel, heated to 300°C and pressurized to 100 MPa. Reactions were allowed to proceed at these conditions for 24 hours, quenched in room temperature water, and once cool, the pressure was released. The capsules were removed from the reaction vessel, rinsed in dichloromethane (DCM, 99.9%, Fisher Scientific), frozen in liquid nitrogen, and opened in glass vials containing 3 mL DCM and 5.9 µL decane (used as an internal standard; 99%, Alfa Aesar). Once thawed, the capsules in DCM/decane were shaken to fully extract organic products. The organic phase was separated from the aqueous phase and analyzed via gas chromatography with flame ionization detection (GC-FID) on a Varian CP-3800 equipped with a 5% diphenyl/95% dimethylsiloxane column (Supelco, Inc). The GC conditions were as follows: an injector temperature of 200°C, and a GC oven heating program that started at 40°C for 4 min, followed by a temperature ramp to 90°C at 2°C/min, followed by another temperature ramp to 300°C at 30°C/min where it was held for 10 min. Products were identified by matching retention times with the retention times of known standards. Quantification was achieved using response factors generated with calibration curves of known standards. Concentrations of structures that did not have authentic standards were determined using a calibration curve made from an authentic standard of a structural isomer. If an isomer was not available, the average GC response

factor for standards with similar structures was used. To determine concentrations of dimeric products, the average of the GC response factors from all the standards was multiplied by two. Products that could not be identified using authentic standards on the GC-FID were characterized via gas chromatography-mass spectrometry (GC-MS). The GC-MS was an Agilent 6890/5973 using the same analytical column and temperature protocol as used with the GC-FID system. Identification of peaks was based on the interpretation of mass spectra as well as comparison against the NIST Mass Spectral Library.

The organic reactants used were *trans*-1,2-dimethylcyclohexane (99%, Aldrich) and 2-methylcyclohexanone (99+%, Sigma-Aldrich). The monomethyl ketone was chosen because the dimethyl ketone was not available commercially and the mono and dimethyl compounds had been shown previously to have similar reactivity at our experimental conditions (Shipp et al., 2013). The minerals used were synthetic powders purchased from Alfa Aesar: Fe_3O_4 (97% metals basis), Fe_2O_3 (99.5% metals basis), FeS_2 (99.9% metals basis), and FeS (99.9% metals basis). X-Ray diffraction (XRD) analysis (Siemens D5000 with copper Kα, 1.541 Å radiation) of powders revealed crystal structures consistent with troilite, pyrite, hematite, and magnetite. Troilite (FeS) is not as common in nature as pyrrhotite ($Fe_{1-x}S$; x= 0 to 0.2) but it is an end member of the pyrrhotite group. I am therefore using troilite as a pyrrhotite analogue in order to avoid the added complication of iron vacancies in the iron sulfide crystal structure. To avoid confusion I will refer to it simply as FeS throughout the rest of the chapter. Surface areas were measured using N_2-absorption (Tristar II 3020) and the BET surface areas were 2.35 m^2/g for pyrite, 1.09 m^2/g for FeS, 7.8 m^2/g for magnetite, and 12.9 m^2/g for hematite.

Results and Discussion

Within our experimental timeframe and P-T conditions (24 h, 300°C, 100 MPa) the minerals do not have time to come to equilibrium with the surrounding water (Holm and Andersson, 2005). However, on their approach to equilibrium, the minerals used in this study will promote a trend toward different H_2 and H_2S concentrations, Figure 10. Addition of these minerals to the experiment should ultimately result in a different end point, but we also find differences in early time reactivity (24 h). Alkanes and ketones represent two ends of the oxidation/reduction-hydration/dehydration pathway in Figure 11. Experiments were performed starting at the two ends of the reaction scheme in order maximize sensitivity to changes in the reaction pathways. Experiments were run to low conversions in order to minimize secondary reactions. The amount of mineral used throughout the study was standardized to give 0.22 m^2 of surface in each capsule, unless otherwise stated.

Experiments Starting with trans-1,2-Dimethycyclohexane

The overall conversion of *trans*-1,2-dimethylcyclohexane into products was altered in the presence of minerals, in some cases dramatically, Figure 12. The percent conversion (calculated from the total number of products formed) changed relative to conversions in experiments with water alone, for all experiments using a mineral. Percent conversions increased in the presence of all minerals except for FeS. The increased conversion was greatest in the presence of pyrite; 10.4 ± 0.3% (n=2) conversion after 24 h, compared to 1.6 ± 0.2% (n=5) conversion in water alone. In contrast, the percent conversion in the presence of FeS was only 0.91 ± 0.02% (n=2). Not only were changes

in extent of conversion observed, but the product distributions were also different, with enhancement of some products and suppression of others as compared to water alone.

The product distribution for reactions with minerals that started with the *trans*-1,2-dimethylcyclohexane provide information on the relative importance of the oxidation-reduction (dehydrogenation/hydrogenation) and hydration-dehydration pathways. The oxidation pathway ultimately forms the aromatic xylene products, almost certainly via the corresponding alkene and diene structures. Formation of the ketone from the alkane involves oxidation (to an alkene), hydration (to an alcohol) and, finally, oxidation (to the ketone). Previous experiments in water alone showed the lifetimes of the alcohol and diene are sufficiently short that they do not build up appreciable concentrations in a 24 h experiment (Shipp et al. 2013). However, detection of xylene or ketone products is evidence that the alcohol and diene must form in the course of the reaction since they are the obvious precursors to ketones and xylenes, respectively. Suppression of oxidation would be expected to result in lower yields of xylene and/or ketone products. Reaction of the alkane may still occur under these conditions, however, and may be detected by formation of the *cis*-stereoisomer (*cis*-1,2-dimethylcyclohexane). Formation of the *cis*-isomer gives information about the primary step in the overall reaction pathways that start from the alkane. Specifically, Shipp et al. (submitted) show that isomerization of *trans*-1,2-dimethylcyclohexane to *cis*-1,2-dimethylcyclohexane is catalyzed in the presence of sphalerite (ZnS) and that the reaction proceeds via an intermediate involving cleavage of a single C-H bond. Isomerization thus represents a probe for the most elementary chemical reaction in the reaction scheme, cleavage of a single covalent bond. In water alone xylenes, ketones and the *cis*-stereoisomers are

produced in roughly equal amounts (Figure 13). This is not the case in the presence of any of the minerals investigated in the present study.

Reaction of the *trans*-alkane with pyrite and with FeS produced oxidation products but, interestingly, no ketones were detected, Figure 13. In water alone, ketones are formed at abundances similar to those of the other products. This suggests that with the iron sulfides, the hydration reaction pathway is suppressed. The two sulfide minerals seem to further affect reactivity differently, and are thus discussed separately.

Unlike all of the other minerals, FeS decreases conversion of the starting *trans*-1,2-dimethylcyclohexane relative to the water-only experiments, Figure 12. The change in product distribution with FeS is similarly dramatic, apart from the *cis*-stereoisomer, only the alkene is formed in detectable quantities, Figure 13. Although the overall conversion is reduced, the yield of the *cis*-stereoisomer is actually increased somewhat compared to the water only experiment. It appears the primary C-H bond cleavage required to initiate the reaction sequence is not suppressed. Thus, the fundamental reactivity of *trans*-1,2-dimethylcyclohexane may not be altered in the presence of FeS, but its propensity to form the more oxidized xylenes and ketones certainly is. From the stability diagram (Figure 10) one can see that at equilibrium FeS is consistent with an aqueous environment that can have both a relatively high H_2 activity and a relatively high H_2S activity; i.e., the FeS is stable in more reducing aqueous environments.

When considering the role of a weakly soluble mineral on organic reactivity, the effects of both the mineral surface and of solution phase reactants should be considered. Although both of these effects may play a role, the dominant one can be distinguished by considering the effect of varying the amount of added mineral. At equilibrium, the

concentration of mineral-derived solution phase reactants is independent of the quantity of added mineral, whereas the surface area obviously increases. Thus, if an effect increases with the addition of ever larger amounts of mineral, there is strong evidence for a dominant mineral surface effect. In contrast, if an observed mineral effect is essentially uninfluenced by adding larger amounts of mineral (above a critical minimum quantity, of course), one may reasonably conclude that solution-phase differences are the dominant mineral effect. In our FeS experiments, the systems are not at mineral-solution equilibrium; never-the-less, the presence of the FeS strongly influences the organic reaction chemistry compared to results in water-only experiments, and there is no apparent dependence on added mineral (i.e., surface area), see Figure 14. Neither the conversion nor the product distribution varies significantly with increasing quantities of FeS. This argues strongly for a dominant role for solution phase reactants and not surface reactions. The suppression of oxidation products is also consistent with a more reducing environment, which is, in turn, consistent with the presence of solution phase H_2 and H_2S. Hydrogenation of covalent double bonds with molecular hydrogen is well known in hydrothermal systems (Reeves et al., 2012; Seewald, 1994), although the detailed mechanism for this process is not; H_2S is also a well-understood reducing agent in organic chemistry. In water alone, the reactions connecting the alkene formed initially with the more oxidized xylene and ketone products are completely reversible, and a plausible explanation for the lack of oxidized structures in the FeS experiments is simply that the rates of the reverse reactions (hydrogenation, dehydration) that take the oxidized species back toward the alkane are increased in the presence of H_2 and H_2S. Thus, FeS

does not suppress reactivity, so much as increase the rate of reactions leading away from the oxidized species.

The situation for reactions in the presence of pyrite (FeS_2) is very different. In this case the overall rate of consumption of the alkane starting material is dramatically increased (Figure 12), and the rate of consumption increases with increasing quantities of added mineral. At low amounts of added surface area, the amount of xylene produced is similar to that which occurs in water alone; however at greater amounts of added surface, the yields increase by almost 100% (Figure 14). Pyrite's enhancement of the *cis*-*trans* isomerization reaction, to form the *cis*-alkane product, happens at even low surface area; the degree of isomerization increases slightly with increasing surface area, relative to a water only experiment, but the increase appears to be non-linear. This result provides strong evidence for a pyrite surface effect rather than an effect due to changes in the solution composition. Relative to FeS, pyrite occupies a position in the stability diagram that supports a lower equilibrium H_2 activity, Figure 10. Consistent with a less reducing environment, significant quantities of xylene are formed in reactions with pyrite as compared to reactions with FeS. The dependence of xylene formation on the amount of mineral added further suggests that pyrite influences the reaction predominantly via a surface effect. This is consistent with the observation that the major product, by far, with pyrite addition is the *cis*-stereoisomer. Isomerization requires activation and cleavage of a C-H bond, and previous experiments using sphalerite (ZnS) also showed dramatically enhanced C-H bond cleavage catalyzed by the mineral surface (Shipp et al., submitted). Effectively pyrite (like sphalerite) reduces the energetic barrier to C-H bond cleavage, which is responsible for the isomerization, and presumably also catalyzes the relatively

rapid progress towards xylene. These experiments do not reveal the exact nature of the surface catalytic effect, however, pyrite has a negative surface charge and has previously been shown to bind aqueous organic species (Bebie and Schoonen, 2000) which likely plays a critical role.

The isomerization reaction does not require formation of the alkene. The results from the work with sphalerite suggested isomerization of *trans*-1,2-dimethylcyclohexane could occur via an intermediate species (between the alkane and alkene) that has lost a single hydrogen atom. The intermediate could either lose another hydrogen atom to form the alkene or a hydrogen atom could be added back to form either the *cis*- or the original *trans*- stereoisomer. By the principle of microscopic reversibility the sphalerite and pyrite minerals catalyze both the C-H bond breaking and the C-H bond formation processes.

Formation of ketone products decreases in the presence pyrite presumably because hydration of the alkene competes less well with dehydrogenation. Hydration of the alkene probably proceeds at the same rate as in the absence of pyrite, since it is catalyzed by hydronium ions, but dehydrogenation to xylene appears to be faster in the presence of pyrite.

Based on my stability diagram, hematite and magnetite both occupy a position lower on the H_2S axis than either pyrite or FeS; hematite and magnetite also fall within different H_2 stability fields (Figure 10). Both of the oxide minerals increase the rate of alkane consumption compared to water alone, but the increase in conversion is not as great as we observed in experiments using pyrite (Figure 12). A major difference in the product distribution for the reactions with iron oxides versus those with iron sulfides, is that the oxides enhance formation of the oxygen containing products at the expense of

xylene formation (Figure 13). With both hematite and magnetite, ketones constitute the major product, while no ketones were ever detected with pyrite or FeS. Hematite and magnetite experiments exhibit similar yields of ketone, and both of these minerals produce more ketones than are produced in experiments without minerals (water alone).

Differences in the equilibrium aqueous redox conditions in the experiments containing magnetite and hematite result almost exclusively from differences in the H_2 activities these minerals promote (note, magnetite is stable at slightly higher aH_2S over some range of aH_2 relative to hematite). The equilibrium hydrogen activity in the presence of hematite is lower than that in presence of magnetite (i.e., at equilibrium the aqueous environment in the presence of hematite is expected to be more oxidizing). Distinguishing the relative importance of solution phase reactants and surface effects is more difficult for the hematite and magnetite experiments (compared to pyrite for example) because the changes in reaction rates are smaller. Never-the-less, experiments using a range of surface areas were performed with the iron oxides in an attempt to distinguish surface effects from solution composition effects. Product distributions in experiments with hematite and magnetite were notably different from those in water alone, where the most abundant product is xylene, and were broadly similar (ketone>alkane>alkene) in experiments with low surface areas (Figure 15). Xylene was, in fact, the least abundant product in experiments with both iron oxides and the xylene yield remained relatively constant in the presence of large amounts of surface. Notably, this effect was not the same for all products. As the amount of hematite surface increases the yield of the *cis*-alkane isomer also increases. This is not the case for the magnetite experiments where the alkane product yield was similar to that in no mineral

experiments, and remained fairly constant at higher amounts of surface. The opposite pattern holds for the alkene products, which are relatively constant and simliar those in experiments with water alone for hematite, but which increase linearly with increasing magnetite surface, although, admittedly, the effect is not very large.

The *cis-trans* isomerization reaction is also influenced by the presence of iron oxide minerals. In experiments with hematite, the efficiency of the isomerization process depends upon the amount of hematite surface used, consistent with surface catalyzed C-H bond cleavage and suggests that the mechanism is similar to what we observe with pyrite. With the mineral loadings studied here, a similar surface effect cannot be observed readily using magnetite, suggesting magnetite is a less effective surface catalyst for C-H bond cleavage than hematite in reactions with the dimethylcyclohexanes.

Magnetite appears to enhance the formation of ketone, apparently at the expense of xylene (Figure 13). The paths to the ketone and to the xylene diverge at the alkene. Dehydrogenation of the alkene leads to xylene, hydration of the alkene leads ultimately to ketone after another dehydrogenation step at the alcohol. In the presence of magnetite the hydration path is apparently enhanced, or the dehydrogenation path is suppressed, compared to water alone. It is important to remember that the pathways are reversible, and the hydration/dehydration reactions linking the alkene and the alcohol are probably very rapid on the timescale of these experiments. Specifically, dehydration of the alcohol was the fastest reaction observed in the hydrothermal reactions of dimethylcyclohexane in water alone (Shipp et al., 2013). In the no-mineral control experiments, it is clear that the alcohol/alkene equilibrium strongly favors the alkene. One plausible explanation for the change in the reaction path in the presence of magnetite is that the alcohol/alkene

equilibrium position is shifted toward the alcohol. Surface binding is necessarily accompanied by a decrease in energy that could be responsible for the increase in the alcohol-derived ketone product in the presence of magnetite.

Experiments Starting with 2-Methylcyclohexanone

The experiments starting with the *trans*-1,2-dimethylcyclohexane suggest a variety of ways in which minerals can influence organic hydrothermal chemistry. It is obviously of interest to see if these effects translate to the chemistry of a very different functional group. Previous work on the hydrothermal chemistry of cycloalkanes in water alone showed that xylenes are quite unreactive under the current experimental conditions, but that ketones, another oxidized functional group, can react to give a range of products (Shipp et al., 2013). Therefore, we have investigated the effect of minerals on the hydrothermal chemistry of a model cyclohexanone.

2-Methylcyclohexanone undergoes hydrothermal reaction in water alone at 300°C and 100 MPa. For a 24 h reaction period, the total conversion of the ketone is 10.6%. No single reaction pathway dominates in water alone and the major products are methylcyclohexenes, toluene, methylcyclohexane and methylcyclohexenones, Figure 16. The methylcyclohexenone (eneone) products are dehydrogenation products, but the formation of alkenes requires hydrogenation followed by dehydration. Based on the results of the mineral experiments with the cycloalkane, we can make predictions as to how the minerals might change the reactivity of the ketone. For the alkane starting material, pyrite was found to catalyze C-H bond breaking, which suggests that the yields of dehydrogenated products might increase for reaction of a ketone in the presence of

pyrite. In alkane experiments with FeS, the formation of oxidized products was significantly suppressed, to the point that overall conversion of the alkane was lowered. So, starting with an oxidized structure (ketone) with FeS, we might expect increased reactivity and formation of reduced products. Both hematite and magnetite favored oxygenated products, with hematite also seeming to facilitate C-H bond cleavage. Thus we predict that similarly, in ketone reactions the oxygenated products might dominate in the presence of hematite and magnetite, effectively lowering conversion of the ketone, and that dehydrogenated products might be favored in the presence of hematite.

In experiments starting with 2-methylcyclohexanone in the presence of FeS, overall conversions were dramatically increased to 87.4% from 10.6% in experiments without minerals. Instead of the large number of products formed in water-only reactions, reduced products are now dominant; 43% of the products formed were alkenes, 21.2% was the alkane, and very little enone or toluene products were formed. Formation of alkenes and the alkane require hydrogenation, i.e., reduction of the ketone. Thus, this observation is in line with our prediction and entirely consistent with the results from experiments starting with the alkane. The effect of a reducing environment is now much more evident because the starting structure is more oxidized (ketone vs. alkane). The high conversion suggests the reduction reactions are rapid on the timescale of the experiment. This, in turn, suggests the decreased amount of conversion of the cycloalkane in the presence of FeS is not due to a decrease in the rate constants for the reactions that consume the alkane, but, rather, to an increase in the rates of reactions that form reduced products in the reversible reaction scheme, i.e., those that reform the alkane.

Addition of pyrite to 2-methylcyclohexanone experiments also dramatically increased the extent of conversion, from 10.6% in water alone to 88.5%. Again, mainly two types of products were formed in contrast to the multiple products observed in water alone; but in this case, the products are enones (9.4%) and toluene (23.4%). Both of these are dehydrogenated (i.e. oxidized) products. Again, this is consistent with predictions and with observations from the dimethylcyclohexane experiments. The pyrite apparently catalyzes cleavage of C-H bonds to enhance the rates of formation of dehydrogenated products in the reversible reaction scheme, so that these accumulate at the expense of the other, more reduced products.

The addition of the iron oxides, hematite and magnetite, changed the extent of conversion of the ketone, but to a much smaller extent than observed for either of the sulfide minerals. The conversions are 20.0% and 6.0% for hematite and magnetite, respectively, compared to 10.6% without mineral, and ~90% in the presence of the iron sulfides (Figure 16). The iron oxide minerals are also less selective in the types of products formed than the sulfide minerals. In experiments with hematite, the major products from reaction of the ketone include toluene and the enones, with very little conversion to the alkane. Toluene and eneone products are dehydrogenated and require C-H bond cleavage, consistent with the predictions above. In the presence of magnetite, the major products from the ketone are the enone, and curiously the alcohol, i.e., oxygenated products; again as predicted from the alkane experiments. We can speculate that the reason for this is a specific interaction of the alcohol, or perhaps the ketone and enone, with the surface of the magnetite, that results in shifting the equilibria to one that favors higher concentrations of oxygen containing structures.

Conclusion

The presence of minerals can affect organic chemical reactions under hydrothermal conditions. Mineral surfaces, coupled with redox state, can in some cases dramatically change the outcome of an organic reaction and the type of functional groups that are can accumulate over time. Some products, ketones for example, are completely eliminated from the product suites when experiments include the reduced iron sulfide minerals: pyrite and FeS. FeS is even more selective than pyrite, allowing only the reversible conversion of alkane to alkene and inhibiting any further oxidation. The iron sulfides enhance dehydration reactions and therefore they enhance the reactivity of ketone functional groups, with pyrite favoring formation of xylenes/toluene and the alkane isomers, and FeS favoring formation of only the alkenes and the alkane isomers. Iron oxides, magnetite and hematite, allow the hydration of alkanes to ketones, but tend to suppress the oxidation to xylene as compared to results in water alone. Magnetite especially favors oxygenated products (ketones, eneones, and alcohols), and exhibits less ketone conversion than is observed in water alone. The elimination of the hydration reaction via pyrite and FeS and the suppression of oxidation to xylene by hematite and magnetite seem to be independent of surface area, and are likely a result of the particular H_2 and H_2S activities which the minerals promote as they approach equilibrium with the solution. The increased rates of isomerization and of oxidation to xylene in the presence of pyrite do seem to have a surface area dependence, and pyrite may be promoting the oxidation reaction via heterogeneous catalysis of C-H bond cleavage at the mineral surface. Reversable alkane isomerization appears to be increased in the presence of hematite and related to the amount of surface area present. In contrast, increased

magnetite surface area seems to enhance dehydrogenation to the alkenes but not the reverse, hydrogenation, which proceeds (presumably in solution) with no apparent rate change.

The minerals studied here, iron oxides and sulfides, are highly abundant in hydrothermal systems and undoubtedly have an effect on the organic reactions taking place in the environment. This work shows that the presence of these minerals can change the functional group distributions of products, and can be used to selectively enhance or suppress specific reaction pathways. This effect is not due to simple redox changes in solution; certain reaction pathways also depend on the amount of available mineral surface area. Further work needs to be done to understand exactly how the minerals interact with the organic functional groups on a mechanistic level in order to understand why the minerals increase or decrease the rates of specific reaction pathways.

References

Akiya N. and Savage P. E. (2001) Kinetics and mechanism of cyclohexanol dehydration in high-temperature water. *Ind. Eng. Chem. Res.* **40**, 1822-1831.

Akiya, N., Savage, P.E. (2002) Roles of Water for Chemical Reactions in High-Temperature Water. *ChemInform* **33**, 293-293.

Andersson, E., Holm, N.G. (2000). The stability of some selected amino acids under attempted redox constrained hydrothermal conditions *Origins Life Evol. B.* **30**, 9-23.

Bebie, J., Schoonen, M.A. (2000) Pyrite surface interaction with selected organic aqueous species under anoxic conditions. *Geochemical Transactions* **1**, 47.

Bell, J.L.S., Palmer, D.A., Barnes, H.L., Drummond, S.E. (1994) Thermal-decomposition of acetate .3. catalysis by mineral surfaces. *Geochim. Cosmochim. Acta* **58**, 4155-4177.

Breier, J.A., Toner, B.M., Fakra, S.C., Marcus, M.A., White, S.N., Thurnherr, A.M., German, C.R. (2012) Sulfur, sulfides, oxides and organic matter aggregated in submarine hydrothermal plumes at 9 degrees 50 ' N East Pacific Rise. *Geochim. Cosmochim. Acta* **88**, 216-236.

Cody, G.D. (2004). Transition metal sulfides and the origins of metabolism. *Annu. Rev. Earth Planet. Sci.* **32**, 569-599.

Cody, G.D., Boctor, N.Z., Brandes, J.A., Filley, T.R., Hazen, R.M., H. S. Yoder, J. (2004) Assaying the catalytic potential of transition metal sulfides for abiotic carbon fixation. *Geochim. Cosmochim. Acta* **68**, 2185-2196.

Cody, G.D., Boctor, N.Z., Filley, T.R., Hazen, R.M., Scott, J.H., Sharma, A., Yoder, H.S. (2000) Primordial carbonylated iron-sulfur compounds and the synthesis of pyruvate. *Science* **289**, 1337-1340.

Ferris, J.P. (2005) Mineral catalysis and prebiotic synthesis: Montmorillonite-catalyzed formation of RNA. *Elements* **1**, 145-149.

Foustoukos, D.I., Seyfried, W.E. (2004) Hydrocarbons in hydrothermal vent fluids: The role of chromium-bearing catalysts. *Science* **304**, 1002-1005.

Fu, Q., Foustoukos, D.I., Seyfried, W.E. (2008) Mineral catalyzed organic synthesis in hydrothermal systems: An experimental study using time-of-flight secondary ion mass spectrometry. *Geophys. Res. Lett*. **35**.

Head I. M., Jones D. M. and Larter S. R. (2003) Biological activity in the deep subsurface and the origin of heavy oil. *Nature* **426**, 344-352.

Holm, N.G., Andersson, E. (2005) Hydrothermal simulation experiments as a tool for studies of the origin of life on earth and other terrestrial planets: A review. *Astrobiology* **5**, 444-460.

Horsfield B., Schenk H. J., Zink K., Ondrak R., Dieckmann V., Kallmeyer J., Mangelsdorf K., Primio R. D., Wilkes H., Parkes R. J., Fry J. and Cragg B. (2006) Living microbial ecosystems within the active zone of catagenesis: Implications for feeding the deep biosphere. *Earth Planet Sci. Lett*. **246 (**1–2), 55-69.

Johnson J. W., Oelkers, E. H., and Helgeson, H. C. (1992) SUPCRT92 - A software package for calculating the standard molal thermodynamic properties of minerals, gases, aqueous species, and reactions from 1 bar to 5000 bar And 0°C To 1000°C. *Comput. Geosci* **18**, 899-947.

Jones D. M, Head I. M., Gray N. D., Adams J. J., Rwan A. K., Aitken C. M., Bennett B., Huang H., Brown A., Bowler B. F. J., Oldenburg T., Erdmann M. and Larter S. R. (2008) Crude-oil biodegradation via methanogenesis in subsurface petroleum reservoirs. *Nature* **451**, 176-180.

Katritzky A. R., Nichols D. A., Siskin M., Murugan R. and Balasubramanian M. (2001) Reactions in high-temperature aqueous media. *Chem. Rev.* **101**, 837-892.

Kvenvolden, K.A., Rapp, J.B., Hostettler, F.D. (1990) Hydrocarbon geochemistry of hydrothermally generated petroleum from Escanaba Trough, offshore California, USA. *Appl. Geochem*. **5**, 83-91.

Kvenvolden, K.A., Rapp, J.B., Hostettler, F.D., Rosenbauer, R.J. (1994) Laboratory simulation of hydrothermal petroleum formation from sediment in Escanaba Trough, offshore from Northern California. *Org. Geochem*. **22**, 935-945.

Lahav, N. (1994) Minerals and the origin of life- hypotheses and experiments in heterogeneous chemistry. *Heterogen. Chem. Rev.* **1**, 159-179.

Martin W., Baross J., Kelley D. and Russell M. J. (2008) Hydrothermal vents and the origin of life. *Nat. Rev. Microbiol*. **6**, 805-814.

Mason O. U., Nakagawa T., Rosner M., Van Nostrand J. D., Zhou J., Maruyama A., Fisk M. R. and Giovannoni S. J. (2010) First investigation of the microbiology of the deepest layer of ocean crust. *PLoS ONE*. **5**, 1-11.

McCollom, T.M., Seewald, J.S., Simoneit, B.R.T. (2001) Reactivity of monocyclic aromatic compounds under hydrothermal conditions. *Geochim. Cosmochim. Acta* **65**, 455-468.

McCollom, T.M., Simoneit, B.R.T., Shock, E.L. (1999) Hydrous pyrolysis of polycyclic aromatic hydrocarbons and implications for the origin of PAH in hydrothermal petroleum. *Energy Fuels* **13**, 401-410.

Mulkidjanian, A.Y. (2009) On the origin of life in the Zinc world: I. Photosynthesizing, porous edifices built of hydrothermally precipitated zinc sulfide as cradles of life on Earth. *Biol. Direct* **4**.

Oldenburg, T.B.P., Larter, S.R., Huang, H. (2006) Nutrient supply during subsurface oil biodegradations - Availability of petroleum nitrogen as a nutrient source for subsurface microbial activity. *Energy Fuels* **20**, 2079-2082.

Reeves, E.P., Seewald, J.S., Sylva, S.P. (2012) Hydrogen isotope exchange between n-alkanes and water under hydrothermal conditions. *Geochim. Cosmochim. Acta* **77**, 582–599.

Russell, M.J., Daniel, R.M., Hall, A.J. (1993) On the emergence of life via catalytic iron-sulfide membranes. *Terr. Nova* **5**, 343-347.

Savage P. E. (1999) Organic chemical reactions in supercritical water. *Chem. Rev*. **99**, 603-621.

Schoonen, M., Smirnov, A., Cohn, C. (2004) A perspective on the role of minerals in prebiotic synthesis. *Ambio* **33**, 539-551.

Schreiner, E., Nair, N.N., Wittekindt, C., Marx, D. (2011) Peptide synthesis in aqueous environments: The role of extreme conditions and pyrite mineral surfaces on rormation and hydrolysis of peptides. *J. Am. Chem. Soc*. **133**, 8216-8226.

Seewald J. S. (1994) Evidence for metastable equilibrium between hydrocarbons under hydrothermal conditions. *Nature* **370**, 285-287.

Seewald J. S. (2001) Aqueous geochemistry of low molecular weight hydrocarbons at elevated temperatures and pressures: Constraints from mineral buffered laboratory experiments. *Geochim. Cosmochim. Acta* **65**, 1641-1664.

Seewald J. S. (2003) Organic-inorganic interactions in petroleum-producing sedimentary basins. *Nature* **426**, 327-333.

Shipp, J., Gould, I.R., Herckes, P., Shock, E.L., Williams, L.B., Hartnett, H.E. (2013) Organic functional group transformations in water at elevated temperature and pressure: Reversibility, reactivity, and mechanisms. *Geochim. Cosmochim. Acta* **104**, 194-209.

Shipp, J., L., S.E., Gould, I., Williams, L.B., Hartnett, H., submitted. Sphalerite is a catalysis for carbon-hydrogen bond breaking reactions. Submitted.

Shock, E.L. (1993) Hydrothermal dehydration of aqueous-organic compounds. *Geochim. Cosmochim. Acta* **57**, 3341-3349.

Shock E. L., Sassani D. C., Willis M., and Sverjensky D. A. (1997) Inorganic species in geologic fluids: Correlations among standard molal thermodynamic properties of aqueous ions and hydroxide complexes. *Geochim. Cosmochim. Acta* **61**, 907-950.

Simoneit, B.R.T. (1993) Aqueous high-temperature and high-pressure organic geochemistry of hydrothermal vent systems. *Geochim. Cosmochim. Acta* **57**, 3231-3243.

Simoneit, B.R.T. (2003) Petroleum generation, extraction and migration and abiogenic synthesis in hydrothermal systems., in: Ikan, R. (Ed.), Natural and laboratory simulated thermal geochemical rocesses. Kluwer Academic Publishers, Kluwer, Amsterdam, pp. 1–30.

Siskin M. and Katritzky A. R. (2001) Reactivity of organic comounds in superheated water: general background. *Chem Rev*. **101**, 825-835.

Tivey, M.K. (1995) The influence of hydrothermal fluid composition and advection rates on black smoker chimney mineralogy: Insights from modeling transport and reaction. *Geochim. Cosmochim. Acta* **59**, 1933-1949.

Vaughan, D.J., Lennie, A.R. (1991) The iron sulfide minerals- their chemistry and role in nature. *Science Progress* **75**, 371-388.

Wang, W., Li, Q., Yang, B., Liu, X., Yang, Y., Su, W. (2012) Photocatalytic reversible amination of alpha-keto acids on a ZnS surface: implications for the prebiotic metabolism. *Chem Commun (Camb)* **48**, 2146-2148.

Wang, W., Yang, B., Qu, Y.P., Liu, X.Y., Su, W.H. (2011) $FeS/S/FeS_2$ Redox system and its oxidoreductase-like chemistry in the iron-sulfur world. *Astrobiology* **11**, 471-476.

Watanabe M., Sato T., Inomata H., Smith, Jr., R. L., Arai K., Kruse A. and Dinjus E. (2004) Chemical reactions of C_1 compounds in near-critical and supercritical water. *Chem Rev.***104**, 5803-5821.

Williams, L.B., Canfield, B., Voglesonger, K.M., Holloway, J.R. (2005) Organic molecules formed in a "primordial womb". *Geology* **33**, 913-916.

Williams L. B., Holloway J. R., Canfield B., Glein C., Dick J., Hartnett H. and Shock E. (2011) Birth of biomolecules from the warm wet sheets of clays near spreading centers. In *Earliest Life on Earth: Habitats, Environments and Methods of Detection* (eds. Golding S. and Glikson M.). Springer Publishing. Chapter 4. pp. 79-112.

Windman T., Zolotova N., Schwandner F. and Shock E. (2007) Formate as an energy source for microbial metabolism in chemosynthetic zones of hydrothermal ecosystems. *Astrobiology* **7**, 873-890.

Yang, Z.M., Gould, I.R., Williams, L.B., Hartnett, H.E., Shock, E.L. (2012) The central role of ketones in reversible and irreversible hydrothermal organic functional group transformations. *Geochim. Cosmochim. Acta* **98**, 48-65.

Table 3. Product distributions for reactions of *trans*-1,2-dimethylcyclohexane with various iron-bearing minerals. Amounts of alkenes, ketones, and xylenes, are the sum of all isomers formed for each type of compound. Note, no alcohols were detected in these experiments. "Others" represent products that are not a part of the main reaction scheme. Percent conversion is an indication of the total amount of products formed compared to starting material.

			Products (µmoles)				
Mineral	Surface Area, (m^2)	Total conversion (%)	*cis*-alkane	alkenes	xylenes	ketones	others
none	n/a	1.6 ± 0.2	0.148 ± 0.007	0.11 ± 0.08	0.3 ± 0.1	0.19 ± 0.06	0.19 ± 0.01
pyrite	0.05	6.3	3.22	nd	0.3	nd	0.2
	0.11	8.3	3.52	nd	0.9	nd	0.2
	0.22	10.4 ± 0.3	3.96 ± 0.10	nd	1.3 ± 0.2	nd	0.1 ± 0.2
FeS	0.05	0.90	0.25	0.07	nd	nd	0.148
	0.11	0.94	0.13	0.01	nd	nd	0.138
	0.22	0.91 ± 0.02	0.23 ± 0.01	0.08 ± 0.02	nd	nd	0.127 ± 0.007
hematite	0.06	1.4	0.20	0.14	0.08	0.28	0.13
	0.11	1.9	0.36	0.10	0.11	0.33	0.18
	0.22	3.1 ± 0.7	0.9 ± 0.3	0.06 ± 0.01	0.19 ± 0.03	0.33 ± 0.06	0.19 ± 0.04
magnetite	0.06	1.0	0.14	0.11	0.049	0.16	0.13
	0.11	1.6	0.14	0.26	0.065	0.27	0.17
	0.22	2.0 ± 0.5	0.15 ± 0.02	0.4 ± 0.1	0.050 ± 0.005	0.36 ± 0.12	0.17 ± 0.03

n/a, not applicable
nd, not detected
product amounts are ± the standard deviation in replicate experiments; n = 5 for no-mineral experiemtns, n = 2 for sulfide mineral experiments and n = 3 for oxide mineral experiments.
Analytical error for µmole amounts is <10%.

Table 4. Product distributions for reactions of 2-methylcyclohexanone with various iron-bearing minerals. Alkenes, alcohols, ketones, dienes, and eneones are the sum of all the isomers formed for each type of compound. Ketones are isomer products of the starting reactant. "Others" represent products that were not part of the main reaction scheme. Dimers are unidentified products with masses consistent with two connected rings. Percent conversion is an indication of the total amount of products formed compared to starting material.

			Products (µmoles)								
Mineral	Surface Area (m^2)	Total conversion (%)	alkane	alkenes	dienes	toluene	alcohols	ketones	eneones	others	dimers
none	n/a	10.6	0.10	1.59	0.02	0.68	0.51	0.17	0.87	0.99	0.51
pyrite	0.22	88.5	0.84	0.22	nd	9.12	0.83	1.83	3.64	1.64	8.16
FeS	0.22	87.4	9.81	19.92	0.01	0.04	3.05	0.07	0.02	4.87	1.31
hematite	0.22	20.0	0.04	0.47	0.03	0.97	0.41	0.43	0.45	0.92	3.36
magnetite	0.22	6.0	0.02	0.29	nd	0.14	0.34	0.03	1.29	0.72	0.21

n/a, not applicable
nd- not detected
Analytical error for µmole amounts is <10%.

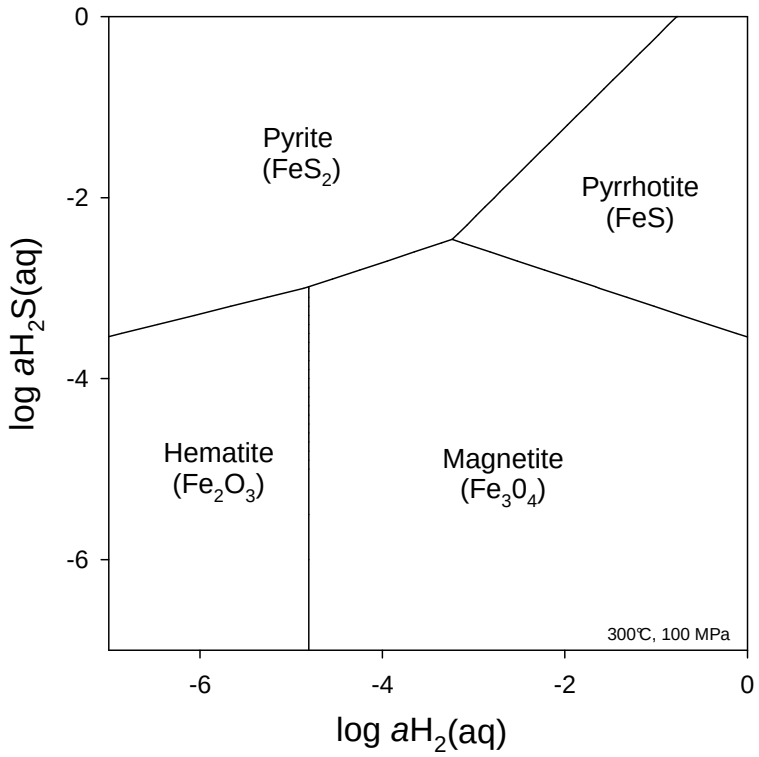

Figure 10. Mineral stability diagram for pyrite, pyrrhotite, hematite, and magnetite in water at 300°C and 100 MPa, calculated using SUPCRT92 (Johnson J., 1992) together with data and parameters from Shock et al. (1997).

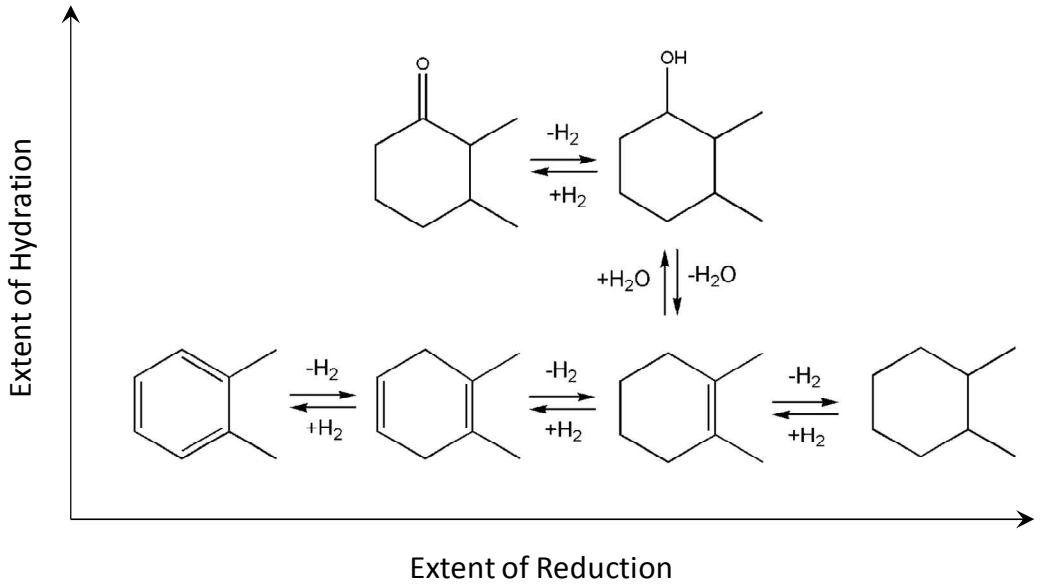

Figure 11. Schematic view of reversible reduction-oxidation and hydration-dehydration reactions of 1,2-dimethylcyclohexane based hydrocarbons under hydrothermal conditions (300^{o}C, 100 MPa).

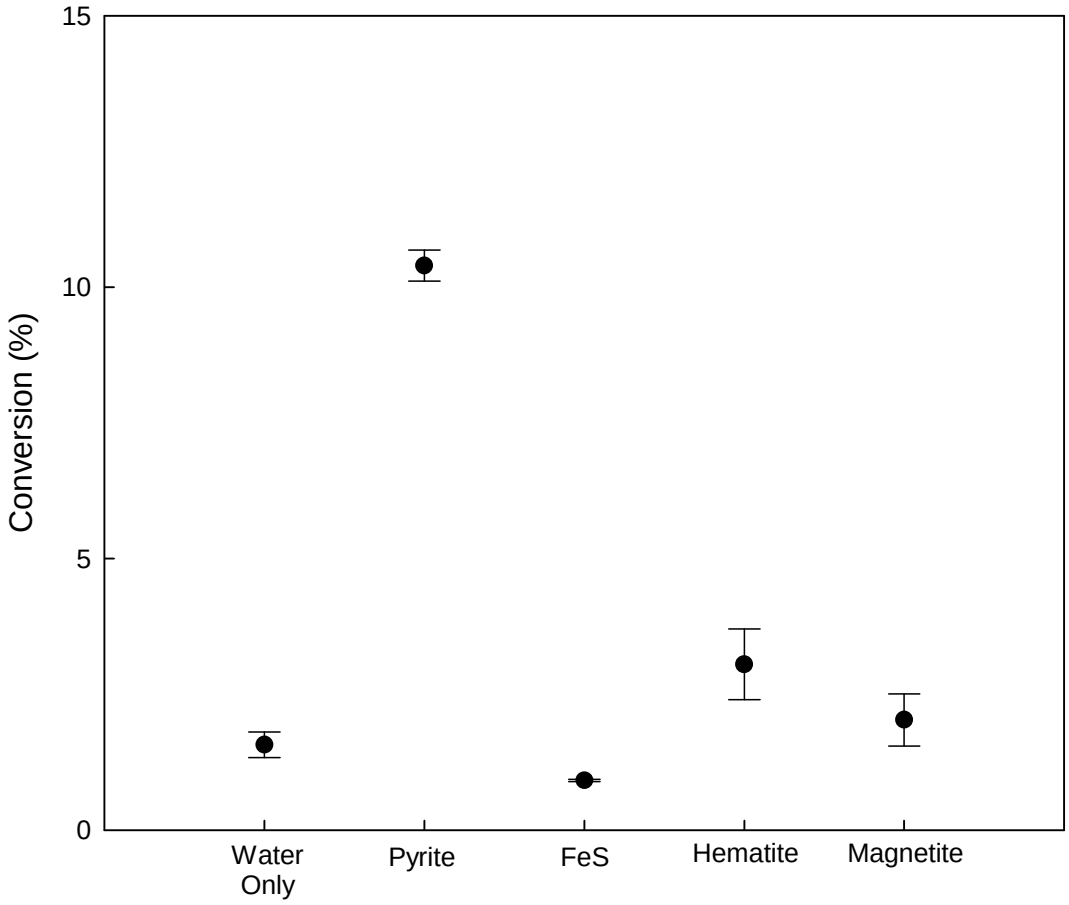

Figure 12. The amount of conversion for 24-hour experiments without mineral (water only), with iron sulfides (pyrite and FeS), and with iron oxides (hematite and magnetite) under hydrothermal conditions (300°C, 100 MPa). Error bars represent the standard deviation in replicate experiments; Water Only had 5 replicates, the sulfide minerals each had 2 replicates, and the oxide minerals each had 3 replicates.

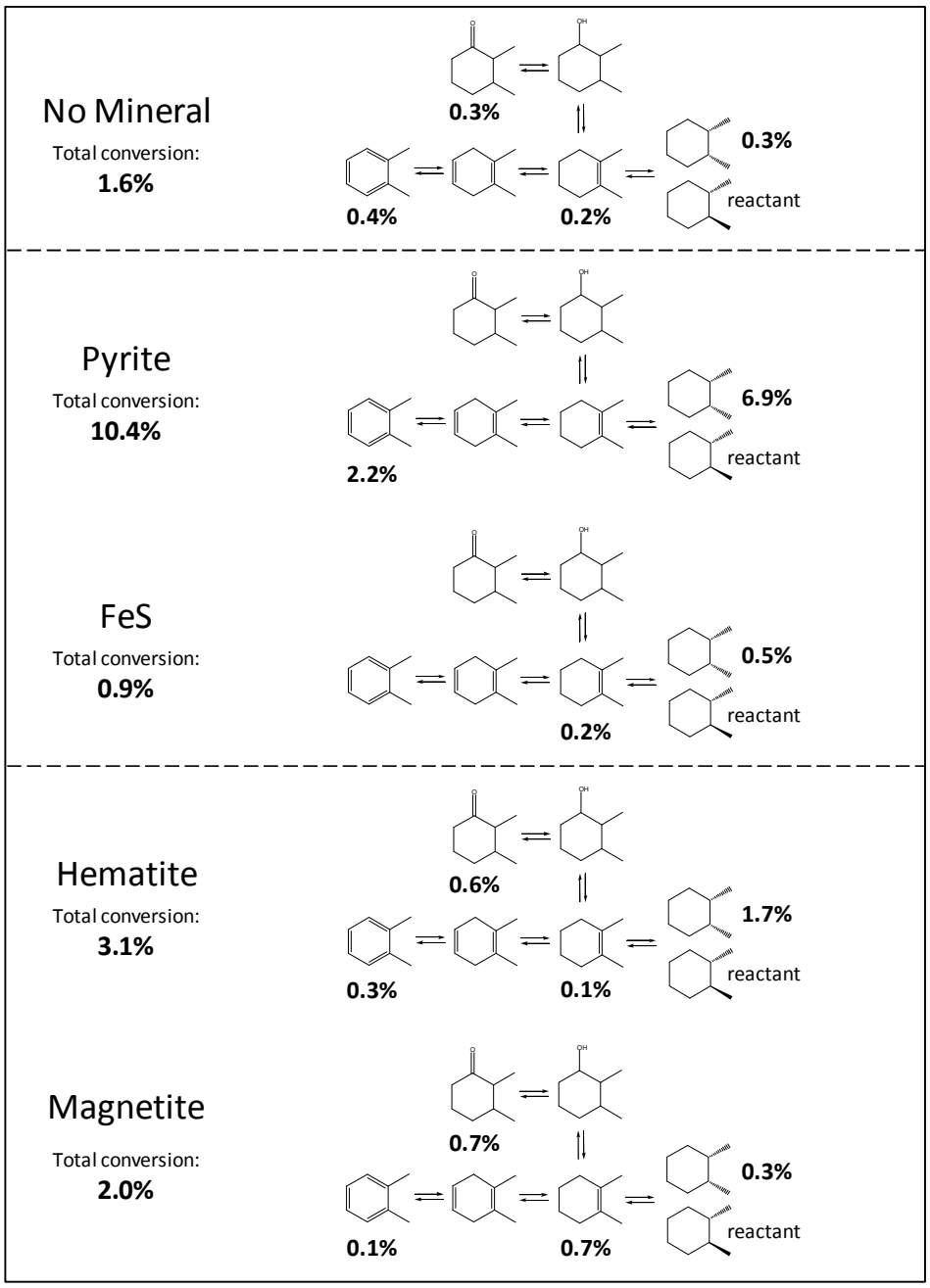

Figure 13. Product distributions for hydrothermal (300°C, 100 MPa) reactions of *trans*-1,2-dimethylcyclohexane without minerals (top panel), with iron sulfide minerals (middle panel), and with iron oxide minerals (bottom panel). Total conversion percentages are based on all products formed (Table 3) and not just the structures illustrated.

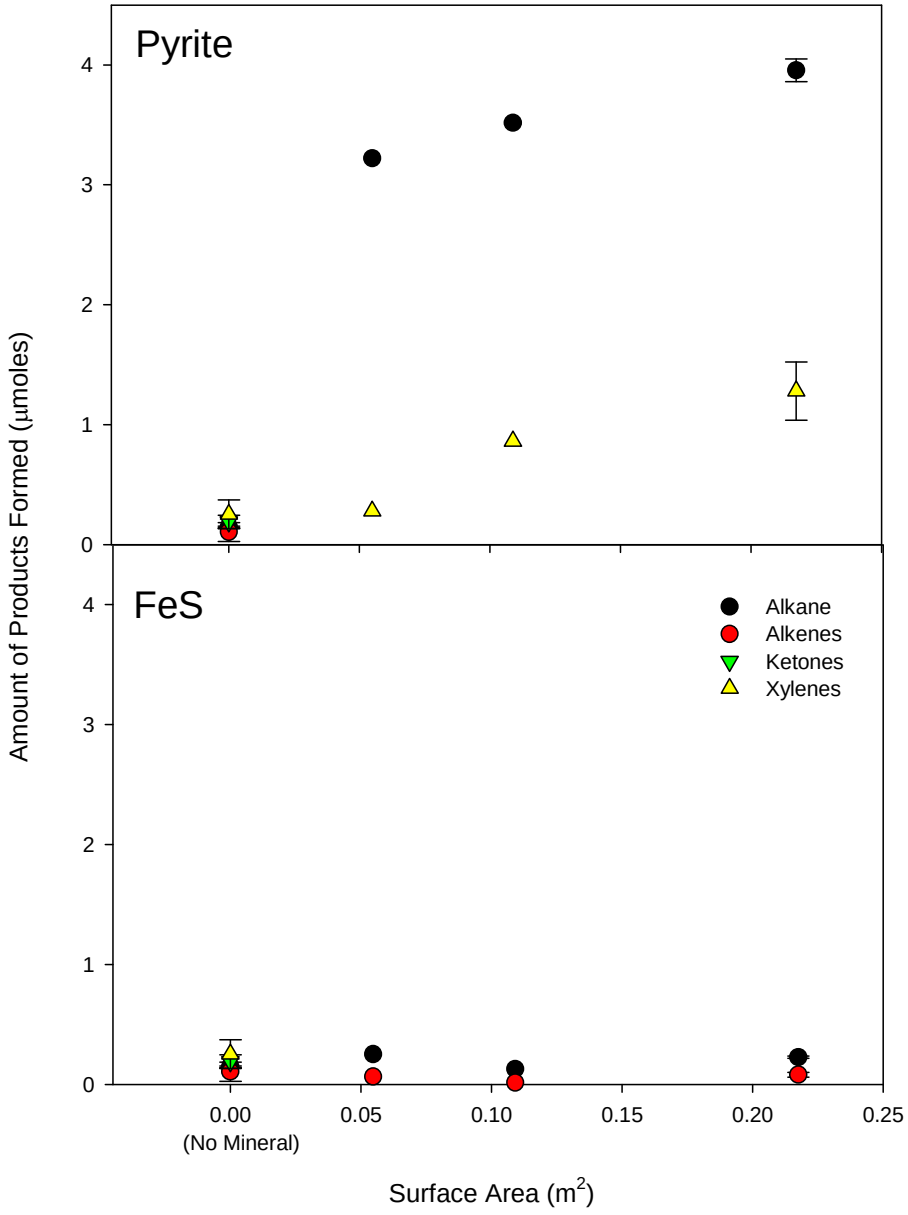

Figure 14. Products formed from hydrothermal reaction (300°C, 100 MPa) of *trans*-1,2-dimethylcyclohexane with iron sulfide minerals, as a function of surface area used. Error bars on "No Mineral" are based on 5 replicate water only experiments. Error bars on 0.22 m^2 surface area points are based on 2 replicate experiments.

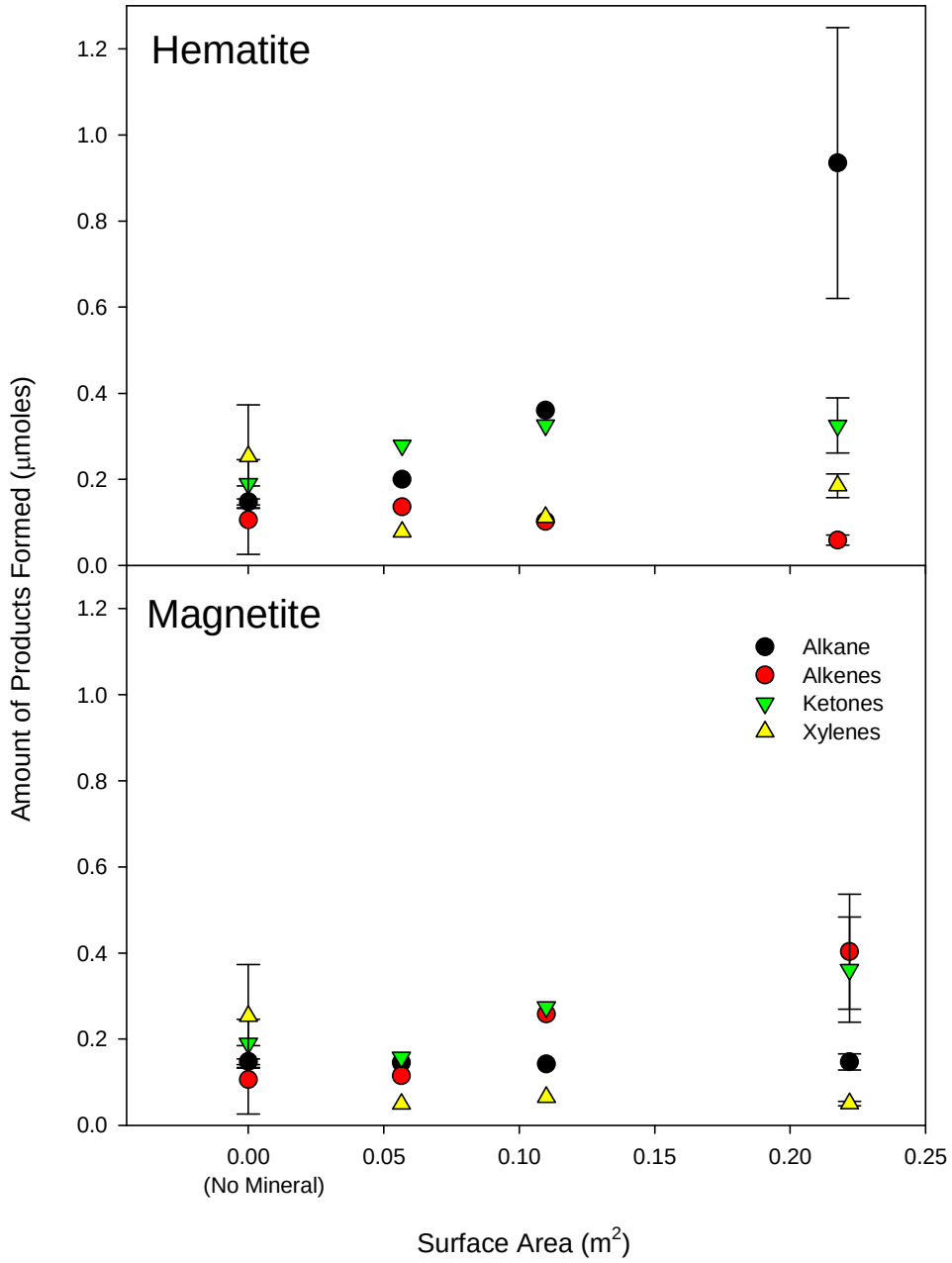

Figure 15. Products formed from hydrothermal reaction (300°C, 100 MPa) of *trans*-1,2-dimethylcyclohexane with iron oxide minerals, as a function of surface area used. Error bars on "No Mineral" are based on 5 replicate experiments. Error bars on 0.22 m^2 surface area points are based on 3 replicate experiments.

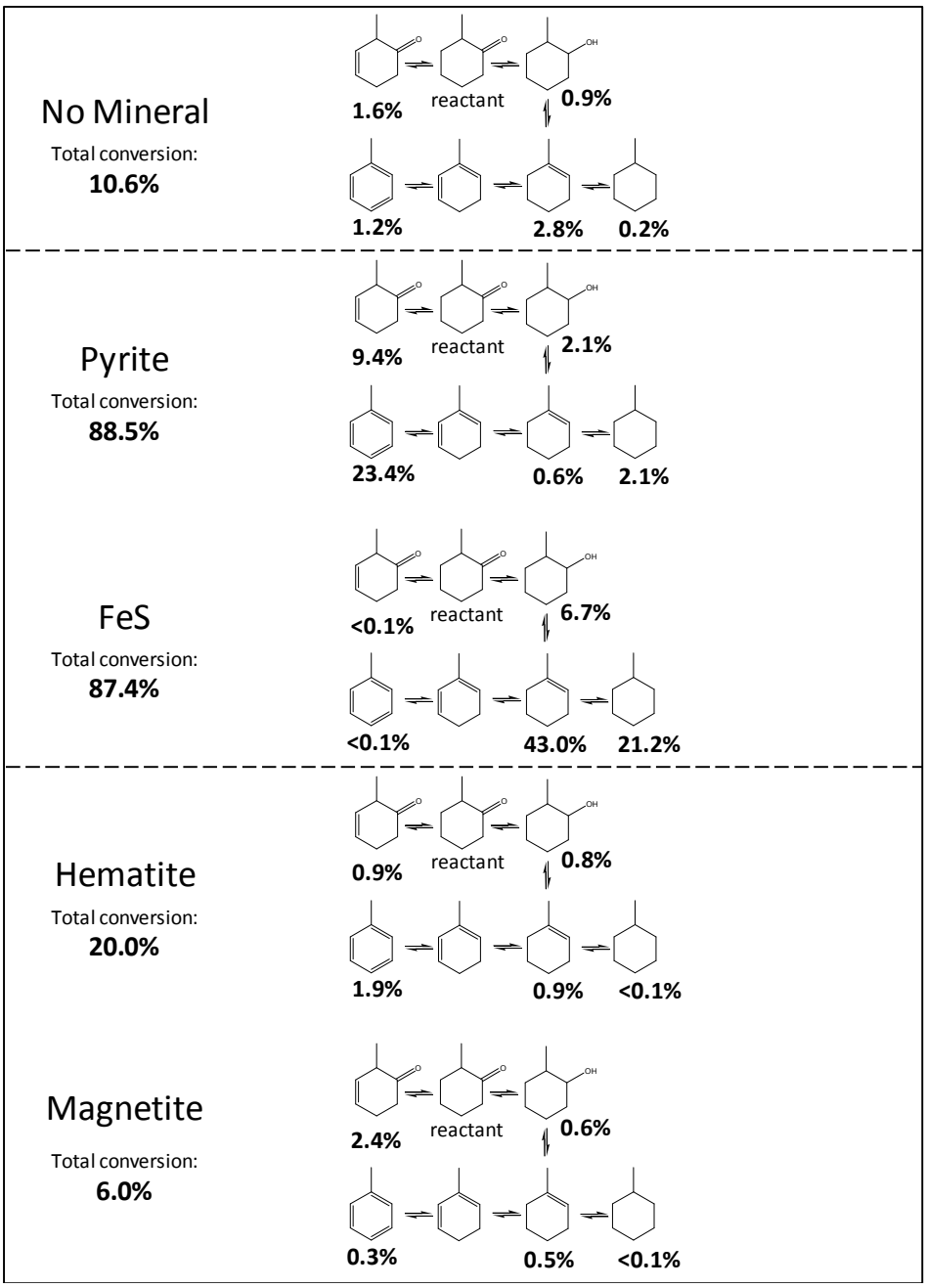

Figure 16. Product distributions for the hydrothermal reaction (300°C, 100 MPa) of 2-methylcyclohexanone without minerals (top panel), with iron sulfide minerals (middle panel), and with iron oxide minerals (bottom panel). Total conversion percentages are based on all products formed (Table 4) and not just the structures illustrated.

Chapter 4

SPHALERITE IS A GEOCHEMICAL CATALYST FOR CARBON-HYDROGEN BOND ACTIVATION

Abstract

Knowing how minerals influence the reactions of organic compounds in hydrothermal systems is a critical component of understanding the deep branch of Earth's global carbon cycle (Amend et al., 2011; Cody, 2004; Hazen and Sverjensky, 2010). Hydrothermal experiments show that both synthesis and decomposition of organic compounds are strongly influenced by the presence of minerals such as transition metal sulfides (Bell et al., 1994; Cody, 2004; Fu et al., 2008). However, there is essentially no predictive understanding of how minerals control the mechanisms of organic reactions, partly because geochemical organic reactions tend to be complex and difficult to study in detail (Burdige, 2006; LaRowe and Van Cappellen, 2011). Here we present the first experimental results that show how a mineral can catalyze the most fundamental component of an organic reaction mechanism–the breaking and making of single covalent bonds. We studied two simple alkanes, *cis*- and *trans*-1,2-dimethylcyclohexane. The stereochemistry of these molecules provides a marker that allows C-H bond cleavage to be probed. In the absence of mineral, hydrothermal reaction (in H_2O at 300˚C, 100 MPa) of either stereoisomer is slow, and generates a large number of products. In the presence of sphalerite (ZnS), the reaction rate is dramatically increased and only one product, the corresponding stereoisomer, is formed. Sphalerite acts as an efficient and highly-specific heterogeneous catalyst for cleavage of single carbon-hydrogen bonds in the dimethylcyclohexanes. The mineral rapidly catalyzes the reaction towards

thermodynamic equilibrium, allowing both the kinetics and thermodynamics of this primary mechanistic process to be fully characterized. Under these conditions, sphalerite is a robust catalyst for carbon-hydrogen bond activation (Bergman, 2007; Labinger and Bercaw, 2002).

Main Text

Organic compounds are almost ubiquitous in natural hydrothermal environments, in deep sedimentary systems, in subduction zones, at spreading centers, and at continental hot spots (Simoneit, 1993). Aqueous organic reactions in hydrothermal environments affect petroleum formation, degradation, and composition (Seewald, 2003; Simoneit, 1993), and provide energy and carbon sources for deep microbial communities (Horsfield et al., 2006). The essential components that control the chemical reactions of organic material in hydrothermal systems are the organic chemicals, hot pressurized water, and associated mineral assemblages. To date, there are many studies of organic reactions in water at high temperatures and pressures (Katritzky et al., 2001; Savage, 1999; Watanabe et al., 2004); however, only a very few of these have incorporated the critical inorganic mineral components present in natural systems. A few experiments have demonstrated sometimes spectacular influences of minerals on organic reactions (Cody et al., 2004; Schoonen et al., 2004; Seewald, 2001; Williams et al., 2005), but attempts to unravel exactly how minerals control functional group transformations are virtually non-existent. Here we describe a mechanistic study of the hydrothermal reactions of simple alkanes that reveals an efficient and highly specific catalytic effect of the mineral sphalerite (ZnS) on a fundamental organic reaction. Sphalerite is a common precipitate in sedimentary

exhalative base metal deposits (i.e., black smokers), along with other common sulfides ($CuFeS_2$, PbS, FeS_2, FeS,) (Breier et al., 2012; Tivey, 1995), and has been the focus of recent origins-of-life investigations (Mulkidjanian, 2009; Wang et al., 2012).

Recent work on the hydrothermal reactions of the model alkanes *cis*- and *trans*-1,2-dimethylcyclohexane at 300°C and 100 MPa in water alone, revealed very slow reactions (<5% conversion over 2 weeks), and the formation of a complex mixture of isomeric products including alkanes, alkenes, ketones, and aromatic functional groups (Shipp et al., 2013). A key finding of this previous work was that the functional group interconversions were reversible. However, equilibrium among the reaction products was not attained even on week-to-month timescales, although at longer reaction times, aromatic xylenes began to accumulate at the expense of other products.

Hydrothermal reaction of *cis*- or *trans*-1,2-dimethylcyclohexane in the presence of sphalerite yields very different results. First, the rate of the reaction is dramatically increased in the presence of the mineral (Figure 17). Second, essentially only one product is formed: the corresponding stereoisomer (*cis*- is formed from *trans*- and vice versa), in sharp contrast to the large number of products formed in the water-only experiments. Some small amounts of xylenes are formed in the reaction with sphalerite but almost four times less than observed in the water-only experiments, despite much higher conversions over a similar time period (see Table 5 for exact product distributions).

Formation of one stereoisomer from the other does not add or take away any atoms, therefore, sphalerite must be acting as a catalyst. The stereoisomerization reaction requires either carbon-carbon bond cleavage, followed by bond reformation, or carbon-hydrogen bond cleavage, and reformation. To test which bond-breaking process is

responsible for the reaction, experiments were performed with the *cis*- and *trans*-1,2-dimethylcyclohexane reactants in D_2O with sphalerite. Deuterium incorporation was found in the isomerized products, with the majority of the products containing only one deuterium for a reaction time of 24 hours. Preferential single deuterium incorporation was also observed in the remaining starting material. These results are consistent with a mechanism in which sphalerite catalyzes breaking of a carbon-hydrogen bond to form a common intermediate (I) that can either revert to the same starting structure, or form the isomer by reformation of the carbon-hydrogen bond (Figure 18). The hydrogen that adds to the common intermediate is not the original hydrogen atom, but rather must be derived from the solvent, since essentially all of the products incorporated at least one deuterium. Small amounts of product with 2 deuterium atoms were also observed after 24 hours of reaction, indicating replication of the exchange process with sequential incorporation of a single deuterium. Reeves et al. (2012) recently reported deuterium incorporation in alkanes under hydrothermal conditions, which was attributed to addition of solvent-derived deuterium to the corresponding alkenes that were also observed under equilibrium conditions. The selective incorporation of a single deuterium in the dimethylcyclohexanes shows that formation of an alkene is not necessary for deuterium incorporation in the presence of sphalerite (alkenes are not detected anyway), confirming catalytic breaking and making of single C-H bonds in the presence of the mineral.

The reaction rate is increased sufficiently in the presence of sphalerite that thermodynamic equilibrium is readily attained; i.e., the mineral *catalyzes* the approach to equilibrium. Starting with the *cis*-1,2 dimethylcyclohexane, only the *trans*-isomer forms in appreciable quantities, and the ratio of *cis*- to *trans*-isomers attains a constant value of

0.354 by day 14 (Figure 19). Starting with the *trans*-isomer, the *cis*-isomer is the only appreciable product, and essentially the same *cis*- to *trans*- ratio of 0.341 is observed over the same time-scale. The apparent equilibrium constant, K_{eq}, must equal the activity product for the reaction *trans*⇆*cis*; therefore, if activity is equated with concentration, K_{eq} = [*cis*]/[*trans*] = 0.348 (the average experimental ratio). The rate law for approach to equilibrium contains both the forward (*k*) and reverse (*k'*) reactions, Figure 19: d[A]/dt = -*k*[A] + *k'*[B]. At infinite t, this expression is reduced to $[A]_\infty = k'[A]_o/(k + k')$ and $[B]_\infty = k[A]_o/(k = k')$; thus $K_{eq} = [B]_\infty/[A]_\infty = k/k'$. The best fit values to the time-resolved data of Figure 19 are, k = 0.0215 hr^{-1} and k' = 0.0078 hr^{-1}, yielding: k/k' = 0.363. The slight difference between K_{eq} derived from the kinetic model (0.363) and that obtained from the measured concentration ratio (0.348) is probably due to the small amounts of xylenes formed in the reaction. The free energy difference between the *cis*- and *trans*-isomers is thus determined to be 4.8 kJ mol^{-1}.

The surface area of the sphalerite used in these experiments, measured using an N_2 BET isotherm, is 12.68 m^2g^{-1}, and so the total mineral surface area available in the experiments is 0.11 m^2. At the concentrations used in the experiments, the area occupied by *trans*-1,2-dimethylcyclohexane is ca. 28 $Å^2$. The total area of the dimethylcyclohexane is ca. 8.3 m^2. Thus, there are many more reactant molecules than can be accommodated by the mineral surface, which means there must be many more molecules than surface active sites. Assuming the mineral surface area available to the dimethylcyclohexane is the same as that available to nitrogen (it is probably smaller), and assuming the area of an active site is the area of a dimethylcyclohexane (it may be larger), the number of active sites on the mineral is less than 3×10^{17}. The number of reactant molecules is ca. 3×10^{19},

and all of these must react at least once by the time equilibrium is reached. This means that each active site must catalyze at least 100 reactions, and probably many more as equilibrium is approached.

Experiments were performed to distinguish between heterogeneous (surface) and homogeneous catalysis mechanisms. The reaction rate prior to equilibrium was found to increase essentially linearly with the mass of sphalerite loaded into the reaction container, Figure 20. The equilibrium concentrations of the stereoisomers are the same at different mineral loadings, equilibrium is just attained more rapidly with more mineral. The available surface area increases linearly with added mineral, whereas the activity of mineral-derived dissolved species at equilibrium is independent of the amount of mineral; this observation argues strongly for a surface catalyzed reaction. Using data and parameters from Shock et al. (1997) and Sverjensky et al. (1997), we calculate an equilibrium concentration of aqueous Zn^{2+} that would be present as a result of sphalerite dissolution at 300^{o}C and 100 MPa to be 4.4 x 10^{-6} mol L^{-1}. Experiments were performed with no mineral, but in the presence of 0.6, 6.0 and 60 mg/L of $ZnCl_2$, which correspond to 1, 10 and 100 times the calculated equilibrium concentration of Zn^{2+} ions, respectively. These experiments gave results that were indistinguishable from water alone, indicating that the sphalerite catalysis was not due to the aqueous Zn^{2+} ions.

Mechanistic study of mineral catalysis of hydrothermal organic reactions is a new field in geochemistry, which has possible implications for green chemistry. The catalysis of carbon-hydrogen bond activation, for example, has been the subject of extensive research, and a wide range of potential catalysts have now been synthesized, mostly based on organometallic chemistry (Bergman, 2007; Labinger and Bercaw, 2002).

Although the reactions described here are rapid and unusually selective in a geochemistry context, the timescales and reaction temperatures are not yet particularly useful for general catalysis. However, the sphalerite used here is not optimized, particularly in terms of surface area. More importantly, minerals are extremely inexpensive, robust and require no synthesis compared to conventional organometallic catalysts. The results described here therefore suggest that the use of naturally occurring and relatively abundant minerals that are appropriately optimized may represent a new approach to the development of useful heterogeneous catalysts for a wide range of organic transformations.

Methods Summary

50 µmoles of reactant, (*trans*- or *cis*-dimethylcylohexane; Aldrich, 99%) plus ZnS synthetic powder (Alfa Aesar, 99.99%) and 250 µL Ar-purged 18.2 MΩ·cm water were sealed into Ar-purged gold capsules by welding. The capsules (3.35 cm x 5 mm OD x 4 mm ID) were placed in a stainless steel, cold-seal reaction vessel, pressurized to 100 MPa with DI water, and heated to 300°C. At each time point, the vessel was quenched, two capsules (one of each reactant) were removed, and the vessel was reheated to 300°C. Capsules were rinsed with dichloromethane (DCM) and frozen in liquid N_2 before opening in 3 mL DCM and 5.9 µL *n*-decane (internal standard). Products were quantified by gas chromatography (GC) with flame ionization detection (Varian CP-3800, 5% diphenyl/95% dimethylsiloxane column, Supelco, Inc). For details see Shipp et al. (2013). For D_2O experiments, D_2O was substituted for H_2O and extracts were analyzed

via GC-mass spectrometry (Agilent 6890/5973) using the same column and temperature protocols.

The ZnS was confirmed to be sphalerite by X-ray diffraction (Siemens D5000 with Cukα radiation) and <0.001% other metals by ICP-MS (Thermo X-Series). BET surface area was also measured by N_2 adsorption (Tristar II 3020).

References

Amend, J.P., McCollom, T.M., Hentscher, M., Bach, W. (2011) Catabolic and anabolic energy for chemolithoautotrophs in deep-sea hydrothermal systems hosted in different rock types. *Geochim. Cosmochim. Acta* **75**, 5736-5748.

Bell, J.L.S., Palmer, D.A., Barnes, H.L., Drummond, S.E. (1994) Thermal-decomposition of acetate .3. catalysis by mineral surfaces. *Geochim. Cosmochim. Acta* **58**, 4155-4177.

Bergman, R.G. (2007) Organometallic chemistry: C-H Activation. *Nature* **446**, 391–393.

Breier, J.A., Toner, B.M., Fakra, S.C., Marcus, M.A., White, S.N., Thurnherr, A.M., German, C.R. (2012) Sulfur, sulfides, oxides and organic matter aggregated in submarine hydrothermal plumes at 9 degrees 50 ' N East Pacific Rise. *Geochim. Cosmochim. Acta* **88**, 216-236.

Burdige, D.J. (2006) Geochemistry of marine sediments. Princeton University Press, Princeton, NJ.

Cody, G.D. (2004). Transition metal sulfides and the origins of metabolism. *Annu. Rev. Earth Planet. Sci.* **32**, 569-599.

Cody, G.D., Boctor, N.Z., Brandes, J.A., Filley, T.R., Hazen, R.M., H. S. Yoder, J. (2004) Assaying the catalytic potential of transition metal sulfides for abiotic carbon fixation. *Geochim. Cosmochim. Acta* **68**, 2185-2196.

Fu, Q., Foustoukos, D.I., Seyfried, W.E. (2008) Mineral catalyzed organic synthesis in hydrothermal systems: An experimental study using time-of-flight secondary ion mass spectrometry. *Geophys. Res. Lett*. **35**.

Hazen, R.M., Sverjensky, D.A. (2010) Mineral surfaces, geochemical complexities, and the origins of life. Cold Spring Harbor Perspect. *Biol*. **2**.

Horsfield B., Schenk H. J., Zink K., Ondrak R., Dieckmann V., Kallmeyer J., Mangelsdorf K., Primio R. D., Wilkes H., Parkes R. J., Fry J. and Cragg B. (2006) Living microbial ecosystems within the active zone of catagenesis: Implications for feeding the deep biosphere. *Earth Planet Sc. Lett.* **246 (**1–2), 55-69.

Katritzky A. R., Nichols D. A., Siskin M., Murugan R. and Balasubramanian M. (2001) Reactions in high-temperature aqueous media. *Chem. Rev.* **101**, 837-892.

Labinger, J.A., Bercaw, J.E. (2002) Understanding and Exploiting C-H Activation. *Nature* **417**, 507–514.

LaRowe, D.E., Van Cappellen, P. (2011) Degradation of natural organic matter: A thermodynamic analysis. *Geochim. Cosmochim. Acta* **75**, 2030-2042.

Mulkidjanian, A.Y. (2009) On the origin of life in the Zinc world: I. Photosynthesizing, porous edifices built of hydrothermally precipitated zinc sulfide as cradles of life on Earth. *Biol. Direct* **4**.

Reeves, E.P., Seewald, J.S., Sylva, S.P. (2012) Hydrogen isotope exchange between n-alkanes and water under hydrothermal conditions. *Geochim. Cosmochim. Acta* **77**, 582–599.

Savage P. E. (1999) Organic chemical reactions in supercritical water. *Chem. Rev*. **99**, 603-621.

Schoonen, M., Smirnov, A., Cohn, C. (2004) A perspective on the role of minerals in prebiotic synthesis. *Ambio* **33**, 539-551.

Seewald J. S. (2001) Aqueous geochemistry of low molecular weight hydrocarbons at elevated temperatures and pressures: Constraints from mineral buffered laboratory experiments. *Geochim. Cosmochim. Acta* **65**, 1641-1664.

Seewald J. S. (2003) Organic-inorganic interactions in petroleum-producing sedimentary basins. *Nature* **426**, 327-333.

Shipp, J., Gould, I.R., Herckes, P., Shock, E.L., Williams, L.B., Hartnett, H.E. (2013) Organic functional group transformations in water at elevated temperature and pressure: Reversibility, reactivity, and mechanisms. *Geochim. Cosmochim. Acta* **104**, 194-209.

Shock E. L., Sassani D. C., Willis M., and Sverjensky D. A. (1997) Inorganic species in geologic fluids: Correlations among standard molal thermodynamic properties of aqueous ions and hydroxide complexes. *Geochim. Cosmochim. Acta* **61**, 907-950.

Simoneit, B.R.T. (1993) Aqueous high-temperature and high-pressure organic geochemistry of hydrothermal vent systems. *Geochim. Cosmochim. Acta* **57**, 3231-3243.

Sverjensky, D.A., Shock, E.L., Helgeson, H.C. (1997) Prediction of the thermodynamic properties of aqueous metal complexes to 1000°C and 5 kb. *Geochim. Cosmochim. Acta* **61**, 1359-1412.

Tivey, M.K. (1995) The influence of hydrothermal fluid composition and advection rates on black smoker chimney mineralogy: Insights from modeling transport and reaction. *Geochim. Cosmochim. Acta* **59**, 1933-1949.

Wang, W., Li, Q., Yang, B., Liu, X., Yang, Y., Su, W. (2012) Photocatalytic reversible amination of alpha-keto acids on a ZnS surface: implications for the prebiotic metabolism. *Chem Commun (Camb)* **48**, 2146-2148.

Watanabe M., Sato T., Inomata H., Smith, Jr., R. L., Arai K., Kruse A. and Dinjus E. (2004) Chemical reactions of C_1 compounds in near-critical and supercritical water. *Chem Rev.***104**, 5803-5821.

Williams, L.B., Canfield, B., Voglesonger, K.M., Holloway, J.R. (2005) Organic molecules formed in a "primordial womb". *Geology* **33**, 913-916.

Acknowledgements

We thank the members of the Hydrothermal Organic Geochemistry group for discussion on this research. This work was funded by NSF grant 0826588.

Table 5. Reaction conditions and products of *cis*- and *trans*-1,2-dimethylcyclohexane in water, at 300°C and 100 MPa, with and without sphalerite (ZnS).

					Products, µmoles (±SD)[a]							
Reactants		Time (d)	MB (%)	% Reacted	*trans*-alkane	*cis*-alkane	alkane isomers	1,2-alkene	alkene isomers	*o*-xylene	xylene isomers	ketone isomers
Water + ZnS	*cis*	1.8	97.4	52.8	25.4 (0.2)	**23.0**[b] **(0.1)**	nd[c]	nd	nd	0.162 (0.002)	0.080 (0.009)	0.032 (0.005)
		3.0	99.3	65.7	32.4 (0.9)	**17.1 (0.4)**	nd	nd	nd	0.153 (0.005)	0.068 (0.002)	trace
		7.0	97.8	72.3	35.1 (0.6)	**13.5 (0.2)**	nd	nd	nd	0.16 (0.04)	0.095 (0.004)	trace
		14.0	98.3	74.0	36.1 (0.2)	**12.78 (0.05)**	nd	nd	nd	0.169 (0.0008)	0.096 (0.003)	trace
	trans	1.8	96.7	19.1	**38.9 (0.1)**	8.99 (0.02)	nd	nd	nd	0.141 (0.007)	0.068 (0.007)	nd
		3.0	95.7	22.3	**37.0 (0.2)**	10.37 (0.06)	nd	nd	nd	0.152 (0.007)	0.077 (0.006)	nd
		7.0	97.4	25.5	**36.2 (0.2)**	12.15 (0.05)	nd	nd	nd	0.144 (0.005)	0.066 (0.006)	nd
		14.0	99.3	25.8	**36.7 (0.5)**	12.5 (0.1)	nd	nd	nd	0.151 (0.007)	0.084 (0.008)	trace
Water only[d]	*cis*	1.0	94.1	2.5	0.76 (0.02)	**55.9 (0.9)**	0.055 (0.006)	0.009 (0.002)	0.17 (0.02)	0.264 (0.002)	0.199 (0.002)	trace
		2.0	83.8	3.1	0.827 (0.004)	**49.6 (0.3)**	0.056 (0.003)	0.021 (0.001)	0.11 (0.03)	0.46 (0.01)	0.103 (0.002)	trace
		6.0	86.5	4.5	1.164 (0.007)	**50.4 (0.2)**	0.165 (0.002)	0.0168 (0.0009)	0.241 (0.006)	0.640 (0.001)	0.151 (0.003)	nd
		16.0	84.4	4.6	1.35 (0.03)	**49.1 (0.9)**	0.194 (0.006)	0.013 (0.002)	0.282 (0.008)	0.441 (0.005)	0.110 (0.002)	nd
	trans	1.0	96.5	0.6	**57.6 (0.1)**	0.0883 (0.0005)	trace	0.040 (0.001)	0.091 (0.009)	0.08 (0.01)	trace	0.04 (0.03)
		2.0	97.0	1.1	**57.6 (0.3)**	0.093 (0.008)	0.02 (0.01)	0.053 (0.004)	0.16 (0.01)	0.272 (0.006)	0.046 (0.002)	trace
		10.0	99.9	1.8	**58.84 (0.09)**	0.22 (0.02)	0.152 (0.005)	0.010 (0.002)	0.096 (0.008)	0.450 (0.004)	0.152 (0.002)	nd
		19.0	96.4	1.9	**56.8 (0.5)**	0.237 (0.004)	0.180 (0.006)	0.007 (0.004)	0.13 (0.01)	0.395 (0.008)	0.134 (0.005)	nd
		24.0	99.0	2.0	**58.2 (0.3)**	0.327 (0.004)	0.213 (0.009)	0.007 (0.002)	0.160 (0.002)	0.351 (0.002)	0.147 (0.002)	nd

MB- mass balance,[a]standard deviation in parenthesis is based on analytical error between triplicate injections [b]**Bold**= remaining starting reactant, [c]nd = not detected, [d]Water-only results used for comparison, previously published by Shipp et al (2013).

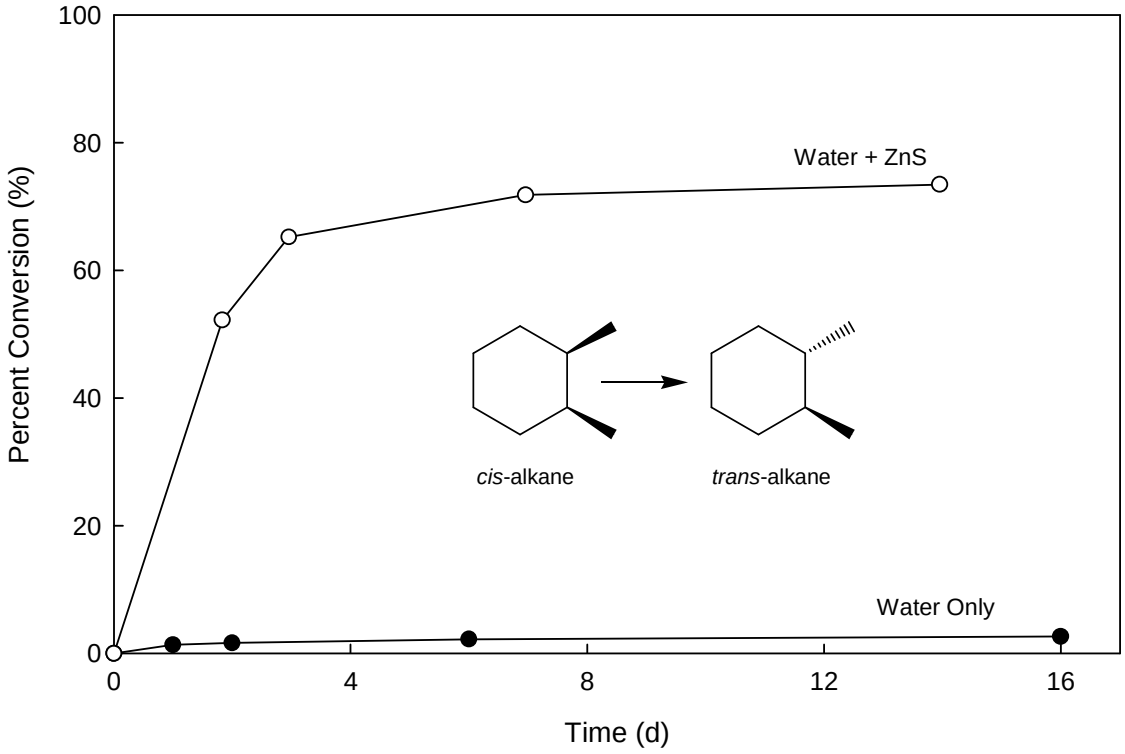

Figure 17. Sphalerite enhancement of stereoisomerization. The extent of conversion of *cis*-1,2-dimethylcyclohexane to the *trans*- stereoisomer, reacted with sphalerite (open symbols) and without sphalerite (closed symbols), under aqueous hydrothermal conditions (300°C and 100 MPa).

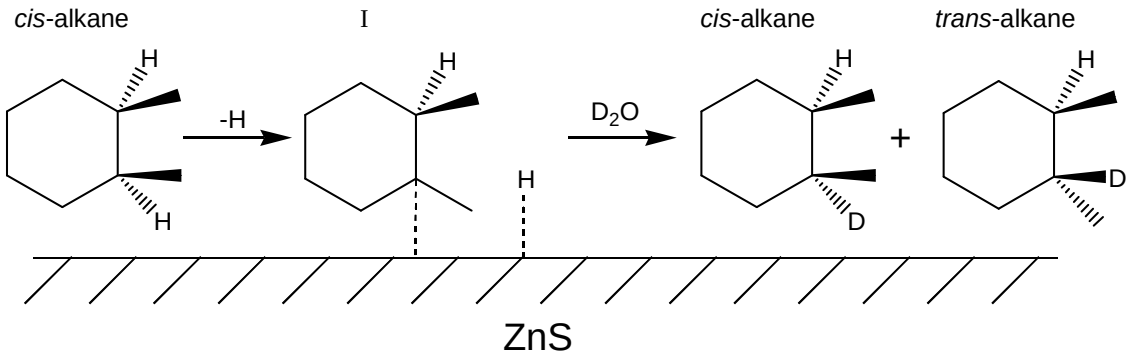

Figure 18. Reaction scheme for C-H bond cleavage on the surface of sphalerite. The surface bound intermediate (I) reacts with solvent derived deuterium to form either stereoisomer with incorporation of a single deuterium.

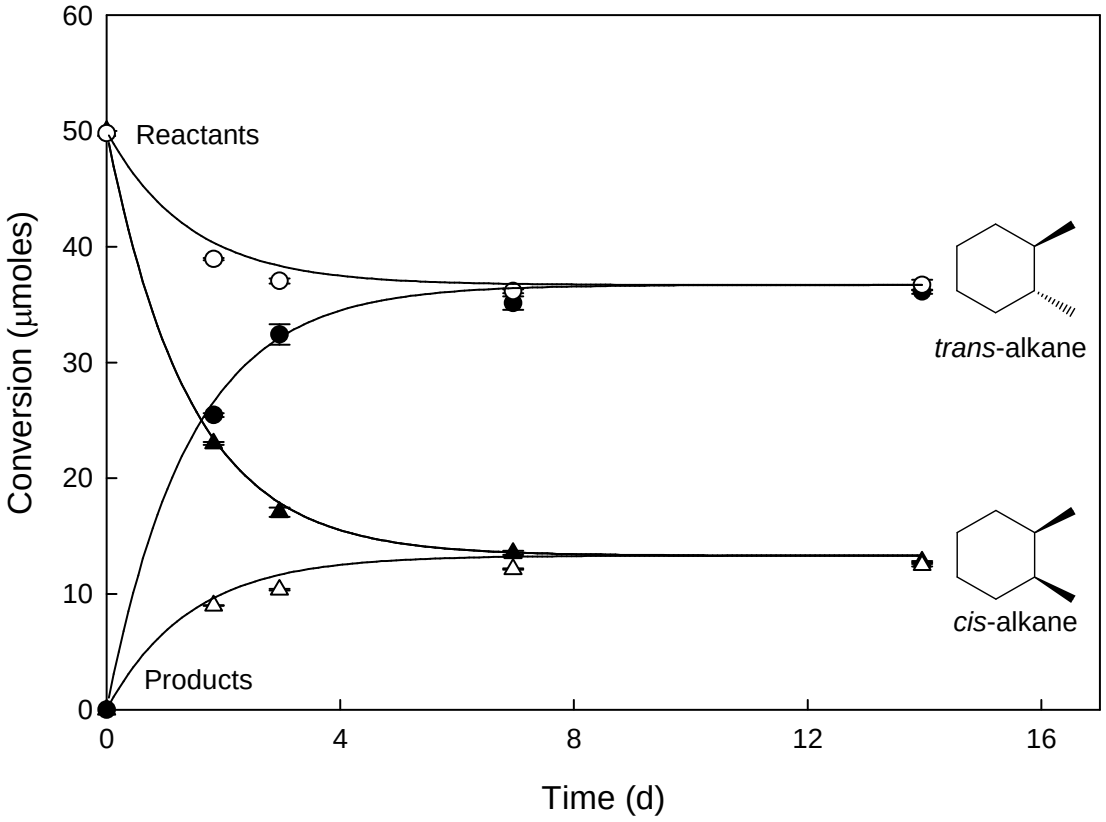

Figure 19. The path to equilibrium for either stereoisomer reacted in water with sphalerite under hydrothermal conditions (300°C and 100 MPa). Experiments with the *cis*-alkane as the reactant have solid symbols; those with the *trans*-alkane as the reactant have open symbols. Concentrations of *trans*-alkane are triangles and concentrations of *cis*-alkane are circles. Error bars are analytical error between replicate analyses.

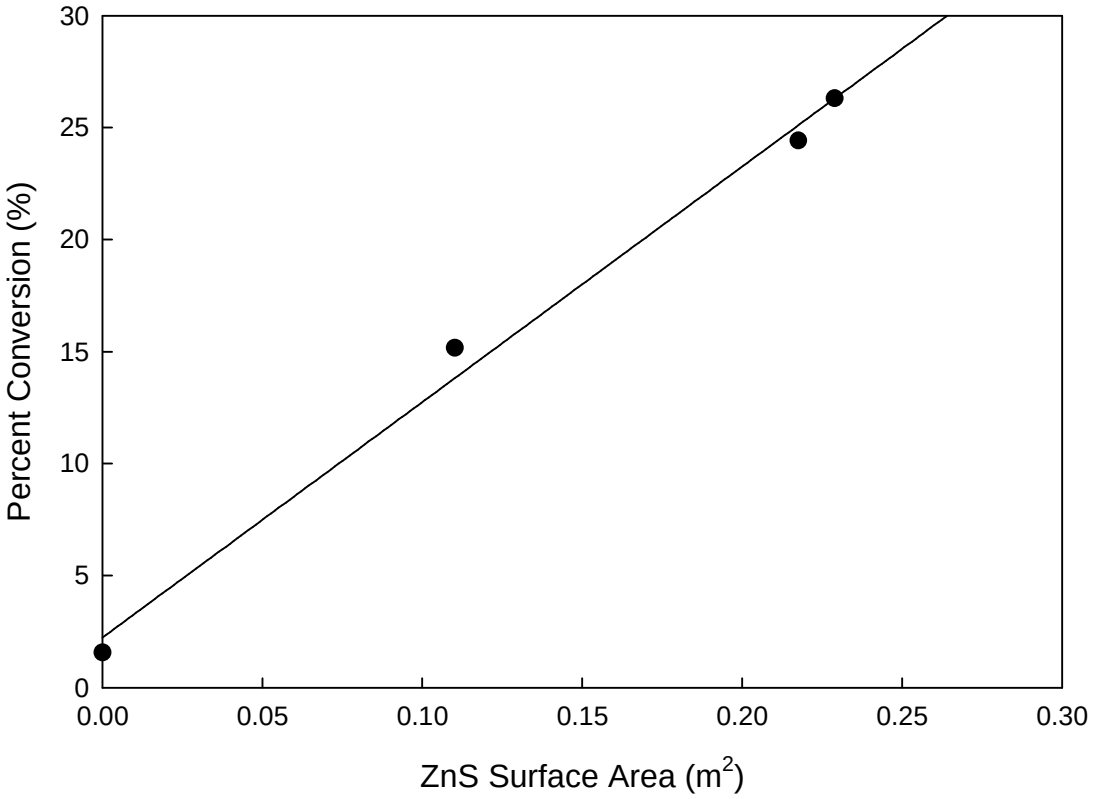

Figure 20: The amount of *trans*-1,2-dimethylcyclohexane conversion in 24 h at 300°C and 100 MPa, with various sphalerite surface areas. Zero surface area represents no mineral (water only) results. Least squares trend line has an R^2 of 0.9928

Chapter 5

CONCLUSION

What have I learned?

Throughout this body of work one thing is consistent: none of it would be possible without water. Not only does water act as a solvent and reaction medium, it is also an active participant in the reactions. Hydration and dehydration reactions use H_2O directly as a reactant and product, and H_2O participates indirectly as a source of hydrogen for reduction reactions. In room temperature water the reactions studied wouldn't be possible. To do the reactions detailed in this thesis using classical organic chemistry methods one would need to utilize strong oxidants, catalysts and reducing agents. Figure 21 depicts the reactions that are necessary to carry out the individual steps of the hydrothermal reactions observed in this study. Cyclohexane based organics are used as the example structures in the figure and are directly comparable with the methyl and dimethylcyclohexane structures used throughout this work. Dehydrogenation of an alkane is typically difficult, the most recent and promising method involves heating the solution over a palladium and titanium dioxide catalyst (Dummer et al., 2010). A multiple step process is then required to make an alcohol from an alkene. The first step uses mercury (II) acetate and water, followed by a second step adding sodium borohydride. To then turn the alcohol into a ketone one then needs sulfuric acid and sodium dichromate. The reverse of these reactions are just as complex. To dehydrogenate an aromatic ring, organic chemists use high pressure hydrogen gas and a platinum catalyst. To reduce a ketone to alcohol, sodium borohydride is used in an ethanol solution, and then to dehydrate the alcohol, concentrated sulfuric acid is added and the solution is heated. Note

that in Figure 21 most of the procedures involve expensive, sometimes toxic reagents and multiple steps. Many of the reactions aren't even possible at ambient conditions (25°C and 0.1 MPa), and additional heat is necessary to promote the reaction. In chapter 2 however, I showed that not only was it possible to go from an alkane to a ketone, but it happens quite readily, and reversibly, in HPW (300°C and 100 MPa) without adding any other reagents or catalysts. Going from a cyclic alkane to an aromatic ring also happens readily at my hydrothermal conditions without added reagents or catalysts. This is a vast improvement over having to work with things like chromium (IV), mercury, palladium , platinum, and concentrated sulfuric acid.

Not only did I eliminate the reagents typically necessary to conduct the functional group transformations depicted in Figure 21, I showed that the addition of minerals to the reaction system can be a powerful tool for product selectivity. I was able to enhance or suppress formation of specific functional group products using naturally abundant, nontoxic minerals. Pyrite (FeS_2) and troilite (FeS) for example can be used to eliminate the formation of ketone functional groups when oxidizing alkanes. FeS also prevents the alkene from further oxidizing to the aromatic products, so that oxidation of the alkane stops with formation of the alkene. Pyrite on the other hand, allows the alkane to be fully oxidized all the way to the aromatic products. Conversely, hematite and magnetite favor formation of the ketones. Therefore, if one wanted to reduce a ketone, they shouldn't use one of the iron oxides, they should use one of the iron sulfides which drive ketone dehydration either to the alkene/alkane (FeS), or to aromatic products (pyrite). These results not only provide useful organic chemistry tools, but all the methods are compatible with "green" chemistry techniques in that they eliminate hazardous reagents,

catalysts, and solvents. Of course, there is a substantial energy input required to carry out the reactions at 300°C, but many of the classical organic reactions also require energy input in the form of heat.

In natural environments, the findings that certain minerals can direct a reaction may have promising predictive uses. For example, I wouldn't expect the natural organic material found in a hydrothermal system composed mostly of pyrite and pyrrhotite ($Fe_{1-x}S$, a more common crystal structure of troilite) to contain many ketone functional groups. On the other hand, a system composed mostly of iron oxides may contain plenty of ketones. These minerals are often found in seafloor hydrothermal systems and petroleum formations (Breier et al., 2012; Kvenvolden et al., 1990; Simoneit, 1993; Tivey, 1995), but more needs to be done to characterize the natural organic functional groups also present in environments with different mineral assemblages to test this theory.

Origins of life investigators have theorized that minerals may act as catalysts for organic reactions in hydrothermal systems (Cody, 2004; Lahav, 1994; Russell et al., 1993). This work confirms that, indeed, minerals have an effect on the reactivity of organic compounds. The results of my mineral/organic reactions in Chapters 3 and 4 provide further evidence that minerals common to hydrothermal vents can be heterogeneous catalysts for organic reactions. Sphalerite, pyrite, and hematite activated carbon-hydrogen bonds which are among the most basic, fundamental bonds in organic chemistry. The development of catalysts that can activate C-H bonds is currently an active area of research. To date, typical methods involve organo-metallic catalysts that use expensive metals, (Re, Fe, Ru, Os, Rh, Ir, Pt) and are almost always unstable

(Bergman, 2007; Labinger and Bercaw, 2002). Sphalerite hasn't yet been optimized as an *efficient* catalyst for C-H bond activation, but in my experiments it's the most effective of the minerals studied, and compared to the organo-metallic catalysts currently being used, it is by far the most abundant and robust.

Future Work

As is typical with novel scientific research, this work generates as many questions as it answers, and leaves room for much future investigation. Toluene and xylene were never able to be reduced in water alone, or even when a mineral was present. This was surprising since FeS inhibited the production of xylene/toluene but could not reduce the aromatic ring when xylene/toluene was the starting reactant. This leaves open the question of whether or not the oxidation of cyclic alkanes to their corresponding aromatic rings is a completely reversible reaction. The only evidence of reversibility from aromatic ring formation was the decrease in xylene concentration shown in the time-series plot of the hydrothermal reaction of *cis*- and *trans*-cyclohexane in water (Figure 9). There was no evidence as to where the xylene was going however; it could have been reduced, or it could have formed dimer or benzene products that were not quantified. Reactions starting with xylene and toluene in water alone, or with pyrite, FeS, or sphalerite, have, thus far, yielded no reaction to detectable quantities of reduced products, even over week-long timescales. This absence of evidence is not, however, proof of irreversibility. Perhaps in a system with alkanes, alkenes, and ketones there are enough sources of hydrogen that the aromatic ring is more reactive. Perhaps future experiments utilizing other hydrogen sources or tracking the progress of xylene molecules after their formation could yield

insight into whether the reaction from a diene to xylene/toluene is truly a reversible reaction.

Thermodynamic calculations of the temperature and hydrogen fugacity dependence of cyclohexane-benzene and methylcyclohexane-toluene equilibrium suggests that by lowering the temperature of my experiments I may be able to push the equilibrium in favor of cyclohexane (Figure 22). Also shown in Figure 22 are the temperature and hydrogen fugacity dependence of common mineral assemblages, pyrite-pyrrhotite-magnetite (PPM) and hematite-magnetite (HM). In order to push the equilibrium in favor of cyclohexane instead of benzene, I might be able to use PPM, or FeS alone, at around 200°C. At 300°C, the conditions used in this study, it is evident that the iron sulfide, and especially the iron oxide, minerals alone wouldn't be able to produce a high enough hydrogen fugacity to reduce the aromatic rings.

Mechanistic details of many of the reactions studied here still remain elusive. Many of the reactions involve adding and removing hydrogen atoms; however, it is unclear if hydrogenation/dehydrogenation proceeds via a hydrogen radical, a cation, or an anion. If hydrogen radicals are involved, radical trapping methods (like addition of an O_2 source) could be investigated for use in these types of experiments. If instead, the reactions are dependent on hydrogen cations, experiments at various pH could prove to be useful avenues for future work. Experiments using addition of NaOH may also indicate if hydrogen cations or anions were involved, by increasing or decreasing the rates of the hydrogen ion's removal; I would expect excess OH^- to encourage removal of H^+ but not of H^-.

Complicating the mechanistic story even further, are the surface interactions between organic compounds and minerals. How and why exactly do the minerals change the rate of reactions and type of reaction pathways available? In Chapter 3 I noted a positive correlation between the abundance of certain products and the amount of available surface. Unfortunately, in order to vary surface area in these experiments, the amount of mineral also changed, causing simultaneous changes in bulk composition. Future studies could utilize a single mineral ground to various surface areas so that the amount of material used could be held constant while varying surface area. That way surface area affects could be better separated from bulk composition effects. Mineral surface properties at these conditions may also be insightful for determining the types of organic-mineral interactions that are involved. Investigations into surface catalysis experimental techniques and semiconductor properties inherent to each mineral might help explain the observed mineral effects on my organic reactions. For example, oxidizing and reducing power of semiconducting minerals can be related to conduction and valence band edge energies (Xu and Schoonen, 2000; Xu et al., 1996)

A mystery that still lingers in my mind is that of the “missing” carboxylic acids. Seewald (2001) showed formation of carboxylic acid products in experiments using similar aqueous temperature and pressure conditions to my experiments, but with an added pyrite-pyrrhotite-magnetite (PPM) mineral buffer. He suggested the acids were forming directly from the ketones that were generated as oxidation products of their starting alkanes. He came to this conclusion by observing a decrease in ketone concentration at the same time as an increase in carboxylic acid concentration. Throughout the chapters presented here, I show no detectable levels of carboxylic acid

products, with minerals or without, even when my starting reactant was a ketone. There was however, one experiment, not reported in any of my published data sets, that formed large quantities of a carboxylic acid. The reactant was *trans*-1,2-dimethylcyclohexane, in a 24 hour long experiment with 0.22 m^2 surface area of pyrite. The carboxylic acid generated was toluic acid, and it was by far the major product. At the time, I considered this experiment to be a fluke. Four identical experiments were conducted, with only this one producing a carboxylic acid product. It was my hypothesis that something went "wrong" with this experiment that allowed the acid to form. The likely culprit is oxygen present in the capsule as a result of insufficient argon purging during experimental procedures. It would be useful to test this hypothesis and determine if carboxylic acid production is a result of a more oxidized environment than can be generated with pyrite alone. I suggested something to this effect in Chapter 2 after comparing the estimated redox state for my system with that generated in the Seewald (2001) experiments using a PPM buffer. Seewald's PPM conditions were more oxidizing than my no mineral conditions and I accounted this to be the likely cause of differences in carboxylic acid production.

Final Thoughts

In summary, this work contributes to a greater understanding of the behavior of organic molecules in natural hydrothermal environments. The multidisciplinary nature of this work leads to diverse implications and advances in organic chemistry, geochemistry, petrology, astrobiology, catalysis, and environmental and green chemistry. It also opens the door for future studies within an emerging subset of hydrothermal organic

geochemistry; one with an emphasis on mineral surface catalysis and mechanistic organic chemistry.

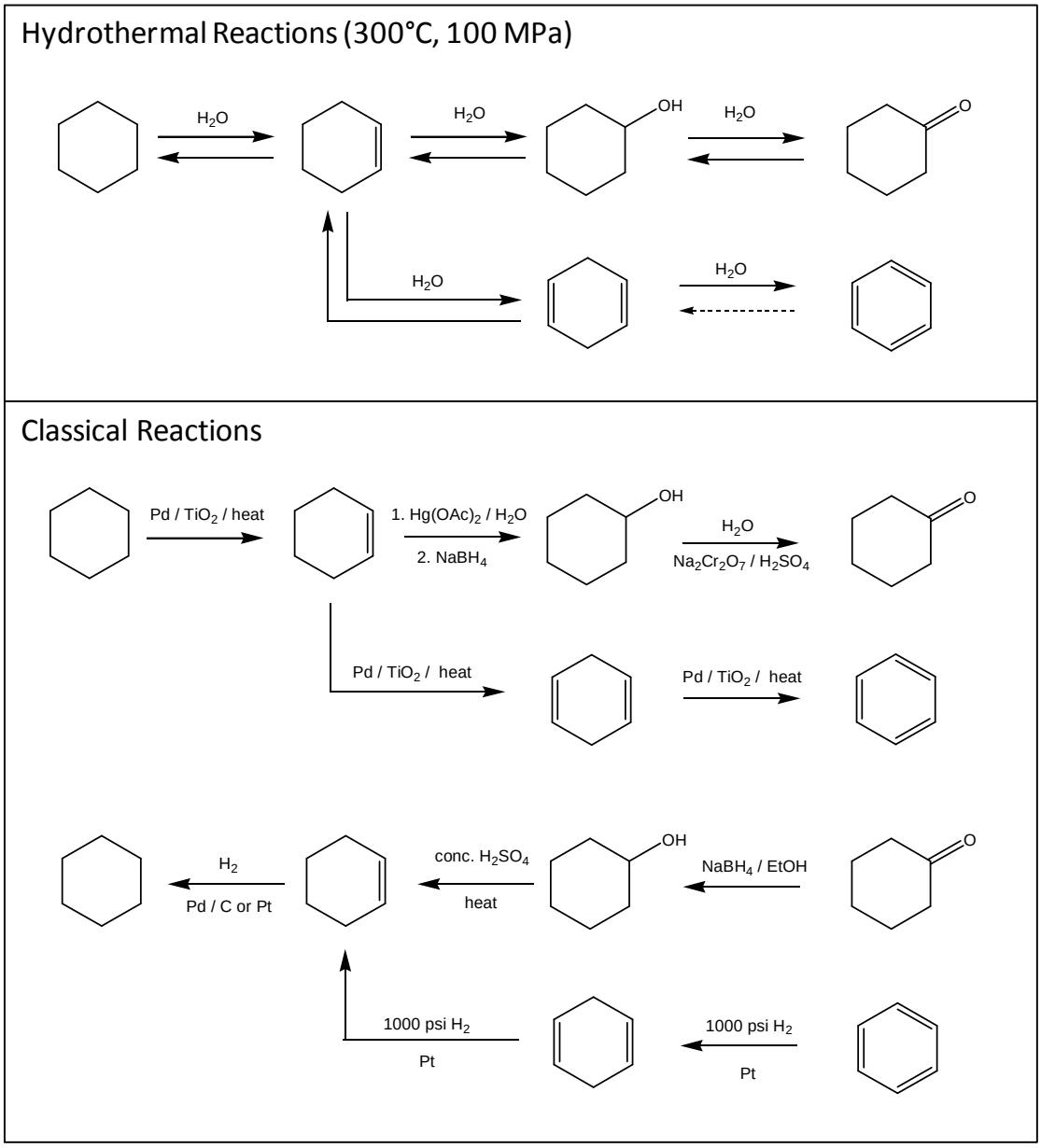

Figure 21. A comparison of the hydrothermal reactions developed in Chapter 2 (upper box) and classical organic chemistry reactions (lower box).

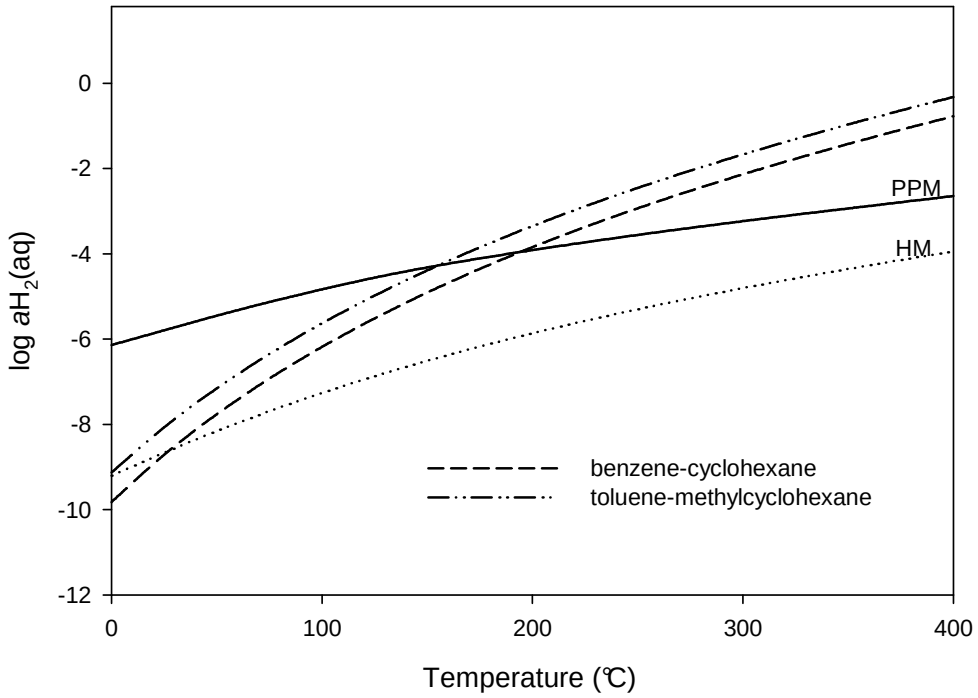

Figure 22. Temperature and hydrogen fugacity dependence of the pyrite-pyrrhotite-matnetite (PPM), hematite-magnetite (HM), benzene-cyclohexane, and toluene-methylcyclohexane equilibriums in water at 100 MPa pressure.

REFERENCES

Akiya N. and Savage P. E. (2001) Kinetics and mechanism of cyclohexanol dehydration in high-temperature water. *Ind. Eng. Chem. Res.* **40**, 1822-1831.

Amend, J.P., McCollom, T.M., Hentscher, M., Bach, W. (2011) Catabolic and anabolic energy for chemolithoautotrophs in deep-sea hydrothermal systems hosted in different rock types. *Geochim. Cosmochim. Acta* **75**, 5736-5748.

Antal, Jr., M. J., Carlsson M. and Xu X. (1998) Mechanism and kinetics of the acid-catalyzed dehydration of 1- and 2-propanol in hot compressed liquid water. *Ind. Eng. Chem. Res.* **37**, 3820-3829.

Andersson, E., Holm, N.G. (2000). The stability of some selected amino acids under attempted redox constrained hydrothermal conditions *Origins Life Evol. B.* **30**, 9-23.

Baross J. A. and Hoffman S. E. (1985) Submarine hydrothermal vents and associated gradient environments as sites for the origin and evolution of life. *Origins Life Evol. B.* **15**, 327-345.

Bebie, J., Schoonen, M.A. (2000) Pyrite surface interaction with selected organic aqueous species under anoxic conditions. *Geochemical Transactions* **1**, 47.

Bell, J.L.S., Palmer, D.A., Barnes, H.L., Drummond, S.E. (1994) Thermal-decomposition of acetate .3. catalysis by mineral surfaces. *Geochim. Cosmochim. Acta* **58**, 4155-4177.

Bergman, R.G. (2007) Organometallic chemistry: C-H Activation. *Nature* **446**, 391–393.

Breier, J.A., Toner, B.M., Fakra, S.C., Marcus, M.A., White, S.N., Thurnherr, A.M., German, C.R. (2012) Sulfur, sulfides, oxides and organic matter aggregated in submarine hydrothermal plumes at 9 degrees 50 ' N East Pacific Rise. *Geochim. Cosmochim. Acta* **88**, 216-236.

Burdige, D.J. (2006) *Geochemistry of Marine Sediments*. Princeton University Press, Princeton, NJ.

Chyba, C.F. (1993) The volent environment of the origin of life- progress and uncertainties. *Geochim. Cosmochim. Acta* **57**, 3351-3358.

Crittendon R. C. and Parsons E. J. (1994) Transformations of cyclohexane derivatives in supercritical water. *Organometallics* **13**, 2587–2591.

Cody, G.D. (2004). Transition metal sulfides and the origins of metabolism. *Annu. Rev. Earth Planet. Sci.* **32**, 569-599.

Cody, G.D., Boctor, N.Z., Brandes, J.A., Filley, T.R., Hazen, R.M., H. S. Yoder, J. (2004) Assaying the catalytic potential of transition metal sulfides for abiotic carbon fixation. *Geochim. Cosmochim. Acta* **68**, 2185-2196.

Cody, G.D., Boctor, N.Z., Filley, T.R., Hazen, R.M., Scott, J.H., Sharma, A., Yoder, H.S. (2000) Primordial carbonylated iron-sulfur compounds and the synthesis of pyruvate. *Science* **289**, 1337-1340.

Colwell, F.S., Onstott, T.C., Delwiche, M.E., Chandler, D., Fredrickson, J.K., Yao, Q.J., McKinley, J.P., Boone, D.R., Griffiths, R., Phelps, T.J., Ringelberg, D., White, D.C., LaFreniere, L., Balkwill, D., Lehman, R.M., Konisky, J., Long, P.E. (1997) Microorganisms from deep, high temperature sandstones: Constraints on microbial colonization. *Fems Microbiol. Rev.* **20**, 425-435.

D'Hondt S., Jørgensen B. B., Miller D. J., Batzke A., Blake R., Cragg B. A., Cypionka H., Dickens G. R., Ferdelman T., Hinrichs K.-U., Holm N. G., Mitterer R., Spivak A., Wang G., Bekins B., Engelen B., Ford K., Gettemy G., Rutherford W. D., Sass H., Skilbeck C. G., Aiello I. W., Guèrin G., House C. H., Inagaki F., Meister P., Naehr T., Niitsuma S., Parkes R. J., Schippers A., Smith D. C., Teske A., Wiegel J., Padilla C. N. and Acosta J. L. S. (2004) Distributions of microbial activities in deep subseafloor sediments. *Science* **306**, 2216-2221.

Dummer, N.F., Bawaked, S., Hayward, J., Jenkins, R., Hutchings, G.J. (2010) Oxidative dehydrogenation of cyclohexane and cyclohexene over supported gold, palladium and gold–palladium catalysts. *Catalysis Today* **154**, 2-6.

Engel, M.H., Macko, S.A. (1993) Organic geochemistry principles and applications. In *Topics in Geobiology*. (eds. Stehli, F.G., Jones, D.S.). Plenum Press, New York.

Ferris, J.P. (2005) Mineral catalysis and prebiotic synthesis: Montmorillonite-catalyzed formation of RNA. *Elements* **1**, 145-149.

Friesen J. B. and Schretzman R. (2011) Dehydration of 2-methyl-1-cyclohexanol: new findings from a popular undergraduate laboratory experiment. *J. Chem. Educ.* **88**, 1141-1147.

Foustoukos, D.I., Seyfried, W.E. (2004) Hydrocarbons in hydrothermal vent fluids: The role of chromium-bearing catalysts. *Science* **304**, 1002-1005.

Fu, Q., Foustoukos, D.I., Seyfried, W.E. (2008) Mineral catalyzed organic synthesis in hydrothermal systems: An experimental study using time-of-flight secondary ion mass spectrometry. *Geophys. Res. Lett*. **35**.

Germanov, A.I. (1965) Geochemical significance of organic matter in hyrothermal process. *Geochemistry International Ussr* **2**, 643.

Hazen, R.M., Sverjensky, D.A. (2010) Mineral surfaces, geochemical complexities, and the origins of life. Cold Spring Harbor Perspect. *Biol*. **2**.

Head I. M., Jones D. M. and Larter S. R. (2003) Biological activity in the deep subsurface and the origin of heavy oil. *Nature* **426**, 344-352.

Hedges, J.I. (1992) Global biogeochemical cycles- progress and problems. *Mar. Chem.* **39**, 67-93.

Helgeson H. C., Knox A. M., Owens C. E. and Shock E. L. (1993) Petroleum, oil-field waters, and authigenic mineral assemblages: Are they in metastable equilibrium in hydrocarbon reservoirs. *Geochim. Cosmochim. Acta* **57**, 3295-3339.

Hinrichs K.-U., Hayes J. M., Bach W., Spivak A. I., Hmelo L. R., Holm N. G., Johnson C. G. and Sylva S. P. (2006) Biological formation of ethane and propane in the deep marine subsurface. *Proc. Natl. Acad. Sci. USA.* **103**, 14,684-14,689.

Holm, N.G., Andersson, E. (2005) Hydrothermal simulation experiments as a tool for studies of the origin of life on earth and other terrestrial planets: A review. *Astrobiology* **5**, 444-460.

Horsfield B., Schenk H. J., Zink K., Ondrak R., Dieckmann V., Kallmeyer J., Mangelsdorf K., Primio R. D., Wilkes H., Parkes R. J., Fry J. and Cragg B. (2006) Living microbial ecosystems within the active zone of catagenesis: Implications for feeding the deep biosphere. *Earth Planet Sci. Lett*. **246 (**1–2), 55-69.

Johnson J. W., Oelkers, E. H., and Helgeson, H. C. (1992) SUPCRT92 - A software package for calculating the standard molal thermodynamic properties of minerals, gases, aqueous species, and reactions from 1 bar to 5000 bar And 0°C To 1000°C. *Comput. Geosci* **18**, 899-947.

Jones D. M, Head I. M., Gray N. D., Adams J. J., Rwan A. K., Aitken C. M., Bennett B., Huang H., Brown A., Bowler B. F. J., Oldenburg T., Erdmann M. and Larter S. R. (2008) Crude-oil biodegradation via methanogenesis in subsurface petroleum reservoirs. *Nature* **451**, 176-180.

Katritzky A. R., Nichols D. A., Siskin M., Murugan R. and Balasubramanian M. (2001) Reactions in high-temperature aqueous media. *Chem. Rev.* **101**, 837-892.

Kompanichenko, V.N. (2012) Inversion concept of the origin of life. *Orig Life Evol Biosph* **42**, 153–178.

Kuhlmann B., Arnett E. M. and Siskin M. (1994) Classical organic reactions in pure superheated water. *J. Org. Chem.* **59**, 3098-3102.

Kvenvolden, K.A. (1980) *Geochemistry of Organic Molecules*, *Benchmark Papers in Geology*. Dowden, Hutchinson and Ross, Inc., Stroudsburg, Pennsylvania.

Kvenvolden, K.A., Rapp, J.B., Hostettler, F.D. (1990) Hydrocarbon geochemistry of hydrothermally generated petroleum from Escanaba Trough, offshore California, USA. *Appl. Geochem*. **5**, 83-91.

Kvenvolden, K.A., Rapp, J.B., Hostettler, F.D., Rosenbauer, R.J. (1994) Laboratory simulation of hydrothermal petroleum formation from sediment in Escanaba Trough, offshore from Northern California. *Org. Geochem*. **22**, 935-945.

Labinger, J.A., Bercaw, J.E. (2002) Understanding and exploiting C-H activation. *Nature* **417**, 507–514.

Lahav, N. (1994) Minerals and the origin of life- hypotheses and experiments in heterogeneous chemistry. *Heterogen. Chem. Rev.* **1**, 159-179.

LaRowe, D.E., Van Cappellen, P. (2011) Degradation of natural organic matter: A thermodynamic analysis. *Geochim. Cosmochim. Acta* **75**, 2030-2042.

Larter S., Wilhelms A., Head I., Koopmans M., Aplin A., Primio R. D., Zwach C., Erdmann M. and Telnaes N. (2003) The controls on the composition of biodegraded oils in the deep subsurface- part 1: biodegradation rates in petroleum reservoirs. *Org. Geochem*. **34,** 601-613.

Leviette, D., Greitzer, Y. (2003) Natural and laboratory-simulated geothermal and geochemical processes, In *Natural and Laboratory Simulated Thermal Geochemical Processes*. (ed. Ikan, R.). Kluwer Academic Publishers, Kluwer, Amsterdam, pp. 239-252.

Lunine, J.I. (1999) *Earth: Evolution of a Habitable World*. Cambridge University Press, Cambridge, UK.

Martin W., Baross J., Kelley D. and Russell M. J. (2008) Hydrothermal vents and the origin of life. *Nat. Rev. Microbiol*. **6**, 805-814.

Mason O. U., Nakagawa T., Rosner M., Van Nostrand J. D., Zhou J., Maruyama A., Fisk M. R. and Giovannoni S. J. (2010) First investigation of the microbiology of the deepest layer of ocean crust. *PLoS ONE*. **5**, 1-11.

McCollom T. M. and Seewald J. S. (2007) Abiotic synthesis of organic compounds in deep-sea hydrothermal environments. *Chem. Rev.* **107**, 382-401.

McCollom, T.M., Seewald, J.S., Simoneit, B.R.T. (2001) Reactivity of monocyclic aromatic compounds under hydrothermal conditions. *Geochim. Cosmochim. Acta* **65**, 455-468.

McCollom, T.M., Simoneit, B.R.T., Shock, E.L. (1999) Hydrous pyrolysis of polycyclic aromatic hydrocarbons and implications for the origin of PAH in hydrothermal petroleum. *Energy Fuels* **13**, 401-410.

Mulkidjanian, A.Y. (2009) On the origin of life in the Zinc world: I. Photosynthesizing, porous edifices built of hydrothermally precipitated zinc sulfide as cradles of life on Earth. *Biol. Direct* **4**.

Nisbet E. G. (1985) The geological setting of the earliest life forms. *J. Mol. Evol.* **21**, 289-298.

Oldenburg, T.B.P., Larter, S.R., Huang, H. (2006) Nutrient supply during subsurface oil biodegradations - Availability of petroleum nitrogen as a nutrient source for subsurface microbial activity. *Energy Fuels* **20**, 2079-2082.

Parkes, R.J., Cragg, B.A., Bale, S.J., Getliff, J.M., Goodman, K., Rochelle, P.A., Fry, J.C., Weightman, A.J., Harvey, S.M. (1994) Deep bacterial biosphere in Pacific-Ocean sediments. *Nature* **371**, 410-413.

Reeves, E.P., Seewald, J.S., Sylva, S.P. (2012) Hydrogen isotope exchange between n-alkanes and water under hydrothermal conditions. *Geochim. Cosmochim. Acta* **77**, 582–599.

Russell, M., Hall, A., Mellersh, A. (2003) On the dissipation of thermal and chemical energies on the early Earth. In *Natural and Laboratory Simulated Thermal Geochemical Processes* (Ikan, R. et al., ed.). 325-388.

Russell, M.J., Daniel, R.M., Hall, A.J. (1993) On the emergence of life via catalytic iron-sulfide membranes. *Terr. Nova* **5**, 343-347.

Savage P. E. (1999) Organic chemical reactions in supercritical water. *Chem. Rev*. **99**, 603-621.

Schoonen, M., Smirnov, A., Cohn, C. (2004) A Perspective on the role of minerals in prebiotic synthesis. *Ambio* **33**, 539-551.

Schreiner, E., Nair, N.N., Wittekindt, C., Marx, D. (2011) Peptide synthesis in aqueous environments: The role of extreme conditions and pyrite mineral surfaces on formation and hydrolysis of peptides. *J. Am. Chem. Soc*. **133**, 8216-8226.

Seewald J. S. (1994) Evidence for metastable equilibrium between hydrocarbons under hydrothermal conditions. *Nature* **370**, 285-287.

Seewald J. S. (2001) Aqueous geochemistry of low molecular weight hydrocarbons at elevated temperatures and pressures: Constraints from mineral buffered laboratory experiments. *Geochim. Cosmochim. Acta* **65**, 1641-1664.

Seewald J. S. (2003) Organic-inorganic interactions in petroleum-producing sedimentary basins. *Nature* **426**, 327-333.

Seewald J. S., Zolotov M. Y. and McCollom T. (2006) Experimental investigation of single carbon compounds under hydrothermal conditions. *Geochim. Cosmochim. Acta* **70**, 446-460.

Shipp, J., Gould, I.R., Herckes, P., Shock, E.L., Williams, L.B., Hartnett, H.E. (2013) Organic functional group transformations in water at elevated temperature and pressure: Reversibility, reactivity, and mechanisms. *Geochim. Cosmochim. Acta* **104**, 194-209.

Shipp, J., L., S.E., Gould, I., Williams, L.B., Hartnett, H., submitted. Sphalerite is a catalysis for carbon-hydrogen bond breaking reactions. Submitted.

Shock E. L. (1988) Organic acid metastability in sedimentary basins. *Geology* **16**, 886-890.

Shock E. L. (1989) Corrections to "Organic acid metastability in sedimentary basins." *Geology* **17**, 572-573.

Shock E. L. (1990) Geochemical constraints on the origin of organic compounds in hydrothermal systems. *Origins Life Evol. B.* **20**, 331-367.

Shock E. L. (1992) Chemical environments in submarine hydrothermal systems. In *Marine Hydrothermal Systems and the Origin of Life* (ed. N. Holm). *Origins Life Evol. B.* **22**, 67-107.

Shock, E.L. (1993) Hydrothermal dehydration of aqueous-organic compounds. *Geochim. Cosmochim. Acta* **57**, 3341-3349.

Shock E. L. (1994) Application of thermodynamic calculations to geochemical processes involving organic acids. In *The Role of Organic Acids in Geological Processes* (eds. M. Lewan and E. Pittman). Springer-Verlag. pp. 270-318.

Shock E. L. (1995) Organic-acids in hydrothermal solutions - standard molal thermodynamic properties of carboxylic-acids and estimates of dissociation-constants at high-temperatures and pressures. *Am. J. Sci.* **295**, 496-580.

Shock E. L. (1996) Hydrothermal systems as environments for the emergence of life. In *Evolution of Hydrothermal Ecosystems on Earth (and Mars?)*. Wiley, Chichester (Ciba Foundation Symposium 202). pp. 40-60.

Shock E. L. and Canovas P. C. (2010) The potential for abiotic organic synthesis and biosynthesis at seafloor hydrothermal systems. *Geofluids* **10**, 161-192.

Shock, E.L., Amend, J.P., Y., Z.M. (2000) The early Earth vs. the origin of life. In *The Origin of the Earth and Moon*. (eds. Canup, R., Righter, K.). University of Arizona Press., pp. 527-543.

Shock E. L. and Schulte M. D. (1998) Organic synthesis during fluid mixing in hydrothermal systems. *Jour. Geophys. Res.* **103**, 28513-28527.

Shock E. L., Helgeson H. C. and Sverjensky D. A. (1989) Calculation of the thermodynamic and transport-properties of aqueous species at high-pressures and temperatures: Standard partial molal properties of inorganic neutral species. *Geochim. Cosmochim. Acta* **53**, 2157-2183.

Shock E. L., McCollom T. and Schulte M. D. (1995) Geochemical constraints on chemolithoautotrophic reactions in hydrothermal systems. *Origins Life Evol. B.* **25**, 141-159.

Shock E. L., McCollom T. and Schulte M. D. (1998) The emergence of metabolism from within hydrothermal systems. In *Thermophiles: the keys to molecular evolution and the origin of life?* (eds. Wiegel and Adams). Taylor & Francis, London. pp. 59-76.

Shock E. L., Amend J. P. and Zolotov M. Y. (2000) The early Earth vs. the origin of life. In *The Origin of the Earth and Moon* (eds. R. Canup and K. Righter) University of Arizona Press. pp. 527-543.

Shock E. L., Sassani D. C., Willis M., and Sverjensky D. A. (1997) Inorganic species in geologic fluids: Correlations among standard molal thermodynamic properties of aqueous ions and hydroxide complexes. *Geochim. Cosmochim. Acta* **61**, 907-950.

Shock, E.L., Schulte, M.D. (1998) Organic synthesis during fluid mixing in hydrothermal systems. *Journal of Geophysical Research-Planets* **103**, 28513-28527.

Simoneit, B.R.T. (1993) Aqueous high-temperature and high-pressure organic geochemistry of hydrothermal vent systems. *Geochim. Cosmochim. Acta* **57**, 3231-3243.

Simoneit, B.R.T. (2003) Petroleum generation, extraction and migration and abiogenic synthesis in hydrothermal systems. In *Natural and Laboratory Simulated Thermal Geochemical Processes*. (ed. Ikan, R.). Kluwer Academic Publishers, Kluwer, Amsterdam, pp. 1–30.

Siskin, M., Katritzky, A.R. (1991) Reactivity of organic-compounds in hot water-geochemical and technological implications. *Science* **254**, 231-237.

Siskin M. and Katritzky A. R. (2001) Reactivity of organic comounds in superheated water: general background. *Chem Rev*. **101**, 825-835.

Stull D. R., Westrum E. F. and Sinke G. C. (1969) *The Chemical Thermodynamics of Organic Compounds*. John Wiley & Sons, Inc., New York. pp. 358-359.

Sverjensky, D.A., Shock, E.L., Helgeson, H.C. (1997) Prediction of the thermodynamic properties of aqueous metal complexes to 1000°C and 5 kb. *Geochim. Cosmochim. Acta* **61**, 1359-1412.

Tivey, M.K. (1995) The influence of hydrothermal fluid composition and advection rates on black smoker chimney mineralogy: Insights from modeling transport and reaction. *Geochim. Cosmochim. Acta* **59**, 1933-1949.

Vaughan, D.J., Lennie, A.R. (1991) The iron sulfide minerals- their chemistry and role in nature. *Science Progress* **75**, 371-388.

Wang, W., Li, Q., Yang, B., Liu, X., Yang, Y., Su, W. (2012) Photocatalytic reversible amination of alpha-keto acids on a ZnS surface: implications for the prebiotic metabolism. *Chem Commun (Camb)* **48**, 2146-2148.

Wang, W., Yang, B., Qu, Y.P., Liu, X.Y., Su, W.H. (2011) $FeS/S/FeS_2$ Redox system and its oxidoreductase-like chemistry in the iron-sulfur world. *Astrobiology* **11**, 471-476.

Watanabe M., Sato T., Inomata H., Smith, Jr., R. L., Arai K., Kruse A. and Dinjus E. (2004) Chemical reactions of C_1 compounds in near-critical and supercritical water. *Chem Rev.***104**, 5803-5821.

Williams, L.B., Canfield, B., Voglesonger, K.M., Holloway, J.R. (2005) Organic molecules formed in a "primordial womb". *Geology* **33**, 913-916.

Williams L. B., Holloway J. R., Canfield B., Glein C., Dick J., Hartnett H. and Shock E. (2011) Birth of biomolecules from the warm wet sheets of clays near spreading centers. In *Earliest Life on Earth: Habitats, Environments and Methods of Detection* (eds. Golding S. and Glikson M.). Springer Publishing. Chapter 4. pp. 79-112.

Windman T., Zolotova N., Schwandner F. and Shock E. (2007) Formate as an energy source for microbial metabolism in chemosynthetic zones of hydrothermal ecosystems. *Astrobiology* **7**, 873-890.

Xu X. and Antal, Jr., M. J. (1994) Kinetics and mechanism of isobutene formation from t-butanol in hot liquid water. *AIChE J.* **40**, 1524-1534.

Xu X., Antal, Jr., M. J. and Anderson D. G. M. (1997) Mechanism and temperature-dependant kinetics of the dehydration of tert-butyl alcohol in hot compressed liquid water. *Ind. Eng. Chem. Res.* **36**, 23-41.

Xu, Y., Schoonen, M.A.A., (2000) The absolute energy positions of conduction and valence bands of selected semiconducting minerals. *American Mineralogist* **85**, 543-556.

Xu, Y., Schoonen, M.A.A., Strongin, D.R. (1996) Thiosulfate oxidation: Catalysis of synthetic sphalerite doped with transition metals. *Geochim. Cosmochim. Acta* **60**, 4701-4710.

Yang, Z.M., Gould, I.R., Williams, L.B., Hartnett, H.E., Shock, E.L. (2012) The central role of ketones in reversible and irreversible hydrothermal organic functional group transformations. *Geochim. Cosmochim. Acta* **98**, 48-65.

Zlatkin, I.V., Schneider, M., deBruijn, F.J., Forney, L.J. (1996) Diversity among bacteria isolated from the deep subsurface. *Journal of Industrial Microbiology* **17**, 219-227.

APPENDIX A

PUBLICATION CITATION

Chapter 2 titled "Organic functional group transformations in water at elevated temperature and pressure: Reversibility, reactivity, and mechanisms" is reprinted in this thesis with permission from co-authors: Ian R. Gould, Pierre Herckes, Everett L. Shock, Lynda B. Williams, and Hilairy E. Hartnett. The original article was published in 2013 in *Geochimica Cosmochimica Acta*, issue 104, pages 194-209.